# International Scientific-Technical and Production Journal

# CONTENTS

# FLASH-BUTT WELDING OF THICK-WALLED PIPES FROM HIGH-STRENGTH STEELS OF K56 STRENGTH CLASS

**S.I. KUCHUK-YATSENKO**[1], **Yu.V. SHVETS**[1], **V.F. ZAGADARCHUK**[1], **V.I. SHVETS**[1], **V.I. KHOMENKO**[2], **S.I. ZHURAVLYOV**[2], **A.Ya. SUDARKIN**[2], **V.L. KOLIKOV**[3], **S.A. KHOMICHENKO**[3]

[1]E.O. Paton Electric Welding Institute, NASU, Kiev, Ukraine
[2]CJSC «Pskovelektrosvar», Pskov, RF
[3]OJSC «Mezhregiontruboprovodstroj», Moscow, RF

Technology was developed for flash-butt welding of 1219 mm diameter pipes with 27 mm wall thickness from 10G2FB steel of strength class K56, designed for construction of off-shore gas pipelines. Admissible limits of variation of the main welding parameters ensuring the required quality of welded joints were determined. Required level of mechanical properties of the joints is achieved by local postweld high-temperature heat treatment in combination with accelerated cooling.

In 1980–1990s flash-butt welding (FBW) was widely used for joining position butts of pipes in construction of various pipelines with up to 20 mm wall thickness from steels of K52–K54 strength class.

Technology and equipment for FBW performance were developed at the E.O. Paton Electric Welding Institute together with Pskov Plant of Heavy Electric Welding Equipment (PPHEWE) with the participation of organizations of USSR Minneftegazstroj. Starting from 1980, PPHEWE mastered industrial production of equipment complexes «Sever-1», which include in-pipe welding machine USO 400 (K700) with internal flash-remover, external flash-remover, device for cleaning pipe inner surface to accommodate contact shoes and mobile electric power plant of 1000 kV·A power. «Sever-1» complexes were used to weld more than 6000 km of 1420 mm diameter pipelines (predominantly in Extreme North regions). Here high productivity of FBW process was achieved at minimum labour consumption [1]. Experience accumulated over many years of FBW application is indicative of stable high quality of welded joints that is practically independent of weather conditions or operator qualifications.

Over the last decade, intensive construction of super high-capacity pipelines operating at increased pressure (12–150 MPa) is observed. They are constructed of pipes from high-strength steels of K56–K65 strength class with wall thickness of 27–36 mm and more. Higher requirements are made of the quality of such pipe joints that is specified in modern normative documents.

As labour consumption of operations on welding position butts of thick-walled pipes in pipeline construction is considerably increased, application of high-efficient FBW process is highly promising.

Equipment available for performance of FBW, as well as «Styk» complexes for flux-cored wire arc welding, which were widely applied in the USSR, cannot be used to solve the above task, because of their technical capabilities. In addition, higher requirements are now made of mechanical property values of welded joints compared to normatives of 1980–1990s.

In this connection in recent years the E.O. Paton Electric Welding Institute and «Pskovelektrosvar» plant (RF) performed integrated development of new generation technology and equipment for FBW of thick-walled pipes. Under this project, weldability of thick-walled pipes from 10G2FB steel of strength class K56 was studied. These steels are applied in construction of off-shore pipelines. The objective of these investigations was development of the technology of welding pipes from the above-mentioned steel with 27 mm wall thickness that ensures improvement of mechanical properties of the joints, in keeping with current standards [2, 3].

Selection of the scope of investigations was determined by customer requirements to the first samples of developed equipment for the purpose of its application at construction of off-shore pipelines.

Development of welding technology was performed on large-size samples-sectors with welded cross-section of 8640 mm$^2$. Sectors of width $B = 320$ mm were cut out of pipes with wall thickness $\delta = 27$ mm, made from sheet steel 10G2FB produced

by controlled rolling with accelerated cooling. Pipe metal had the following composition, wt.%: 0.06 C; 0.21 Si; 1.42 Mn; 0.12 Ni; 0.07 Mo; 0.04 V; 0.04 Al; 0.02 Ti; 0.05 Cr; 0.02 Nb; 0.004 S; 0.012 P.

Mechanical properties of pipe metal were as follows:

$$\sigma_t = 546.7 - 556.8 \text{ MPa}; \ \sigma_y = 484.4 - 493.5 \text{ MPa};$$
$$KCV_{+20} = 334.7 - 336.6 \text{ J}/\text{cm}^2;$$
$$KCV_{-40} = 333.0 - 336.6 \text{ J}/\text{cm}^2.$$

Mechanical testing of welded butt joints was performed at the E.O. Paton Electric Welding Institute and Strength Laboratory of TsNIITMASh in keeping with the normative requirements [2, 3]. Metallographic investigations were conducted in light microscope «Neophot-32» in the Laboratory of Metallographic Investigations. The above laboratories are certified in keeping with the international standards.

FBW technology is based on the process of continuous flash-butt welding with programmed variation of the main parameters of the mode which was verified with positive result in welding by «Sever-1» complexes that allowed elimination to a considerable extent of the influence of accuracy of pipe fit up before welding on welded joint formation.

Welding mode is determined by selection of the program of variation of the main parameters of FBW process. Program (Figure 1) envisages four periods of the welding process [4].

In period *I* a stable flashing process is excited. In period *II* heating of the ends of pipes being welded up to the specified temperature is performed. In period *III* the flashing process is intensified to ensure optimum conditions for joint formation in the spark gap. In period *IV* deformation of heated ends and joint formation take place.

In addition to the main parameter values ($v_{fl}$ — pipe feed rate in periods of excitation of the process of ends flashing and heating; $U_{2o.c}$ — welding transformer open-circuit voltage; $t_w$ — welding time; $P_{up}$ — upset force; $v_{up}$ — upsetting speed), preset by the program, for each of the above flashing periods it is necessary to determine the algorithm of control of feedbacks between individual parameters at selection of the optimum welding mode.

The objective of these studies was selection of optimum welding modes providing the required mechanical properties of welded joints, as well as the possibility of producing sound welded joints at minimum values of consumed power and metal losses for flashing.

Welding of sectors cut out of pipes was performed in upgraded K1000 machine. The taken ratio of sector width, welded section area ($B \times \delta$) and resistance of this machine welding circuit, allowed a sufficiently accurate simulation of the process of flashing of a full-scale pipe of 1219 mm diameter, its power values
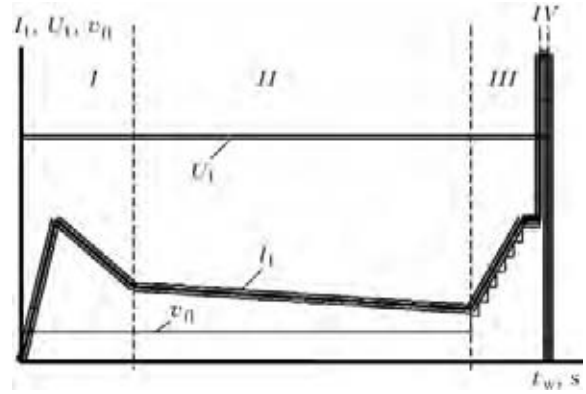
**Figure 1.** Program of variation of the main parameters of the mode of FBW of pipes: $I_1$, $U_1$ — primary welding current and voltage, respectively; $I$–$IV$ — programming periods

and determination of the main parameters of the developed machine for FBW of such pipes.

As follows from the above, at the first stage conditions are created for excitation of a stable flashing process, in which the angle of edges bevel (chamfer) $\alpha$ at pipe ends has an essential role. In this connection, studies of the influence of the angle of edge preparation of pipe ends on power required for excitation of the flashing process were conducted.

Sample ends in the welding area were cut by gas cutting, and edge preparation angle was changed from 0 up to 45° (Figure 2). Power required for excitation of stable flashing decreases with $\alpha$ increase (Figure 3) [5]. At $\alpha > 15°$ the consumed power during excitation of the flashing process (period *I*) and achievement of stable flashing (period *II*) remains constant. It is rational to assume the same loading of the power source at the initial and final periods of welding, then the optimum groove angle is equal to $\alpha = 15°$. In sample welding groove angle was taken to be $\alpha = 15°$.

At determination of optimum duration of stable flashing (period *II*), in order to obtain sound joints it is necessary to ensure heating zone larger than in welding of parts 15–20 mm thick. Maximum possible heating at continuous flashing is limited by achieving such a quasi-equilibrium thermal state, at which extension of flashing duration is not accompanied by heat increment in the ends of parts being heated. In samples of used dimensions such a state is reached in the case of increase of flashing duration up to 200 s
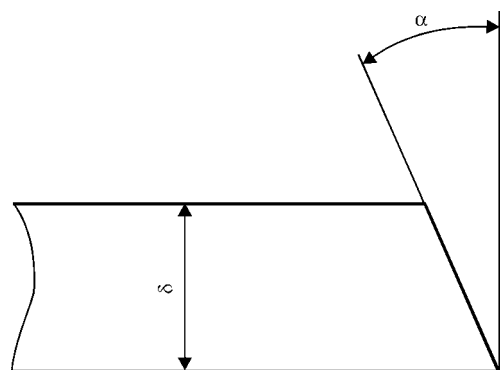


**Figure 2.** Edge preparation on sample ends

$\Delta p$, V·A/mm²
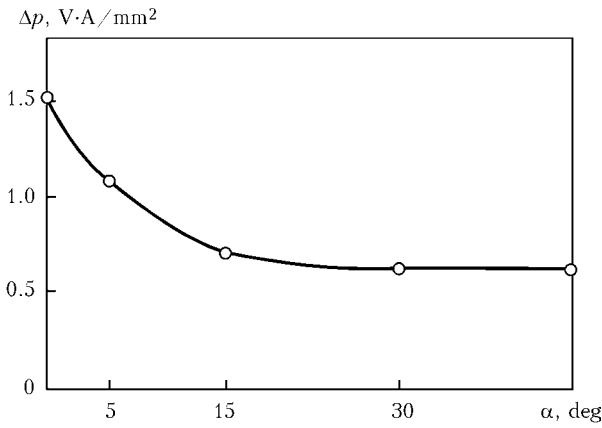


**Figure 3.** Dependence of specific power $\Delta p$ on groove angle $\alpha$ of edges [5]

$\Delta p_{\text{fin}}$, V·A/mm²



**Figure 5.** Dependence of specific consumed power $\Delta p_{\text{fin}}$ on final flashing speed $v_{\text{fin}}$

at optimum speed $v_{\text{fl}} = 0.2$ mm/s [6]. As such a «soft» heating mode corresponds to minimum consumed power, the above parameters are taken as the optimum ones at determination of the program for basic mode of welding sample batches in period *II*. Duration of period *III* and program of increase of displacement speed up to final speed $v_{\text{fin}}$ were taken allowing for the results of earlier research [6]. Figure 4 gives a record of oscillograms of the main welding parameters with the used «soft» mode.

Specific consumed power during stable flashing is equal to $\Delta p_{\text{fl}} = 6.1$ V·A/mm², and in the final period of flashing before upsetting it is increased up to $\Delta p_{\text{fin}} = 13$ V·A/mm² for 2–3 s. At the same program of variation of speed $v_{\text{fin}}$, values of consumed power rise in proportion to increase of $v_{\text{fin}}$ in the range of 0.8–1.4 mm/s. Figure 5 gives dependence $\Delta p_{\text{fin}} = f(v_{\text{fin}})$ at voltage $U_{\text{2o.c}} = 6.8$ V. Value of $\Delta p_{\text{fin}}$ determines set power of power source [7]. In welding pipes of the above cross-section a power source with set power of 1320 kV·A will be required. But as the modern mobile power stations allow short-time overloading of up to 10–15 %, the power can be even lower.

The above data show that determination of optimum $v_{\text{fin}}$ value has an essential influence on power source selection and technico-economic indices. In this connection, the influence of $v_{\text{fin}}$ values on welded joint



**Figure 4.** Oscillograms of the main parameters of welding in the soft FBW mode

quality was studied. For this purpose four batches of butt joints were welded in the «soft» mode with final speed $v_{\text{fin}} = 0.9$, 1.0, 1.1 and 1.2 mm/s. Each batch consisted of five butt joints: three were used for evaluation of mechanical properties, and two were broken in the joint plane. Samples were tested for rupture and bending in keeping with the standards [2, 3]. In order to determine mechanical properties of welded joint metal, bend testing of samples with a sharp notch along the joint line was performed. Results of mechanical testing of welded joints are given in Table 1.

Tensile testing of standard samples did not reveal any rejection indications, except for strength lowering by approximately 5.5 %. Sample fracture occurred at a distance of 21 mm from the joint plane. Bend testing of welded samples showed that at $v_{\text{fin}} = 1.1$ and 1.2 mm/s any rejection indications were absent. At $v_{\text{fin}} = 1.0$ mm/s cracks initiated in the joint plane, which by their length (not more than 6 mm) were not in the category of rejection indication by the normative documents [2, 3]. Bend angle of samples was equal to 180°.

Further lowering of final speed to 0.9 mm/s led to formation of cracks of the length not exceeding the value allowed by the standards. Testing of notched samples showed that such cracks are an indication of presence of sections of structural inhomogeneity that is characteristic for insufficiently intensive flashing before upsetting. In samples of welded joints made at $v_{\text{fin}} = 1.1$ and 1.2 mm/s, defects in the joint plane are absent on fracture surface. At $v_{\text{fin}} = 1.0$ mm/s,

**Table 1.** Mechanical properties of welded joints made at different final flashing speed*

| Batch # | $v_{\text{fin}}$, mm/s | $\sigma_t$, MPa | Rejection indication |
|---------|------------------------|-----------------|----------------------|
| 1 | 0.9 | 518.6 | Cracks > 6 mm, $\sigma_t \leq 94.5$ % |
| 2 | 1.0 | 518.0 | $\sigma_t \leq 94.5$ % |
| 3 | 1.1 | 518.4 | |
| 4 | 1.2 | 518.3 | |

*Here and in Table 2 bend angle was equal to 180°, 12 tensile samples and 30 bend samples were tested in each batch.

**Table 2.** Mechanical properties of welded joints made with different upset value

| Batch # | Upsetting, mm | $\sigma_t$, MPa | Rejection indication |
|---------|---------------|-----------------|----------------------|
| 1 | 8 | 515.9 | 6 % softening |
| 2 | 10 | 516.8 | 5.5 % softening |
| 3 | 12 | 518.6 | Same |
| 4 | 14 | 518.3 | » |

individual fine defects appear, so-called mat spots of up to 20 mm². In butt joints welded at $v_{fin} = 0.9$ mm/s, frequency of such defect occurrence becomes higher, and their area can reach 30—35 mm². Proceeding from the obtained results, a program with $v_{fin} = 1.2$ mm/s was accepted in further research.

In order to determine the optimum value of upsetting, four batches of pipe butts were welded in the basic «soft» mode with different upsetting. Each batch consisted of five butt joints: three were used to evaluate mechanical properties of the welded joint, and two were broken in the joint plane (Table 2). Obtained results of tensile testing of these specimens were practically identical. At their testing the reject indication was lowering of ultimate strength of up to 6 % with samples failing in the HAZ away from the joint plane. At bend testing of samples, cracks (small-sized delaminations within normative limits) appeared in some batches of joints welded with upsetting of 8—10 mm. Bend angle of these samples also corresponded to normative values (Figure 6). At bend testing with notches, microimperfections of the structure were found in fractures in the joint plane of some samples made with 8—10 mm upsetting (Figure 7), which were caused by local accumulation of non-metallic inclusions, namely manganese alumosilicates.

In welding of pipes with large developed cross-section, deformation of heated metal can be non-uniform. Therefore, $l_{up} = 13$ mm was taken as the optimum upsetting value. In order to achieve such deformation when the «soft» mode is used, specific upset force of 45 MPa is required.

Proceeding from investigation results, an optimum welding mode is given below, which can be reproduced in a production unit for welding pipes from 10G2FB steel 27 mm thick:

**Table 3.** Mechanical properties of test batch of samples*

| Test results | $\sigma_t$, MPa | $KCV_{+20}$, J/cm² | $KCV_{-20}$, J/cm² |
|--------------|-----------------|----------------------|----------------------|
| After welding | $\dfrac{516.0-523.4}{520.0}$ | $\dfrac{13.3-17.1}{15.0}$ | $\dfrac{6.1-9.7}{8.1}$ |
| After heat treatment | $\dfrac{550.6-561.4}{554.6}$ | $\dfrac{147.9-219.5}{173.2}$ | $\dfrac{86.8-171.1}{137.9}$ |

*Bend angle was 180°; no cracks.
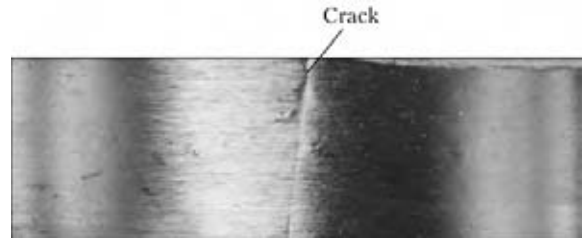


**Figure 6.** Crack in a sample tested for bending ($\alpha = 180°$)

Secondary voltage, V ................................................. 7
Welding time, s .............................................. 180—210
Feed rate at heating, mm/s ........................... 0.19—0.20
Flashing allowance at heating, mm ...................... 32—38
Allowance for speed increase, mm ........................... 6—9
Final speed before upsetting, mm/s ......................... 1.2
Specific upset force, MPa ..................................... 45
Upsetting, mm .................................................. 13

The above mode was used to weld test batches of samples and perform mechanical testing in keeping with standards [2, 3]. Test results are given in Table 3, from which one can see that at rupture testing, ultimate strength of welded joints decreases by 5.5—6.0 %. This occurs in HAZ region, where heating temperature reaches 700—800 °C and is caused by lowering of the effect of steel heat hardening, achieved during its controlled rolling. Impact toughness values $KCV_{+20}$ and $KCV_{-20}$ of the joints do not meet the specified requirements [2, 3].

As is seen from Figure 8, the greatest lowering of impact toughness occurs in the local region in the weld center, the length of which is equal to $l = 0.5-1.0$ mm from the joint plane, that is confirmed by the conducted metallographic investigations. This is readily seen at comparison of the structures of base metal (Figure 9, *a*) and joint line with regions of coarse grain of up to 0.5 mm length adjacent to it (Figure 9, *b*), where metal was subjected to short-term heating up to the temperature of 1300 °C and higher. Base metal microstructure is a ferritic fine-grained matrix (ferrite grains, class 11) with carbide stringers which are elongated along the rolling direction (Figure 9, *a*). Structures with a considerable coarsening of bainite grain (class 3) and high content of polygonal ferrite form in the region adjacent to the joint plane.
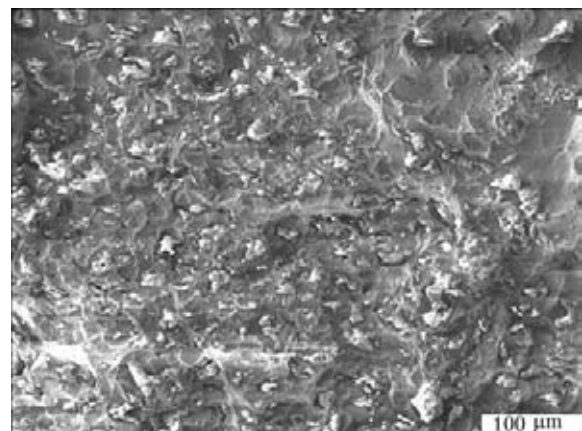


**Figure 7.** Accumulation of manganese alumosilicates in sample fractures made with upsetting of 8—10 mm

$KCV_{+20}$, J/cm$^2$
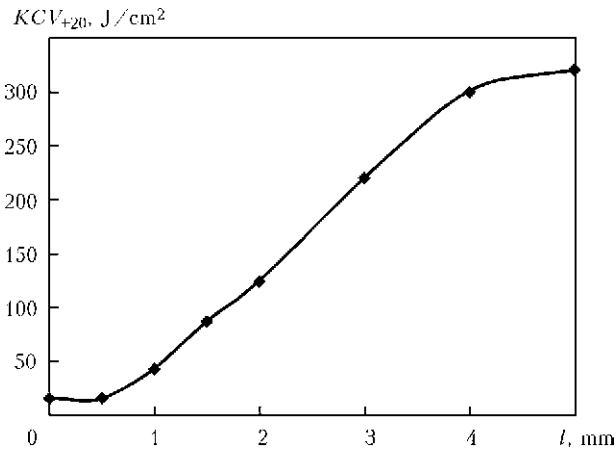


**Figure 8.** Distribution of impact toughness $KCV_{+20}$ in the HAZ metal

These structures are characterized by low values of impact toughness.

In order to check the possibility of increasing the values of impact toughness and strength of welded joints, a batch of samples was welded in the «rigid» mode, the parameters of which are given below:

```
Secondary voltage, V ................................................. 7
Welding time, s ................................................. 45–50
Feed rate at heating, mm/s ..................................... 0.3
Flashing allowance at heating, mm ........................... 12
Allowance for speed increase, mm ........................... 5–6
Final speed before upsetting, mm/s ......................... 1.2
Specific upset force, MPa ................................. 120–140
Upsetting, mm ................................................... 5–6
```
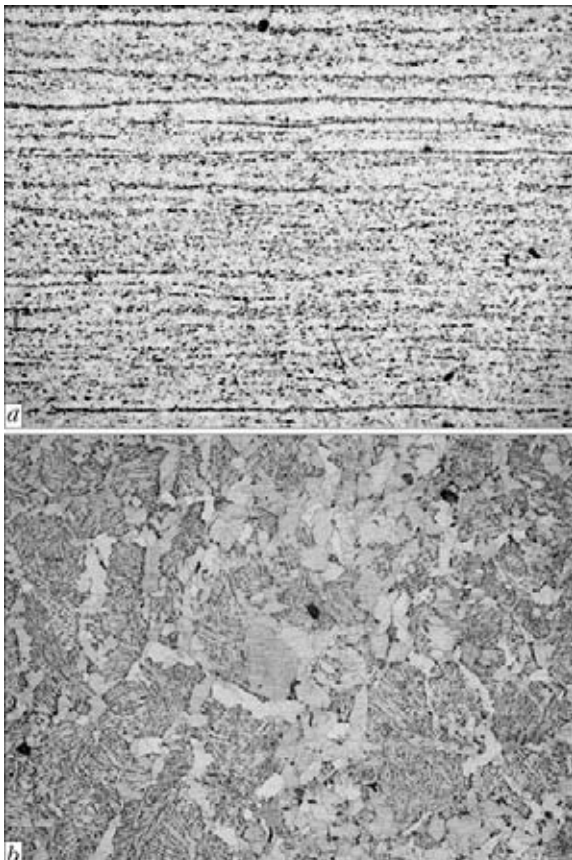


**Figure 9.** Microstructures (×100) of base metal of pipes (*a*) and metal of joint line with coarse grain regions (*b*)

The above mode features a shorter flashing duration in period *II*, increased final speed and greater specific pressure. Mechanical properties of metal of joints made in the «rigid» mode, are as follows: $\sigma_t$ = = 546.0–553.6 MPa; $KCV_{+20}$ = 16.3–22.6 J/cm$^2$; $KCV_{-20}$ = 6.1–9.7 J/cm$^2$; bend angle was equal to 180°; cracks were absent. In welding in the «rigid» mode total process duration is reduced to 50 s, flashing allowance — to 12 mm, and power consumed in the final period of welding increases up to 23 V·A/mm$^2$, i.e. it is almost 2 times higher compared to the «soft» mode. All the other indices correspond to normative requirements except for impact toughness, which increased slightly as a result of lowering of polygonal ferrite content and refinement of primary austenite grains, but its values are below the normative level [2, 3].

In view of the fact that the «rigid» mode requires an essential increase of consumed power at flashing, and great upsetting forces, but only slightly increases welded joint impact toughness, its application is not rational.

It is known that in order to increase the ductile properties of welded joints made by FBW, it is necessary to apply high-temperature heat treatment [8]. In this connection, investigations were performed and technology was developed for heat treatment of welded joints of thick-walled pipes. Samples of welded joints, made in the reference mode, were subjected to local heating by a circular inductor with 2.4 Hz frequency, using thyristor frequency converter TPChT-160. Heating was performed up to the temperature of 950 °C for 5 min, soaked at this temperature for 2.5–3.0 min, and then samples were cooled in an accelerated mode by water-air mixture from two sides up to approximately 300 °C. Accelerated cooling is required, as it eliminates lowering of hardness and ultimate strength in the heating region.

After heat treatment and accelerated cooling of butt joints in the above mode, ultimate strength of welded joints corresponded to base metal values (see Table 3). Bend angle of samples was 180°, cracks on
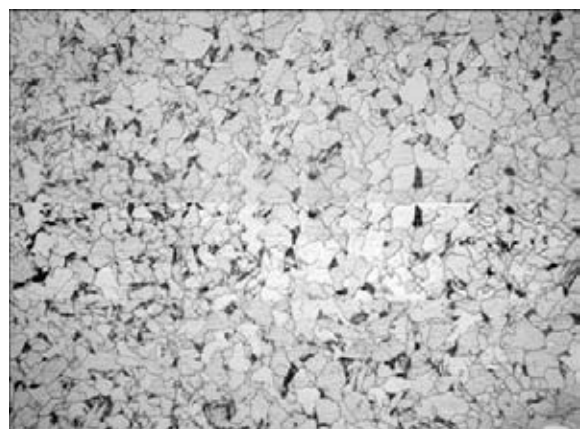


**Figure 10.** Microstructure of metal (×400) of joint line with coarse grain regions after heat treatment and accelerated cooling

the joint line and in the HAZ were absent. Impact toughness $KCV_{+20}$ and $KCV_{-20}$ was equal to 173.2 and 137.9 J/cm$^2$, respectively. These indices are by an order of magnitude higher than impact toughness values of the joints after welding. Mechanical properties of the joints after heat treatment and accelerated cooling fully comply with the requirements of both Russian [2] and international standards [3].

Microstructure of metal of the joint line and coarse grain region is a ferritic matrix with inclusions of residual austenite, which partially decomposes with granular bainite formation. Microstructure of the joint line and coarse grain regions after heat treatment is shown in Figure 10.

Ferrite grain is class 9. Hardness along welded joint line and in the HAZ is on the level of $HV5$ 1900 ± ± 50 MPa that does not exceed the required values [2, 3].

Postweld local heat treatment and accelerated cooling allow leveling the disadvantages of mechanical properties of the joints due to improvement of weld metal structure.

**CONCLUSIONS**

1. Technology of FBW of pipes from high-strength stainless steels of strength class K56 with up to 27 mm wall thickness was developed. In order to obtain sound joints of pipes from such steels, it is necessary for the power source and welding machine upset drive to ensure the values of consumed specific power of not less than 12 V·A/mm$^2$, and specific upset force of not less than 45 MPa in welding.

2. Integrated mechanical testing and metallographic investigations of pipe steel welded joints were conducted. Application of high-temperature heat treatment (normalizing) after welding in combination with accelerated cooling ensures meeting the standard requirements.

3. Proceeding from the results of the conducted studies, statements of work on development of new generation equipment for FBW of thick-walled pipes of 1220−1420 mm diameter were prepared.

1. Mazur, I.I., Serafin, O.M., Karpenko, M.P. (1988) Resistance welding of pipelines: ways of improvement. *Stroitelstvo Truboprovodov*, **4**, 8−11.
2. *STO 2-3.7-380−2009*: Manual on welding technology of sea off-shore pipelines. Introd. 2009.
3. *DNV-OS-F101*: Offshore standard. Submarine pipeline systems. Jan. 2000.
4. Kuchuk-Yatsenko, S.I. (1992) *Flash-butt welding*. Kiev: Naukova Dumka.
5. Kuchuk-Yatsenko, S.I., Mosendz, I.N., Kazymov, B.I. (1987) Programming of parameters of flash-butt welding with large developed sections. *Avtomatich. Svarka*, **6**, 14−18.
6. Kuchuk-Yatsenko, S.I., Lebedev, V.K. (1976) *Continuous flash-butt welding*. Kiev: Naukova Dumka.
7. Kuchuk-Yatsenko, S.I., Krivenko, V.G., Sakharnov, V.A. et al. (1986) *Resistance butt welding of pipelines*. Kiev: Naukova Dumka.
8. Lebedev, V.K., Skulsky, Yu.V., Kuchuk-Yatsenko, S.I. et al. (1977) Local heat treatment of welded joints of 1420 mm diameter gas pipes. *Avtomatich. Svarka*, **10**, 38−40.

# EXPERIMENTAL STUDY OF THE MECHANISM OF HYDROGEN EMBRITTLEMENT OF METALS WITH THE BCC LATTICE[*]

**V.S. SINYUK, I.K. POKHODNYA, A.P. PALTSEVICH** and **A.V. IGNATENKO**

E.O. Paton Electric Welding Institute, NASU, Kiev, Ukraine

The study gives results of investigations of the effect of hydrogen on the mechanism of metal fracture. In metal containing diffusible hydrogen, plastic deformation leads to formation of residual hydrogen, which is connected to formed dislocations and microcracks. The presence of hydrogen connected to dislocations leads to localisation of plastic deformation of metal. Initiation of microcracks occurs by the shear mechanism, and their further growth takes place due to formation of new defects at the old crack apex and their coalescence.

Welding of structures of high-strength low-alloy steels involves a problem of formation of hydrogen-induced cold cracks, which is caused by such a phenomenon as hydrogen embritlement (HE) of metal. The HE mechanism is based on interactions of hydrogen with dislocations and a change in properties of dislocation clusters under the effect of hydrogen. Theoretical aspects of the HE mechanism are considered in study [1]. The present study is dedicated to experimental investigation of the HE mechanism.

Ferritic-pearlitic steel VSt3sp (killed) of the following composition, wt.%: 0.12 C, 0.14 Si, 0.42 Mn, 0.1 Ni, 0.12 Cr, 0.022 S and 0.012 P, was used as the investigation material (Figure 1). Specimens of this steel were annealed at a temperature of 600 °C.

Mechanical properties of the hydrogen-containing specimens of steel VSt3sp were determined in the first



**Figure 1.** Microstructure (×500) of steel VSt3sp

series of experiments. The specimens were saturated with hydrogen by the electrolytic method in the 5 % sulphuric acid solution with an addition of 0.05 % sodium thiosulfate for 8–13 h, the current density being 4 mA/cm$^2$. Re-grinding of the specimens after hydrogenation took no more than 1 min. Before the mechanical tests the specimens were stored in liquid nitrogen. The contents of diffusible and residual hydrogen were determined by the chromatographic method [2].

In the second series of experiments, the specimens of steel VSt3sp were subjected to tension to different degrees of plastic deformation (10, 15 and 17 %). After that hydrogen was removed by heating the specimens to 50 °C and holding for 7 days. After the removal of hydrogen, the specimens were tensioned to fracture. The specimens that contained no hydrogen were subjected to the identical test cycle. Mechanical tests to uniaxial tension were carried out on cylindrical specimens with a gauge lengh of 30 mm and diameter of 5 mm.

Mechanical tests to uniaxial tension testing were conducted by using servohydraulic machine «Instron-1251». Prior to the tests the specimens were heated in alcohol to room temperature. It took no more than 3 min to heat a specimen and then place it in the grips, as well as fix the strain gauge. The strain rate in tension of the specimens was of $1 \cdot 10^{-3}$ s$^{-1}$.

Fractographic analysis was carried out by using JEOL scanning electron microscope JSM-35CF.

Results of the uniaxial tension tests in the proof stress $\sigma$–relative strain $\varepsilon$ coordinate system are shown in Figure 2. Mechanical properties of steel VSt3sp were recovered after hydrogenation and subsequent degassing (curves *1* and *2* in Figure 2). Increase in diffusible hydrogen content $[H]_{diff}$ leads to fracture of metal at a lower degree of plastic deformation
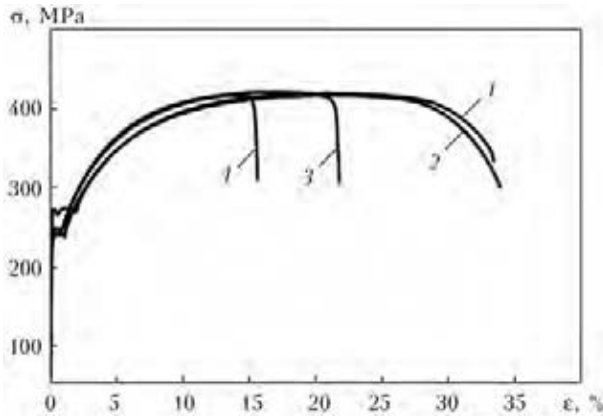
**Figure 2.** Effect of the content of diffusible hydrogen $[H]_{diff}$ on fracture of steel VSt3sp specimens in uniaxial tension: *1* — initial state ($\psi = 54$ %); *2* — after hydrogenation to $[H]_{diff} \approx 7$ cm$^3$/100 g and degassing ($\psi = 62$ %); *3* — $[H]_{diff} = 6.5$ cm$^3$/100 g ($\psi = 23$ %); *4* — $[H]_{diff} = 8.5$ cm$^3$/100 g ($\psi = 15$ %)

(curves *3* and *4* in Figure 2). Fracture of the hydrogen-containing metal occurs after stresses reach the value of tensile strength, i.e. at the beginning of localisation of plastic deformation in the form of a neck. The values of ductility of metal, i.e. elongation and reduction in area, are most sensitive to HE.

After mechanical tests the specimens were held at room temperature for 7 days. The content of residual hydrogen in fractured metal was measured by thermal desorption analysis. For this the specimens were cut out from a region with a uniform plastic deformation. The analysis results are shown in Figure 3. The first peak in the thermal desorption spectrum corresponds to hydrogen at dislocations ($[H]_{disl}$), and the second one — to molecular hydrogen ($[H]_{mol}$) located in microcracks, this being evidenced by its desorption temperature. New dislocations acting as hydrogen traps initiate during the process of plastic deformation. Accumulation of hydrogen at the dislocations facilitates their coalescence [1] and leads to initiation of microcracks. Molisation of hydrogen takes place after it gets into the formed defects.

To determine the effect of hydrogen on the mechanism of initiation of microcracks, the specimens of steel VSt3sp were preliminarily deformed to an elon-
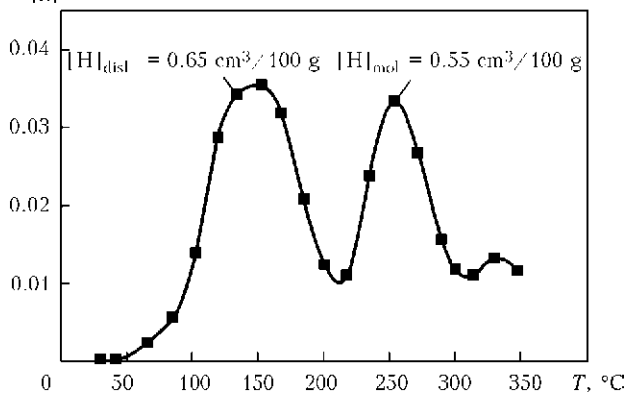


**Figure 3.** Rate of removal of residual hydrogen $v_{[H]}$,
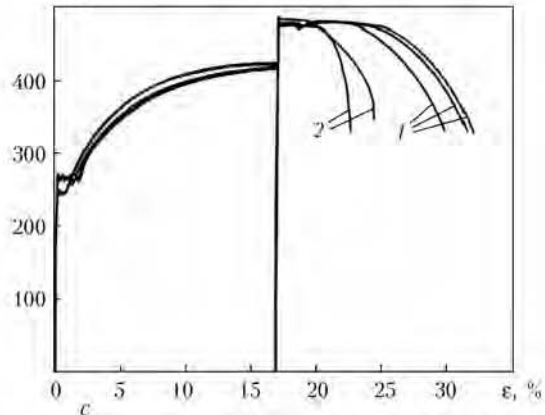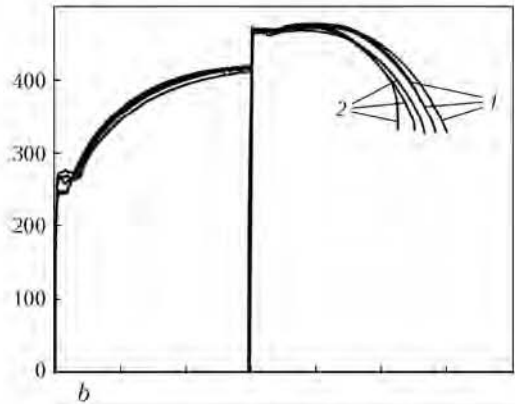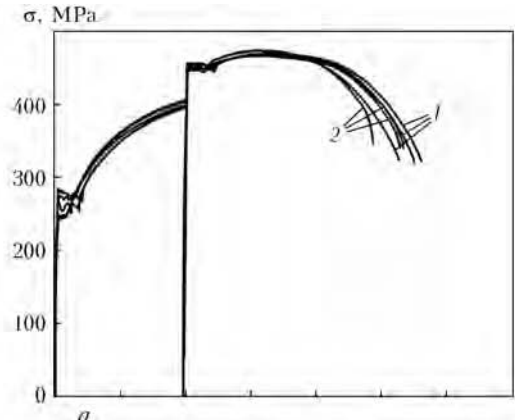


**Figure 4.** Tension diagrams for specimens of steel VSt3sp with different preliminary deformations: *a* — $\varepsilon = 10$ % ($\psi_{[H]} = 51$ %, $\psi = 62$ %); *b* — $\varepsilon = 15$ % ($\psi_{[H]} = 49$ %, $\psi = 57$ %); *c* — $\varepsilon = 17$ % ($\psi_{[H]} = 39$ %, $\psi = 62$ %); $\psi_{[H]}$, $\psi$ — average reduction in area of hydrogen-containing and hydrogen-free specimens, respectively; *1* — initial state; *2* — hydrogen content 7 cm$^3$/100 g (the specimens were degassed after preliminary deformation)

gation of 10, 15 and 17 % and then degassed, after which they were deformed to fracture. The content of diffusible hydrogen in the specimens after electrolytic saturation was 7 cm$^3$/100 g. As shown by the thermal desorption analysis, after degassing of the deformed specimens of steel VSt3sp at a temperature of 50 °C for 7 days the hydrogen was desorbed from them at a temperature above 200 °C. Therefore, the hydrogen at dislocations was removed during degassing. The mechanical test results are shown in Figure 4. Strain ageing of metal takes place after unloading and holding at a temperature of 50 °C. The value of strengthening does not depend on the presence of hydrogen
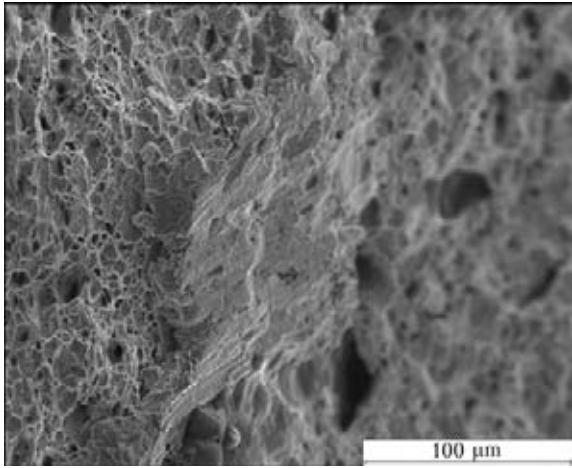
**Figure 5.** Microstructure of the surface of shear microcrack at the centre of steel VSt3sp specimen with a hydrogen content of 7 $cm^3/100$ g after preliminary deformation of 17 %
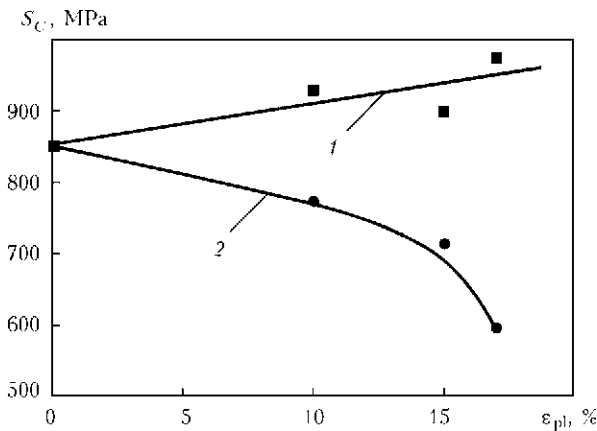


**Figure 6.** Effect of preliminary plastic deformation $\varepsilon_{pl}$ of specimens of steel VSt3sp on fracture stress $S_C$: $1$ — initial state; $2$ — $[H]_{diff}$ = 7 $cm^3/100$ g (the specimens were degassed after preliminary deformation)
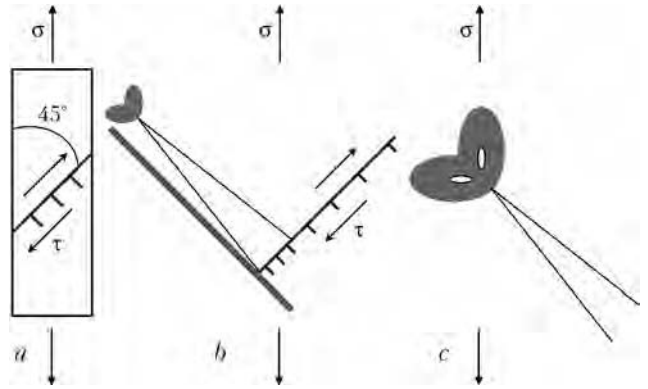


**Figure 7.** Schematics of initiation and growth of crack in hydrogen-containing metal: $a$ — formation of slip systems in tension; $b$ — initiation of microcrack in slip plane; $c$ — growth of crack due to initiation of new microcracks at its apex; $\tau$ — tangential stress

and equals 50 MPa. At a deformation of 10 %, the hydrogen has no substantial effect on mechanical properties of the specimens of steel VSt3sp (see Figure 4, $a$). The same takes place also at a deformation of 15 % (Figure 4, $b$). At a deformation of metal at a level of 17 %, the effect of hedrogen on mechanical properties of steel VSt3sp was much aggravated (Figure 4, $c$). A microcrack oriented at an angle of 45° to the specimen axis appeared on the fracture surface of the specimens with a hydrogen content of 7 $cm^3/100$ g after a preliminary plastic deformation of 17 % (Figure 5). No such cracks were detected in the hydrogen-free specimens. The fracture stress was calculated to evaluate the impact of microcracks formed under the effect of hydrogen on metal fracture [3]. The Bridgeman's relationships [4], allowing for those suggested by Kopelman [5], were used to calculate the maximal stress value in the neck of a specimen at the time point of fracture:
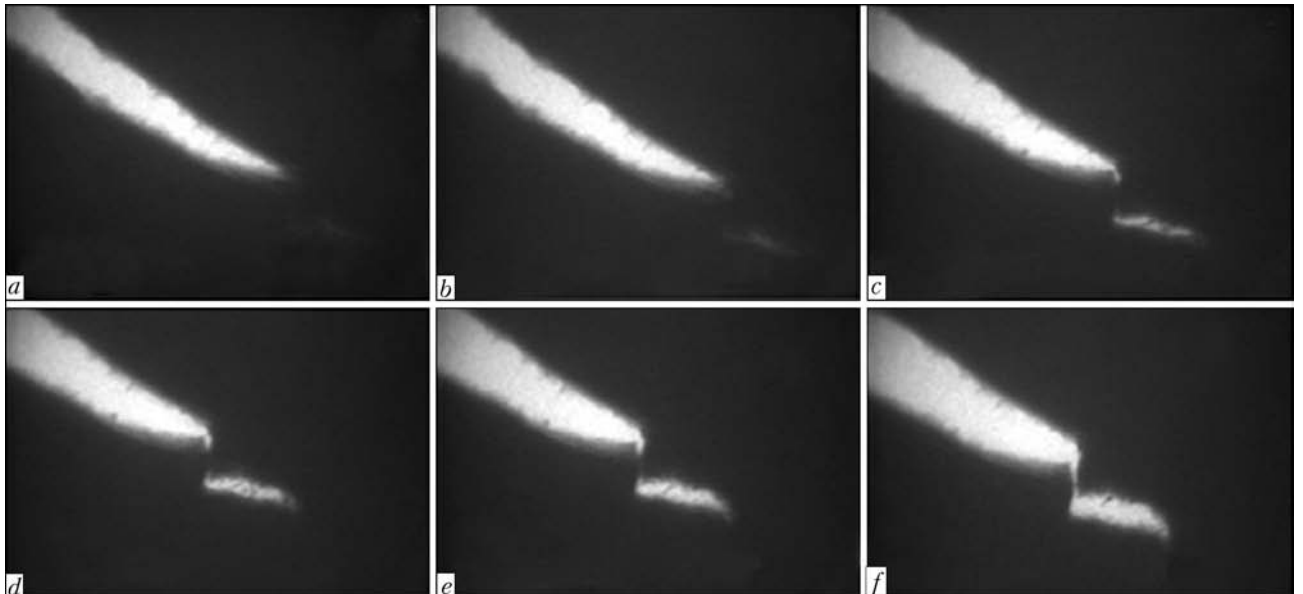


**Figure 8.** Propagation of crack in specimens of steel IN903 without hydrogen ($a$) and by adding it after 17 ($b$), 22 ($c$), 29 ($d$), 32 ($e$) and 39 ($f$) s

$$S_C = S_K \frac{1 + \ln (1 + \eta/2)}{(1 + \eta/2) \ln (1 + \eta/2)},$$

where $\eta = 0.92(e - 0.1)$,; $e = \ln (1/(1 - \psi))$; and $S_K$ is the average stress at the neck at the time point of fracture of a specimen. As seen from Figure 6, the value of fracture stress of metal in the initial state grows with increase of the preliminary plastic deformation [6]. This is related to the fact that microcracks, which form in metal as a result of plastic deformation and do not lead to fracture at the moment of their formation, become blunted with further plastic deformation [7]. At the presence of diffusible hydrogen in metal, the trend is reversed, i.e. the fracture stress decreases with growth of the preliminary plastic deformation. This is indicative of the fact that in the hydrogen-containing metal the microcracks that formed during plastic deformation do not blunt but continue growing.

Plastic deformation of metal leads to initiation of new dislocations, which act as hydrogen traps. The presence of hydrogen at dislocations leads to decrease in the force of repulsion of the dislocations and localisation of plastic deformation [1]. The key stage of the HE mechanism is coalescence of dislocations at the crack apex [8]. Schematic of initiation and growth of a crack in specimens testing is shown in Figure 7. Growth of the crack by the brittle and quasi-brittle mechanism occurs due to initiation of a new microcrack at the apex of the old one and its subsequent coalescence. The dislocation model of this process for the hydrogen-free metal is considered in study [9]. In the hydrogen-containing metal, the formed microcracks continue growing during plastic deformation due to initiation of new defects at the crack apexes (Figures 8 and 9) [10].

It can be concluded from the above-said that the HE mechanism consists in the following. Plastic deformation of metal results in formation of dislocations, which act as traps for diffusible hydrogen and lead to redistribution of the latter. The presence of hydrogen around dislocations leads to their coalescence at a lower external stress, at a macrolevel this showing up as facilitation of shear deformation and localisation of plastic deformation. Further growth of a crack occurs due to initiation of a new microcrack at the apex of the old one as a result of plastic deformation localised here under the effect of hydrogen.
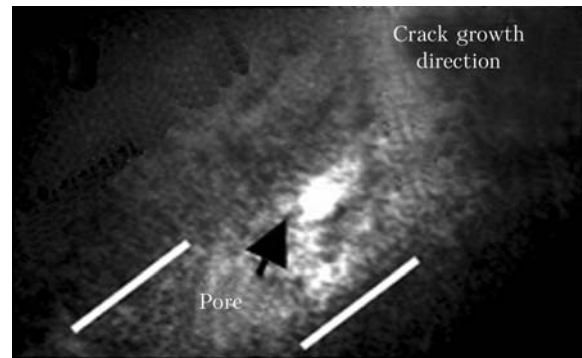


**Figure 9.** Formation of micropore in slip shear line ahead of the crack apex in a hydrogen-containing specimen of steel IN903

## CONCLUSIONS

1. As established by thermal desorption analysis, the cause of hydrogen embrittlement of metal in plastic deformation is hydrogen at dislocations.

2. The presence of hydrogen at dislocations leads to facilitation of shear deformation and initiation of a microcrack at a lower external stress, compared to the hydrogen-free metal.

3. Brittle growth of a crack occurs due to initiation of a new microcrack at the apex of the old one as a result of localisation of plastic deformation at the crack apex under the effect of hydrogen.

1. Ignatenko, A.V., Pokhodnya, I.K., Paltsevich, A.P. et al. (2012) Dislocation model of hydrogen-enhanced localizing of plasticity in metals with bcc lattice. *The Paton Welding J.*, **3**, 15−19.
2. Paltsevich, A.P. (1999) Chromatographic method for determination of hydrogen content in electrode coating components. *Avtomatich. Svarka*, **6**, 45−48.
3. Pokhodnya, I.K., Shvachko, V.I., Stepanyuk, S.N. (2000) The evaluation methods of HSLA steels susceptibility to hydrogen embrittlement. In: *Proc. of Int. Conf. on HSLA Steels* (Xi'an, Chine, 2000), 453−458.
4. Bridgeman, P. (1955) *Investigation of high plastic deformation and fracture*. Moscow: Inostr. Literatura.
5. Kopelman, L.A. (1978) *Resistance of welded assemblies to brittle fracture*. Leningrad: Mashinostroenie.
6. Margolin, B.Z., Shvetsova, V.A., Karzov, G.P. et al. (2009) Development and application of local PROMETEY-approach for prediction of brittle fracture of reactor casing steels. *Voprosy Materialovedeniya*, **3**, 290−314.
7. Kotrechko, S.A., Meshkov, Yu.Ya. (2008) *Ultimate strength*. Kiev: Naukova Dumka.
8. Gerberich, W.W., Stauffer, D.D., Sofronis, P.A. (2009) Coexistent view of hydrogen. In: *Proc. of Int. Conf. on Effects on Mechanical Behavior of Crystals: HELP and HEDE Effects of Hydrogen on Materials* (Wyoming, Sept. 7−10, 2008). Materials Park: ASM Int., 38−45.
9. Vladimirov, V.I. (1986) *Physical nature of metal fracture*. Moscow: Metallurgiya.
10. Robertson, I.M., Birnbaum, H.K. (2005) Dislocation mobility and hydrogen. In: *Brief Rev. of Int. Conf. on Fracture* (Turin, Italy, March 20−25, 2005). *http://www.icf11.com/proceeding/EXTENDED/5759.pdf*

# NEW CAPABILITIES OF MECHANIZED ARC SPOT WELDING USING PULSE EFFECTS

**L.M. LOBANOV, V.A. LEBEDEV, S.Yu. MAKSIMOV, A.N. TIMOSHENKO, P.V. GONCHAROV, I.V. LENDEL** and **R.I. KLOCHKO**

E.O. Paton Electric Welding Institute, NASU, Kiev, Ukraine

The issues related to producing of spot joints of structures on vertical plane using mechanized equipment for arc shielded-gas welding were considered. It was established that application of pulse electrode wire feed with controllable parameters allows essential simplification of process of producing welded joint, providing its necessary quality and repeatability of results. The prospects of application of this welding method were shown including also those with application of welding current sources with pulse algorithms of operation synchronized with pulse electrode wire feed.

***Keywords:*** *arc spot welding, electrode wire, feed, pulse, control, formation, repeatability, equipment*

The mechanized and automatic arc welding using consumable electrode in carbon dioxide atmosphere found wide application due to the complete complex of favorable properties: simplicity, availability of materials, reducing of works terms and costs for structure manufacture, possibility to conduct process in different spatial positions, etc. The most frequent application has the process with natural periodic short circuits of arc gap and electrode metal transfer. In this case the quality of welded joint, economic characteristics of the process significantly depend on stability of electrode metal drops transfer [1].

The basic methods of electrode metal transfer stabilization are [2]:

• selection of optimal parameters of welding process and their stabilization;

• application of activated electrode wires;

• application of pulse-arc process;

• development and application of pulse methods of electrode wire feed.

The pulse electrode wire feed with adjustable parameters of pulsed movement (frequency, relative pulse duration, acceleration) is one of the most effective methods of stabilization of electrode metal transfer characteristics with a number of additional effects [3]. In particular, it relates to welding using thin electrode wires in $CO_2$. Nowadays there is enough information about significant influence of pulse feeding on quality of welded joint produced in different spatial positions [4–6]. However these data relate to welding at different conditions of welds of different length. It is important also to give a prospective evaluation of influence of pulse electrode wire feed on the process of arc spot welding (ASW) which is the aim of present work.

The ASW process is an effective method for joining of sheet structures with elements of frame during lining, for example, railway cars, small ships, other transport vehicles and objects of the kind.

During ASW in flat position it is not difficult in most cases to produce the quality spot joint. In welding on the vertical plane it is far more difficult to produce a spot joint, in particular, if sheets of more than 1 mm thickness are welded.

In the work [4] the algorithm of producing a spot joint in vertical plane using ASW in $CO_2$ was proposed, the principle of which consists in dividing the welding process cycle into several stages. At the beginning of the cycle the burnout of lining sheet at increased values of current and voltage is performed. Then, the obtained space is filled with electrode metal and base metal to which lining is welded on. The problems arise namely during filling the space of burnout.

The basic difficulties and occurring defects during making of a spot joint consist in instability of repeatability of a shape of a spot joint; distortion of lining sheet; overlaps and even metal flows (Figure 1); lack of penetration of base metal, sufficient to provide strength characteristics.

According to carried out investigations the causes for unsatisfactory quality of a spot joint produced using arc process are:

• instability of parameters of welding process (in particular, arc voltage), arising due to a number of natural reasons (changes of real electrode wire stickout, conditions of current supply in current-carrying tip);

• changes of electrode wire feed conditions resulting in incontrollable fluctuations of feed rate and consequently current, influencing the characteristics of fusion;

• heating of metal from performance of previous welded spot joints;

• lack of control of heat input into the pool of molten metal to produce a spot.

Mathematic model of ASW process presented in the work [7] allowed the evaluation of optimal parameters of heat input and also residual stresses after welding. The result of this evaluation appeared to be a development of the algorithm for selection of welding parameters of performance of arc spot joint in-

cluding several cycles of synchronous change of current and voltage of arc process, i.e. the condition modulation. It allows performing control of heat input into a weld pool within some ranges and somewhat stabilize the process of producing a spot joint by selection of modulation parameters. However it is not always possible to find the complete solution for the problems connected with formation of a weld spot joint. Moreover, it is necessary to consider also the conditions of preparation of a structure for welding, first of all, providing surfaces being welded, tightly adjacent one to another. Here, a gap should be not only minimal, but also stable.

The great problem in welding with effective (deep) modulation of conditions is the periodical interruption of burning and exciting of welding arc, in this case the repeated arc excitement, as investigations showed, is not always stable due to formation of electrode metal drop of different size at the edge of a wire. As is seen from Figure 2, where different variants of a shape of a frozen drop are presented, only the shape of drop 3 and 4 allows reliable repeated arc exciting.

It is possible to exclude the basic factors of influence on formation of spot joint using methods of control of electrode metal transfer, in particular, controllable pulsed electrode wire feed. Figure 3 shows the testing-investigation stand for practicing of conditions for welding of spots in vertical plane. As a mechanism of pulse feeding, a new design of a gearless pulsed feeding mechanism based on a valve computerized electric drive with a wide range of control of parameters of pulsed movement of electrode wire such as pitch, frequency, relative pulse duration, shape [8] was used, in application of which a number of tasks on formation of welded joint with long welds as well as on energy- and resources-saving has been already solved until now [9].

It should be noted that the aims of control of electrode metal transfer at pulse electrode wire feed can be considered achieved in that case if the moment of electrode metal transfer corresponds to one pulse of feeding. In welding using thin wires Sv-08G2S in $CO_2$ (short arc welding) this transfer occurs at the moment of short circuiting of arc gap. In other types of controllable transfer the process is realized with consid-
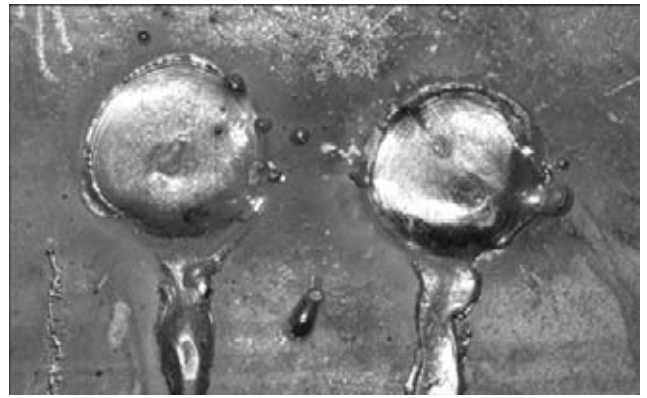


**Figure 1.** Appearance of spot during welding in the vertical plane with flowing out of molten metal and non-uniform formation of spot joint

erable power consumption and should be solved by other complex of equipment combining pulse algorithms of welding current source and pulse mechanism of electrode wire feed.

The cycle of producing a spot joint can be largely split up into two stages: burnout of metal being welded on at the increased process conditions, and formation of a spot joint.

The second stage of spot joint welding was tested on the stand using pulse electrode wire feed. The purpose of experimental investigation was revealing the possibility of stabilization of making of a spot joint in vertical plane in this welding method. Here, one of the basic tasks to be solved was the determination of parameters of a pulsed feeding, the most sufficiently influencing the process and optimization of the most important characteristics of a spot joint, possibility of their multiple reproduction at minimal deviations in sizes and penetration.

For the work the combinations of steels St3 and 09G2S of 1.0 + 4.0 and 2.5 + 7.0 mm thickness, used in transport machine building, were used. The welding was performed using wire Sv-08G2S of 1.2 mm diameter with recommended consumptions of $CO_2$ under conditions: for joining of metals of thickness 1.0 + 4.0 mm the voltage of welding was 26—28 V, the average value of current for all investigated parameters of pulse feeding was 160 A; for joining of metals of thickness 2.5 + 7.0 mm the voltage of welding was 28—30 V, the average value of current was 200 A.
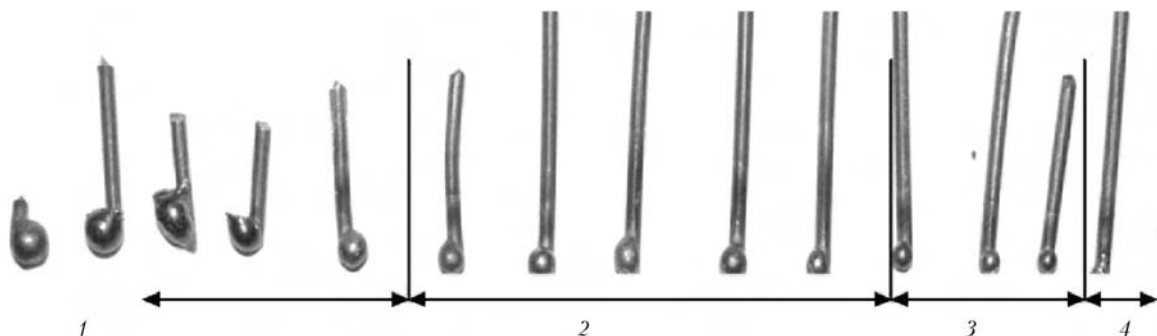


**Figure 2.** Appearance of electrode wire of 1.2 mm diameter with frozen drop at the moment of termination of arc burning: *1, 2* — repeated excitement of arc is difficult; *3, 4* — reliable ignition
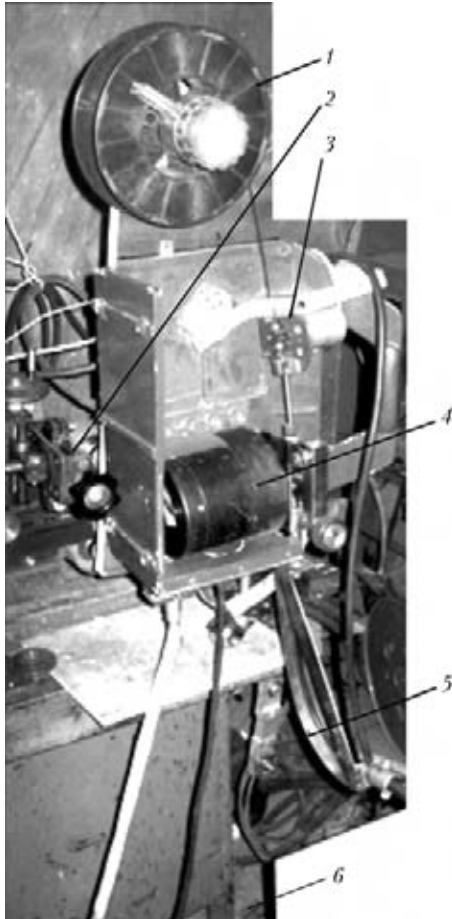
**Figure 3.** Stand for automatic welding of spots in the vertical plane with pulse electrode wire feed: *1* — cassette with electrode wire; *2* — mechanism of torch movement; *3* — sensor of wire feed rate; *4* — wire feed mechanism; *5* — torch for welding in the vertical plane; *6* — product

Figure 4 shows the «perfect» cycle pattern of a pulsed feeding. Basing on the gained experience of application of the pulse electrode wire feeding [10] the following adjustable parameters were used: frequency, relative pulse duration, pitch, rate of feed in pulse and in reverse of feed. In this case the relative pulse duration in accordance with designations in Figure 4 can be determined by the following relation:
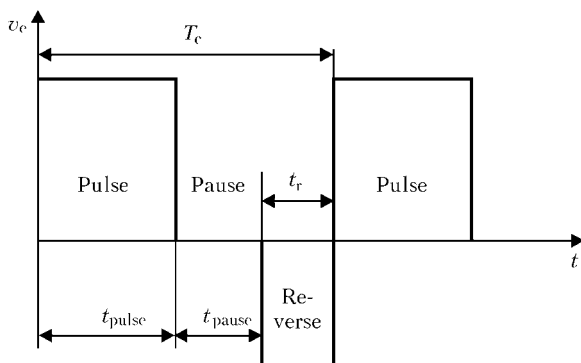


**Figure 4.** «Perfect» cyclogram of pulse feeding: $v_e$ — feed rate; $t_r$, $t_{pulse}$, $t_{pause}$ — time of action of reverse, pulse and pause, respectively; $T_c$ — time of pulse feed cycle
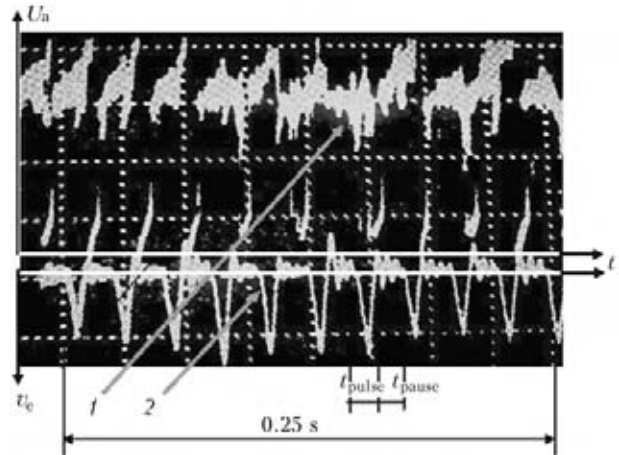


**Figure 5.** Oscillograms of welding process with frequency of pulse electrode wire feed of 40 Hz and relative pulse duration $S = 2$: *1* — $U_a$; *2* — $v_e$

$$S = T_c / t_{pulse}.$$

The influence of frequencies was investigated within the range of 1–10, 20–30 and 40–60 Hz. The experiments were carried out with relative pulse duration $S = 2$ and two variants of changes of a pulse feed of electrode wire: 50 % of time is pulse, 40 % — pause, 10 % — reverse, 50 % of time is pulse, 50 % — pause.

Figure 5 shows characteristic oscillogram with a pulse and pause of ASW process, performed in the vertical plane at frequency of a pulsed feeding of 40 Hz and relative pulse duration $S = 2$. The analysis of oscillograms evidences about high degree of stability of transfer process (one pulse of feed is one drop of electrode metal) and, consequently, about stability of the process as a whole.

At the frequencies in the range of 1–10 Hz it was not possible to obtain the process with formation of a weld spot, as the intensive spattering and leaks of metal from the molten pool were observed. At the frequencies of 20–30 Hz the welding process was more controllable, weld spot is formed, but rather intensive spattering of electrode metal and pool metal occurs. The most quality formation of weld spot was obtained at the frequencies in the range of 40–60 Hz, and at the frequency of 60 Hz the welding process has the best values with minimal (not more than 2–3 %) value of spattering. The result of this algorithm of functioning of controllable pulse feeding mechanism is a repeated number of spots without leaks of metal given in Figure 6. The spots of 12 mm diameter were obtained with a good appearance, deviations of not more than ±0.7 mm and stable guaranteed penetration of base metal providing the required mechanical properties of the welded joint (shear, tear strength, etc.). The destructing shear force for the thickness of specimens being joined 1.0 + 4.0 mm was 14,600–16,000 N, tear force — 12,450–14,700 N, diameter of nugget of weld spot was 5.2 mm; for thicknesses 2.5 + 7.0 mm the shear strength was within 16,900–22,000 N, tear

**Figure 6.** Appearance of spots produced by pulse electrode wire rate at 40 Hz frequency



**Figure 7.** Transverse macrosection of spot of welded joint of sheets 2.5 + 7.0 mm thick at the frequency of pulse electrode wire feed of 60 (*a*) and 40 (*b*) Hz and relative pulse duration $S = 2$

strength — 15,000—20,000 N, diameter of weld spot nugget was 8.5 mm. Geometric sizes of spot joints meet the GOST 14776—79 («Arc welding. Spot welded joints. Main types, design elements and sizes»).

Unsatisfactory running of spot welding process at the frequencies of up to 20 Hz can be explained not by a value of frequency as itself, but by excessively large pitch of electrode wire feed, which is inevitable from the conditions of providing the preset integral feed rate and, consequently, by the average current of arc process which is provided by the new development of applied modern computerized valve electric drive.

The important condition for application of electrode wire pulsed feed is the repeated excitement of arc at technological interruption of the process (additional low-frequency control of heat inputs into the pool). This is possible at such form of a metal drop which is presented in Figure 2, pos. *3* and *4*.

It should be noted that in the process of work the levels of direct consumptions of electric power for conduction of welding process were recorded. Moreover, these consumptions were compared for the process with a conventional electrode wire feed at the same electrode wire consumption. It was determined that at the frequency of pulse feed of 40 Hz and $S = 2$ the direct saving of electric power is 15—20 %, and it is obvious that in these ranges the decrease of heat input into the pool of molten metal occurs, which is an important factor for this work.

The influence of parameters of a pulsed feeding on the formation of a welded joint and penetration can be evaluated on macrosections of a cross section of weld spots given in Figure 7.

The further investigations in this direction are connected with other ranges of thicknesses of material being welded, application of wider variety of parameters of a pulse feed and welding conditions basing on the methods of mathematical design of experiments.
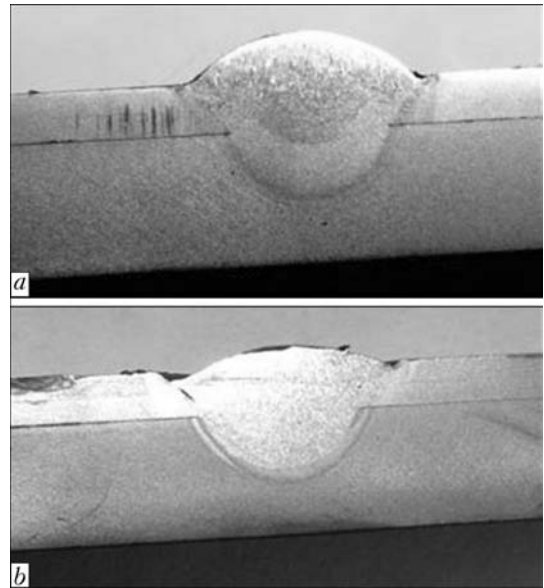
The further modernization of ASW technology, including that in the vertical plane, is connected with new types of equipment and possibilities of producing combined pulse effects. In the work [11] the possibilities of influence on the arc mechanized welding process of a combined pulse effect from a pulse mechanism of electrode wire feed and pulse welding current source with pulse current components in output voltage on the process of arc mechanized welding were analyzed. Previously the technical realization of this welding method could not be completely realized as far as during design of equipment for this solution fulfillment several rather complicated problems arise, especially among them are control of parameters of pulses for effective influence on a molten drop and also establishment and maintaining of sequence of pulse coming from a feeding mechanism and source.
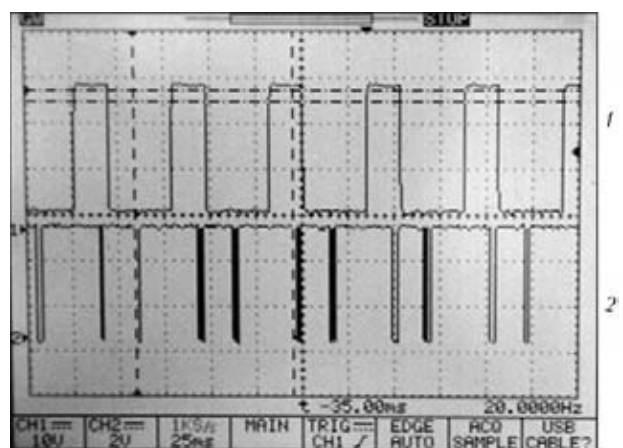


**Figure 8.** Oscillograms of synchronous formation of pulses of electrode wire feed mechanism (*1*) and welding current source (*2*) for combined effect on electrode metal transfer

The new types of gearless mechanisms of electrode wire feeding and modern welding current sources of inverter type with adjustable parameters of pulse effects, development of special software and a number of special technical means mentioned in this work allow solving these tasks providing new opportunities in welding.

In Figure 8 the oscillograms of pulse output effects from a feed mechanism and source are presented, algorithmically matched by parameters and phase shear relatively one another.

## CONCLUSIONS

1. The producing of spot overlap joint using thin electrode wire in $CO_2$ is connected with a number of difficulties (unsatisfactory weld spot formation, flowing of base and electrode metals, low repeatability of results), predetermined both by possibilities of the process itself as well as difficulties of preparation of a structure for welding (pressing of sheets in the place of spot arrangement).

2. The pulse electrode wire feeding in $CO_2$ welding of steels by spots of overlap joints in the vertical has a significant influence on stabilization of the process, welded joint formation, its repeatability, considerably improving these characteristics of the process at optimally selected parameters of a pulse feeding.

3. The carried out investigations, proved by experimental verification, show that a method of producing weld spot joints with a pulse electrode wire feeding can be offered for application in industrial production of welded structures already at this stage and will be continued to study the range of conditions, parameters and combinations with other technological solutions.

4. The further modernization of ASW technology and also stabilization of electrode metal transfer is the combination of processes of a pulse electrode wire feed with a superposition of current pulses.

1. Potapievsky, A.G. (2007) *Consumable electrode gas-shielded welding*. Pt 1: Welding in active gases. 2nd ed. Kiev: Ekotekhnologiya.
2. Lebedev, V.A. (2010) Tendencies in development of mechanized welding with controlled transfer of electrode metal (Review). *The Paton Welding J.*, **10**, 37–44.
3. Lebedev, V.A., Gedrovich, A.I. (2010) *Technique and technology of arc welding and surfacing (nonstationary processes and operating conditions)*. Lugansk: Knowledge.
4. Lobanov, L.M., Timoshenko, A.N., Goncharov, P.V. (2009) Arc spot welding of overlap joints in vertical position. *The Paton Welding J.*, **1**, 26–28.
5. Pekoz, T., McGuire, W. (1980) Welding of sheet steel. In: *Proc. of 5th Int. Spec. Conf. on Cold-Formed Steel Structures* (St.-Louis, 1980).
6. Snow, G.L., Easterling, W.S. (2008) Strength of arc spot welds made in single and multiple steel sheets. In: *Proc. of 9th Int. Spec. Conf. on Cold-Formed Steel Structures* (St.-Louis, 2008).
7. Makhnenko, O.V., Timoshenko, A.N., Muzhichenko, A.F. et al. (2010) Improvement of the technology for arc spot welding of overlap joints based on the results of mathematical modeling. *The Paton Welding J.*, **11**, 21–26.
8. Lebedev, V.A., Rymsha, V.V., Radimov, I.N. (2009) Current valve electric drives in systems of mechanized welding equipment. *Elektromashynobud. ta Elektrooblad.*, Issue 74, 22–24.
9. Paton, B.E., Lebedev, V.A., Pichak, V.G. et al. (2002) Analysis of technical and technological possibilities of electrode wire pulsed feed in processes of arc welding and surfacing. *Svarochn. Proizvodstvo*, **2**, 24–31.
10. Lebedev, V.A. (2007) Peculiarities of welding of steels with pulsed feed of electrode wire. *Ibid.*, **8**, 30–35.
11. Paton, B.E., Lebedev, V.A., Mikitin, Ya.I. (2006) Method of combined control of electrode metal transfer in mechanized arc welding. *Ibid.*, **8**, 27–32.

# EFFECT OF STRUCTURAL-PHASE TRANSFORMATIONS IN ALUMINIUM-LITHIUM ALLOY 1460 JOINTS ON PHYSICAL-MECHANICAL PROPERTIES

**L.I. MARKASHOVA, A.Ya. ISHCHENKO, O.S. KUSHNARYOVA** and **V.E. FEDORCHUK**

E.O. Paton Electric Welding Institute, NASU, Kiev, Ukraine

Analysis of experimental data on evaluation of mechanical properties of the alloy joints was performed by taking into account the weld metal composition, grain and sub-grain sizes, real dislocation density, volume content of phase precipitates, etc. The effect of each of the specific structural-phase parameters on mechanical characteristics of the welded joints and their change under the influence of postweld heat treatments and external loading was determined.

***Keywords:*** *heat treatment, weld metal, aluminium alloy, scandium, fine structure, phase precipitates, dislocation density, composite phase precipitates*

At present there is a growth of commercial demand for materials with special properties. Especially this applies to super-light materials used in aircraft and aerospace engineering, where it is necessary to ensure the sufficient level of specific strength, ductility and crack resistance under complex service conditions [1, 2]. Such materials include, in particular, aluminium-lithium alloys, which are characterised by a high technological effectiveness and the required level of properties at cryogenic and increased temperatures.

However, some important properties of Al−Li alloys dramatically change during fabrication and operation of structures, which is related primarily to special structural-phase transformations occurring in these materials in the course of different technological operations [2, 3], including under the effect of the welding process. As to Al−Li alloys with scandium additions, in this case their phase composition may become even more complicated, since alloys of this type belong to materials that are susceptible to ageing and feature, as a rule, a special complexity of phase transformations occurring under a thermal effect, including heat treatment [4, 5]. It is significant from this standpoint that mechanical properties of alloys of this type also change under the effect of heat treatment, this being related to the impact of structural factors [2, 4−8] (Table).

Therefore, allowing for a complex structural state of this type of materials, and particularly for the phase formation processes under various thermal-deformation impacts, it is important to evaluate the effect of specific structural-phase components on changes in mechanical characteristics of the welded joints that are most significant for service conditions, i.e. strength and toughness values.

It is of interest to investigate the effect of structure of metal of the welded joints on the character of its deformation under external loading, i.e. the effect of structural and phase components on the processes of accumulation of internal stresses and the probability of their plastic relaxation, which is an indicator of crack resistance of the deformed material.

To address the tasks posed, first of all it is necessary to have the comprehensive experimental data base, giving a real view of the structural-phase state of an investigated material, which is formed by using the technological welding parameters, as well as of the changes in this state under conditions of postweld heat treatments and external loading.

The basic experimental information on the structural-phase state of the weld metal of the joints on aluminium alloy 1460 (Al−3 % Cu−2 % Li−0.08 % Sc) welded by using filler wire Sv1201 (Al−6.5 % Cu−0.25 % Zr−0.3 % Mn) with 0.5 % Sc and without it, which is required for analytical evaluation of mechanical properties of the materials studied, was generated from the investigations conducted at the following

Mechanical properties of metal of the joint on alloy 1460 welded by using filler wires Sv1201 and Sv1201 + Sc in the as-welded state and after heat treatment

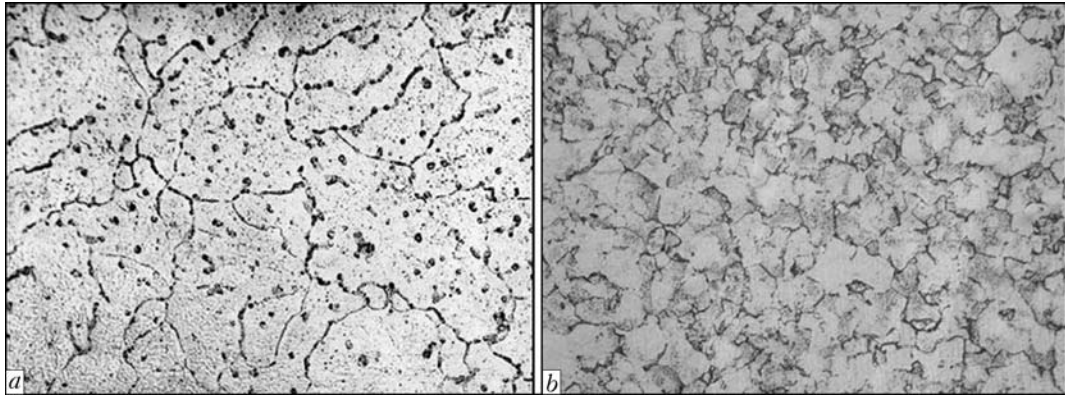| Type of treatment | Sv1201 | | | Sv1201 + Sc | | |
|---|---|---|---|---|---|---|
| | $\sigma_t$, MPa | $\sigma_{0.2}$, MPa | *HRB* | $\sigma_t$, MPa | $\sigma_{0.2}$, MPa | *HRB* |
| As-welded | 250.0 | 175.0 | 75.0 | 282.2 | 189.6 | 81 |
| After artificial ageing ($T$ = 150 °C, $t$ = 22 h) | 316.0 | 281.5 | 78.0 | 337.0 | 240.3 | 85 |
| After annealing ($T$ = 350 °C, $t$ = 1 h) | 248.2 | 204.3 | 71.7 | 345.5 | 295.0 | 92 |

**Figure 1.** Microstructure (×500) of weld metal of the joint on alloy 1460 welded by using filler wires Sv1201 (*a*) and Sv1201 + 0.5 % Sc (*b*)

stages: immediately after argon-arc welding (*I*), after postweld heat treatments (*II*) (artificial ageing at $T = 150$ °C, $t = 22$ h, and annealing at $T = 350$ °C, $t = 1$ h), and after external dynamic loading (*III*). The comprehensive investigations, including chemical analysis of metal of the welded joint, character of the grain, sub-grain and dislocation structure, as well as phase precipitates of complex composition, morphology and distribution at different stages of their formation, were carried out by using optical, analytical scanning microscopy (SEM-515, «Philips», the Netherlands), as well as microdiffraction transmission electron microscopy (JEM-200CX, JEOL, Japan) with an accelerating voltage of 200 kV. Thin foils for transmission microscopy were prepared by the method of ion thinning with ionised argon flows in a specially developed unit [9].

The following was established as a result of preliminary investigations [10–12]. No special differences in distribution of chemical elements in the weld metal were detected during the solidification process (as-welded state) at the absence of scandium in filler wire (*I*) and with scandium added to filler wire (*II*). A complex saturated solid solution of main alloying elements of copper and lithium was formed in both cases, the weight content of copper being minimal at the centre of grains and increasing to some extent towards the grain boundaries. However, the characteristic feature of alloying with scandium was formation of isolated scandium segregations (0.06–0.80 %).

Changes in grain structure were more substantial — alloying with scandium led to a considerable (two-times) refinement of the grain structure (Figure 1). More substantial differences were noted also in the character of fine structure. Whereas the weld metal without addition of scandium (*I*) was characterised by a comparatively uniform distribution of dislocations (Figure 2, *a*) at their low density (approximately $(2–5) \cdot 10^9$ cm$^{-2}$), in the case of scandium additions (*II*) the density of dislocations grew by an order of magnitude (from $6 \cdot 10^9$ to $(5–6) \cdot 10^{10}$ cm$^{-2}$) and their distribution was irregular (Figure 3, *a*, *b*), the tendency being to formation of intragranular, slightly disoriented sub-structures.

As to the phase formation processes, formation of phases of rather big sizes (more than 1–2 μm) (complex conglomerates of the Al–Cu and Al–Li phases), as well as phases of more dispersed sizes (Zr- and Li-containing phases) was fixed in both cases in the bulk of grains in the as-welded state.

However, the most characteristic peculiarity (refers to the Sc-containing states) was formation of a special type of structures, i.e. the Guinier–Preston (GP) zones, in the Sc-containing weld metal, the said zones looking like dense dislocation loops (see Figure 3, *a*) distributed in the segregation clusters of scandium, which was most probably related to the initial stages of decomposition of solid solution.

Some differences in structure of the grain boundaries were fixed also in the as-welded state for the investigated cases of alloying of the weld metal. For instance, fairly wide (approximately 0.1–0.4 μm) interlayers consisting of dense clusters of the globular lithium phases were clearly seen along the grain boundaries at the absence of scandium additions (see Figure 2, *b*). In addition, also characteristic is appearance of extended grain-boundary eutectic formations: either complex phases of Al–Cu type, or conglomerate of phases of Al–Cu, Al–Li type, the composition of grain boundary eutectics being similar to that of coarse intragranular phase precipitates (Figure 2, *a*).

The weld metal in the case of alloying with scandium was characterised by differences both in structure of the grain boundaries proper and in phase formation in this zone. For instance, phases of a different type (Al$_3$Li, Al$_3$Sc) and of a smaller size formed in the grain boundary zones (Figure 3, *b*).

The grain boundary eutectics characterised by non-uniform sizes and morphologies were also much different. Moreover, along with dense, monolithic eutectic formations, which are more typical of a case of the absence of scandium, increase in volume of friable eutectics with inclusions of the dispersed Sc-containing phases was fixed (Figure 3, *a*).

Investigations of the state of the weld metal after heat treatment ($T = 350$ °C, $t = 1$ h) showed a more active redistribution of chemical elements and a change in structure (see Figure 1) independently of

**Figure 2.** Fine structure of weld metal of the joint on alloy 1460 welded by using filler wire Sv1201 in the as-welded state (*I*), after heat treatments at $T = 150$ °C, $t = 22$ h (*II*) and at $T = 350$ °C, $t = 1$ h (*III*): *a* — extended grain-boundary eutectics (phases of the Al−Cu type) (×30,000); *b* — precipitation of phases of the Al−Li type along grain boundaries (×30,000); *c*, *d* — distribution of dislocations and dispersed phases, respectively, in the bulk of grains (×30,000) and along the grain boundaries (×20,000); *e* — decrease in density of distribution of phases (θ′, δ′) and dislocations in near-boundary PFZ (×50,000); *f* — eutectics at the grain boundaries (×20,000)

the type of filler wire, this most probably being caused by the processes of decomposition of solid solution and subsequent formation of new phases. In addition, in a case of the presence of scandium there was a marked increase in general density of dislocations and activation of the processes of their redistribution. The latter is likely to be caused by a considerable violation of coherency of the matrix−phase precipitations lattices related to intensification of the phase formation processes during heat treatment, alloying in this case, which leads to an even more intensive refinement of not only the grain structure but also of the sub-structure, i.e. blocks and sub-grains (Figure 3, *e*, *f*). Moreover, activation of the phase formation processes after heat treatment, when using the indicated types of the fillers, is confirmed by a considerable increase in volume content of the intragranular phase precipitates

of both medium (0.2−0.5 μm) and finer (approximately 0.01−0.03 μm) sizes.

With a change in alloying, the differences could be seen also in structure of the grain boundaries after heat treatment. For example, expansion and structural complication of the grain boundary regions after heat treatment ($T = 350$ °C, $t = 1$ h) were detected in the Sc-free weld metal. Formation of the extended grain-boundary zones free from phase precipitates (PFZ), which were also characterised by a substantial decrease in the dislocation density, was fixed, in addition to the zones with dense layers of the Li-containing phases. As a result, the PFZ regions were a laminated, grain boundary interlayers directed along the boundaries, characterised by a dramatic gradient of the dislocation density and the presence of phases (see Figure 2, *a*).
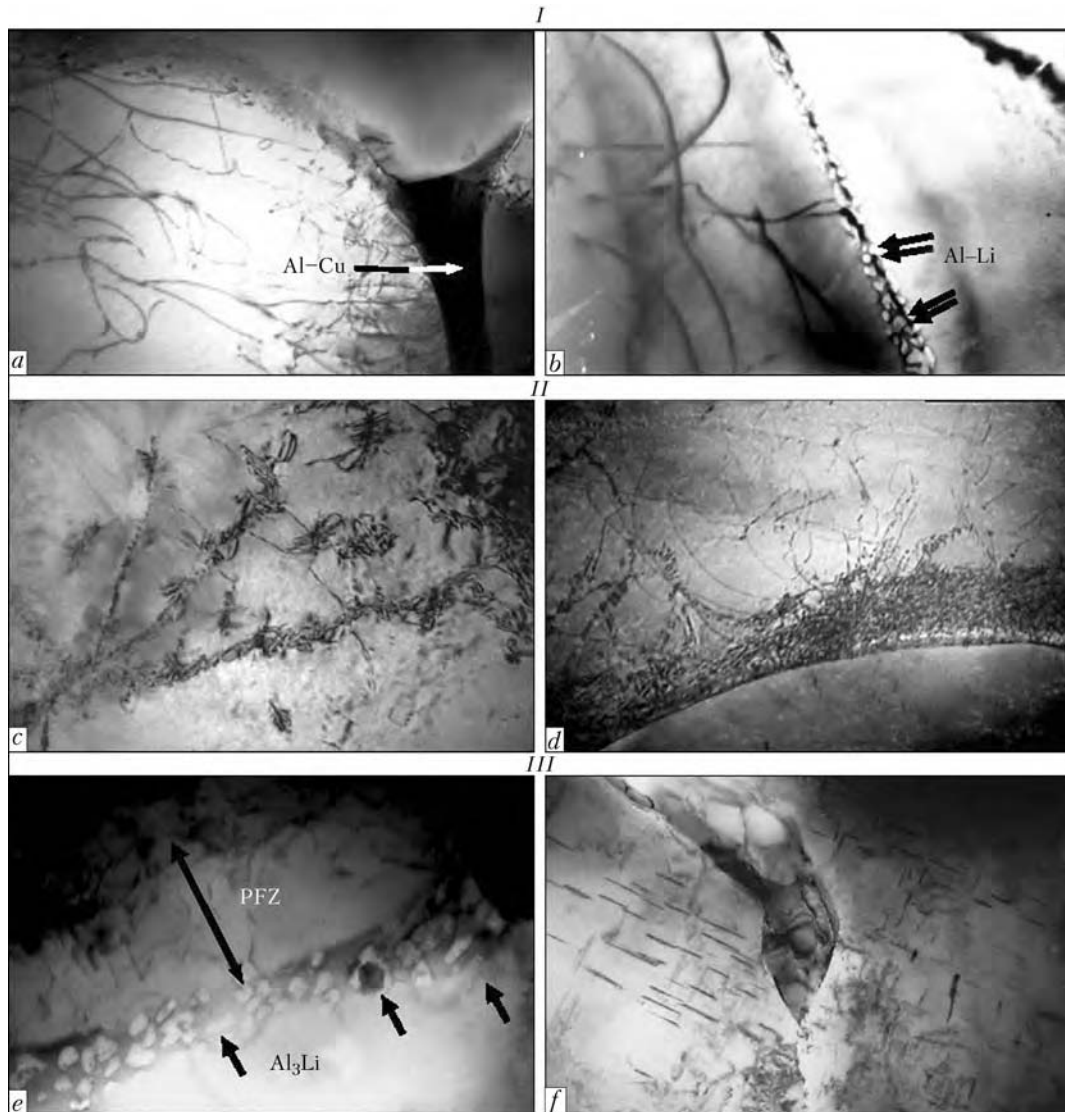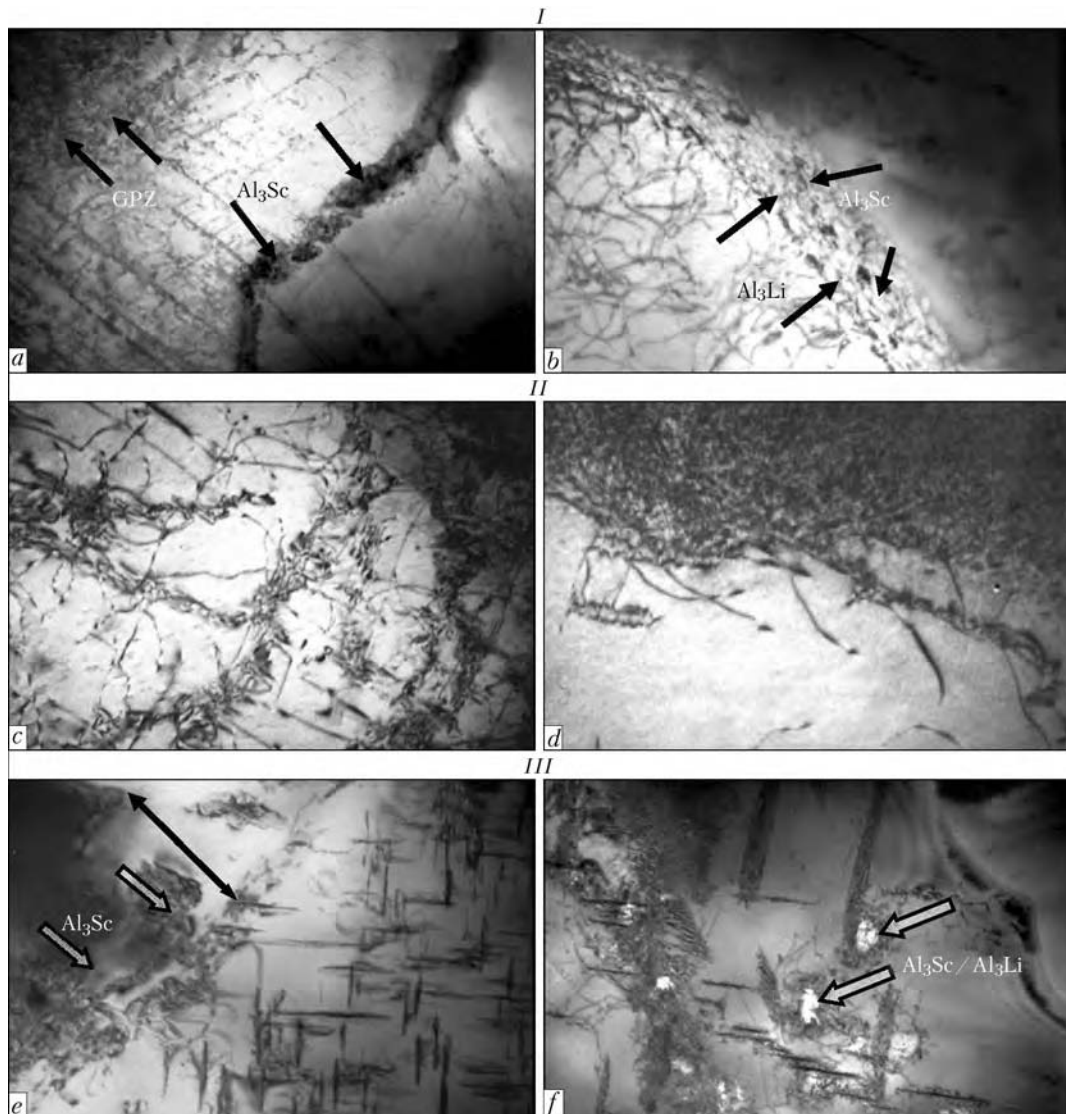
**Figure 3.** Fine structure of weld metal of the joint on alloy 1460 welded by using filler wire Sv1201 + Sc in the as-welded state (*I*), after heat treatments at $T$ = 150 °C, $t$ = 22 h (*II*) and at $T$ = 350 °C, $t$ = 1 h (*III*): $a$ — segregation and phase precipitates in grain boundary zones of weld metal of the Al–Cu type with scandium additions (×20,000); $b$ — precipitation of Al–Li phases along grain boundaries (×37,000); $c$, $d$ — distribution of dislocations and ultra-dispersed phases in the bulk of grains (×30,000) and along the grain boundaries (×37,000); $e$ — filling of PFZ along the grain boundary with phase precipitates $Al_3Sc$ (×30,000); $f$ — distribution of Sc- and Li-containing phases in the bulk of grains (×30,000)

In the case of an addition of scandium to the weld metal, firstly the grain boundary structure lost some of its density, i.e. the boundaries became more friable, and secondly, the volume content of the Li-containing phases along the grain boundaries substantially decreased, while the phase precipitates forming during heat treatment filled up (or made much narrower) the PFZ region adjoining the grain boundaries (Figure 3, *f*), this leading to levelling of the negative effect of this zone clearly defined at the absence of scandium.

As far as the grain boundary eutectic formations are concerned, whereas massive eutectics for the Sc-free weld metal were more stable (both in the as-welded state and after heat treatment), in the weld metal with scandium additions the eutectic during heat treatment became much more friable and decomposed into separate isolated phase formations, this leading to substantial refinement of the individual

phases forming the eutectic, while a number of dispersed phase precipitates in the eutectic lost their clear outlines, this evidencing occurrence of the active processes of their diffusion dissolution.

The experimental results obtained at different structural levels, i.e. from the macro- (grain) to microlevel (dislocation), allowed analytical evaluation of the specific (differentiated) contribution made by different structural-phase parameters (phase composition, grain and sub-grain sizes, dislocation density, etc.) under corresponding thermal-deformation conditions to a change in total (integrated) values of mechanical properties, i.e. strength, ductility and crack resistance.

Evaluation of the total value of increment in yield stress $\Sigma\sigma_y$ for the weld metal of the investigated alloy (without and with scandium), allowing for chemical composition (solid solution strengthening $\Delta\sigma_{ss}$), real
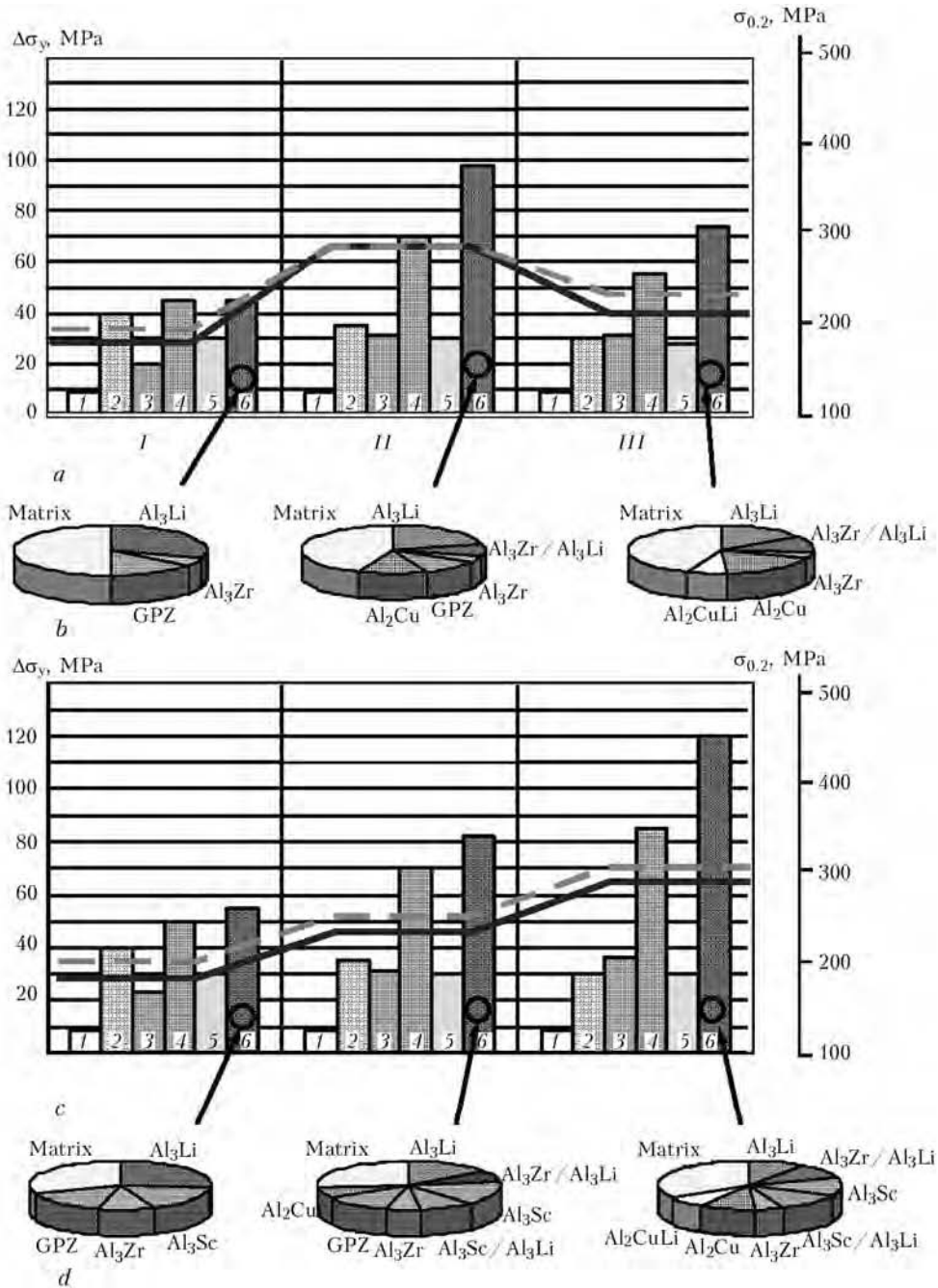
**Figure 4.** Histograms (*a*, *c*) of differentiated contribution of individual structural $\Delta\sigma_y$ parameters to the total (integrated) change of yield stress $\Sigma\sigma_y$ of the 1460 alloy weld metal obtained by using filler wires Sv1201 (*a*) and Sv1201 + 0.5 % Sc (*c*), and sector diagrams of volume content of the phases forming under the investigated conditions (*b*, *d*): *I* — as-welded; *II*, *III* — after heat treatments at $T = 150$ °C, $t = 22$ h, and at $T = 350$ °C, $t = 1$ h; solid line — $\sigma_{0.2}$; dashed line — $\sigma_y$; *1* — $\Delta\sigma_0$; *2* — $\Delta\sigma_{ss}$; *3* — $\Delta\sigma_g$; *4* — $\Delta\sigma_s$; *5* — $\Delta\sigma_d$; *6* — $\Delta\sigma_p$

dislocation density (dislocation strengthening $\Delta\sigma_d$), grain strengthening $\Delta\sigma_g$, sub-grain strengthening $\Delta\sigma_s$, particles of phase precipitates $\Delta\sigma_p$, etc., was made by using the Hall–Petch, Orowan and other similar relationships [13–17].

As seen from Figure 4, the total value of yield stress $\Sigma\sigma_y$ of the weld metal and the specific contribution of different $\Delta\sigma_y$ structural factors to the said characteristic vary depending on the process conditions (welding, heat treatment) and alloying. For instance, for the weld metal (compared to alloying with scandium and without it) a higher level of increment

of strength characteristics $\sigma_y$ was detected, i.e. approximately by 20 (10 %) and 85 MPa (26 %) higher in the as-welded state and after heat treatment ($T = 350$ °C, $t = 1$ h).

The maximal contribution to strengthening $\Delta\sigma_y$ is made by phase formations (approximately by 40 %), and the minimal contribution — by dislocation density (by about 10 %) (see Figure 4).

Specific information on the contribution to strengthening made by other structural factors for the investigated weld metal compositions under the considered conditions is given in Figure 4.
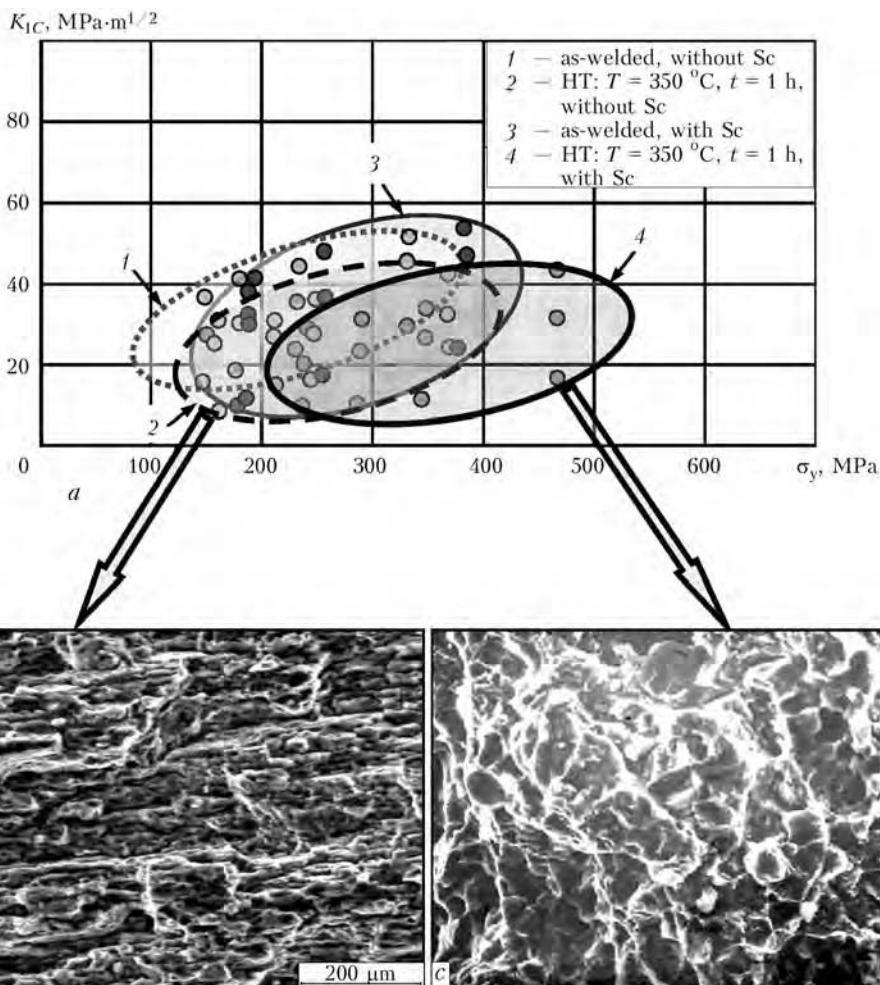
**Figure 5.** Diagram of changes in values of $\Sigma\sigma_y$ and fracture toughness $K_{1C}$ of weld metal of the welded joint on alloy 1460 without scandium in the as-welded state (*1*) and after heat treatment at $T = 350$ °C and $t = 1$ h (*2*), as well as in the as-welded state with scandium (*3*) and after heat treatment of the Sc-containing weld metal performed by using the said parameters (*4*): *a* — character of fracture of the weld metal under external dynamic loading conditions; *b* — quasi-brittle fracture of metal (Sv1201); *c* — tough fracture (Sv1201 + 0.5 % Sc) with the clearly defined pit-like structure
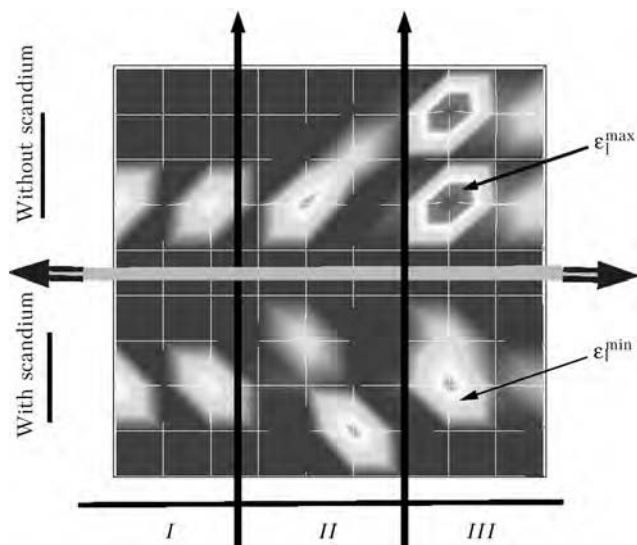


**Figure 6.** Diagrams of distribution of $\varepsilon_l$ deformation localization zones in the 1460 alloy weld metal obtained by using filler wires Sv1201 and Sv1201 + Sc in the as-welded state (*I*) and after heat treatment at $T = 150$ °C, $t = 22$ h (*II*) and at $T = 350$ °C, $t = 1$ h (*III*)

The effect of structural factors on changes in parameters of fracture toughness $K_{1C}$ of the weld metals with different types of alloying was evaluated as well (Figure 5, *a*). The $K_{1C}$ value was determined from the Krafft relationship: $K_{1C} = (2E\sigma_y d_f)^{-1/2}$ [18], which includes experimental data of fractographic analysis of fractures, where $d_f$ is the size of facets or pits on the fracture surface, the value of which is equated to the value of critical crack opening displacement $\delta_c$; $E$ is the Young modulus; and $\sigma_y$ is the calculated strengthening. As shown by analysis of the results, whereas fracture toughness parameter $K_{1C}$ of the weld metal in the as-welded state for the investigated alloying cases (without and with scandium) hardly changes with increase in the level of $\sigma_y$ and equals approximately 35–36 MPa·m$^{1/2}$ (see Figure 5), in heat treatment ($T = 350$ °C, $t = 1$ h) the character of alloying does affect $K_{1C}$. An approximately 20 % decrease in the fracture toughness parameter was fixed at the absence of scandium, whereas in alloying with scandium, although there is an increase in strength characteristics, fracture toughness parameter $K_{1C}$ hardly changes, this indicating to a good combination
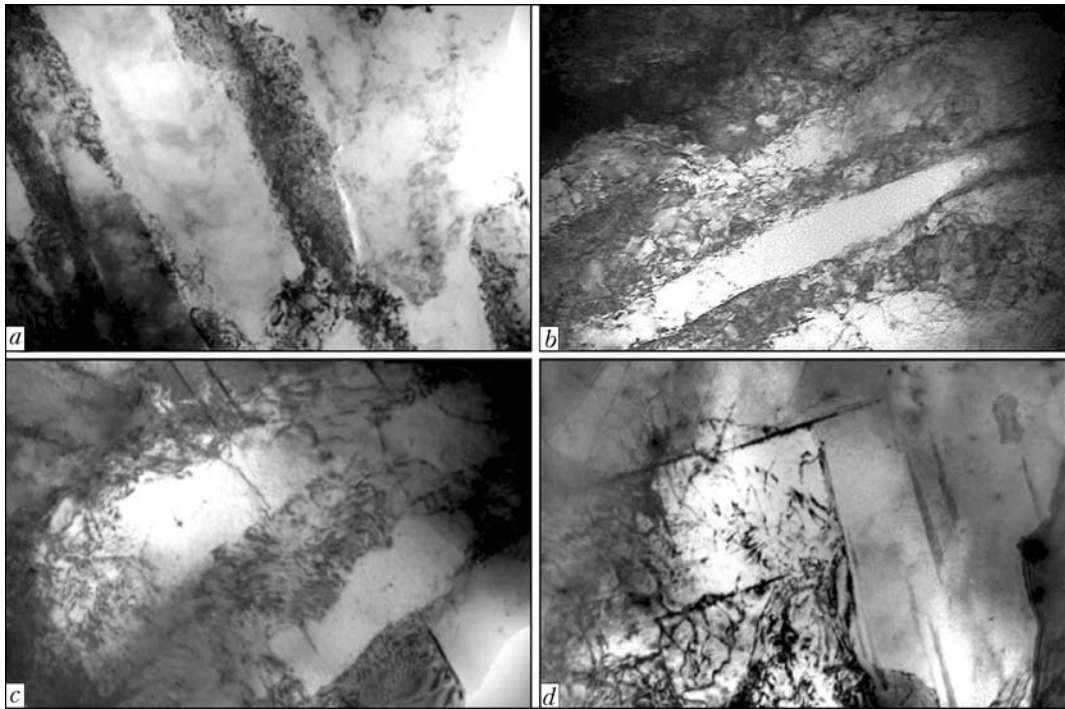
**Figure 7.** Changes in fine structure of heat-treated ($T$ = 350 °C, $t$ = 1 h) weld metal on alloy 1460 under conditions of dynamic loading depending on the alloying method (without and with scandium): $a$, $b$ — intensive SBs in metal without scandium (×20,000 and ×30,000, respectively); $c$, $d$ — fragmentation of structure due to blocking of SBs by the scandium phases in Sc-containing metal (×30,000)

of strength and ductile characteristics of the weld metal (see Figures 4 and 5, $a$).

As to such mechanical characteristic as crack resistance, here very significant is the character of changing of the structural state of the investigated material under external loading, especially under extreme conditions, i.e. dynamic external loadings for the welded joint with and without scandium, which was evaluated by transmission examinations of fine structure.

Examinations of the fine structure showed that, firstly, a non-uniform distribution and clearly defined

localisation of deformation $\varepsilon_l$ in microvolumes of metal take place in the Sc-free weld metal after heat treatment ($T$ = 350 °C, $t$ = 1 h) and subsequent dynamic loading (Figure 6). Secondly, the deformed metal acquires an unstable (meta-stable) structural state, which shows up in an avalanche-like barrier-free metal flow, this being evidenced by the presence of intensive slip systems and shear bands (SB) (Figure 7, $a$, $b$). Moreover, substantial non-uniformity in distribution of dislocation density $\rho$ along SB is fixed in this case, where $\rho \sim 10^8{-}2{\cdot}10^9$ cm$^{-2}$ (region inside SB) and $\rho \sim 8{\cdot}10^{10}{-}2{\cdot}10^{11}$ cm$^{-2}$ (directly along the band bounda-
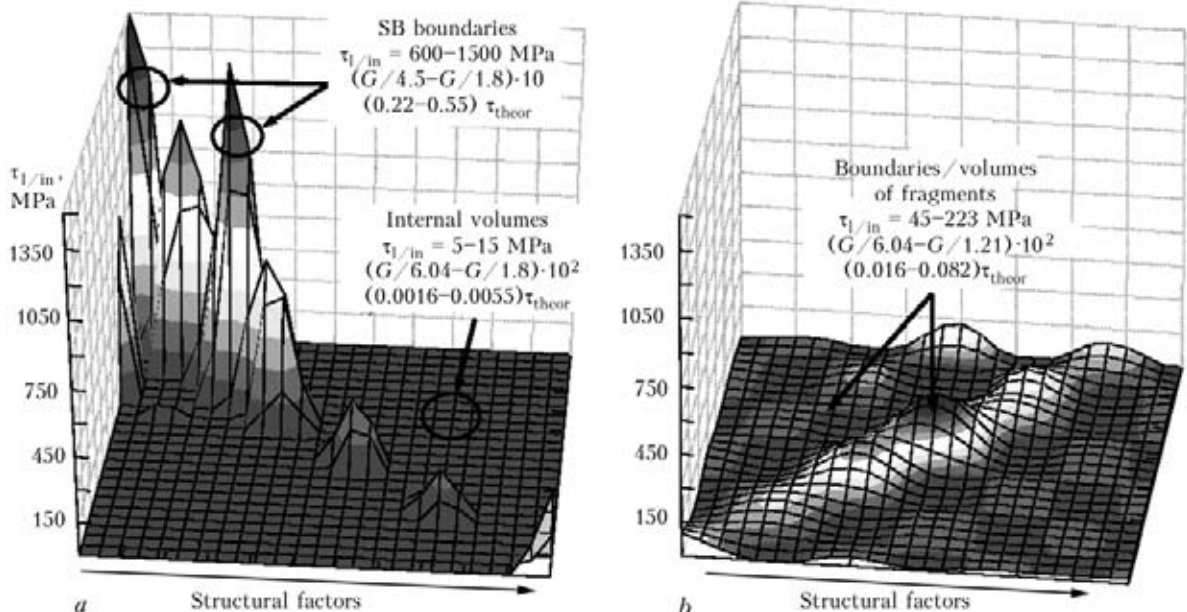


**Figure 8.** Distribution of local internal stresses $\tau_{l/in}$ in weld metal of the Sv1201 ($a$) and Sv1201 + 0.5 % Sc ($b$) types (heat treatment at $T$ = 350 °C, $t$ = 1 h) after external dynamic loading
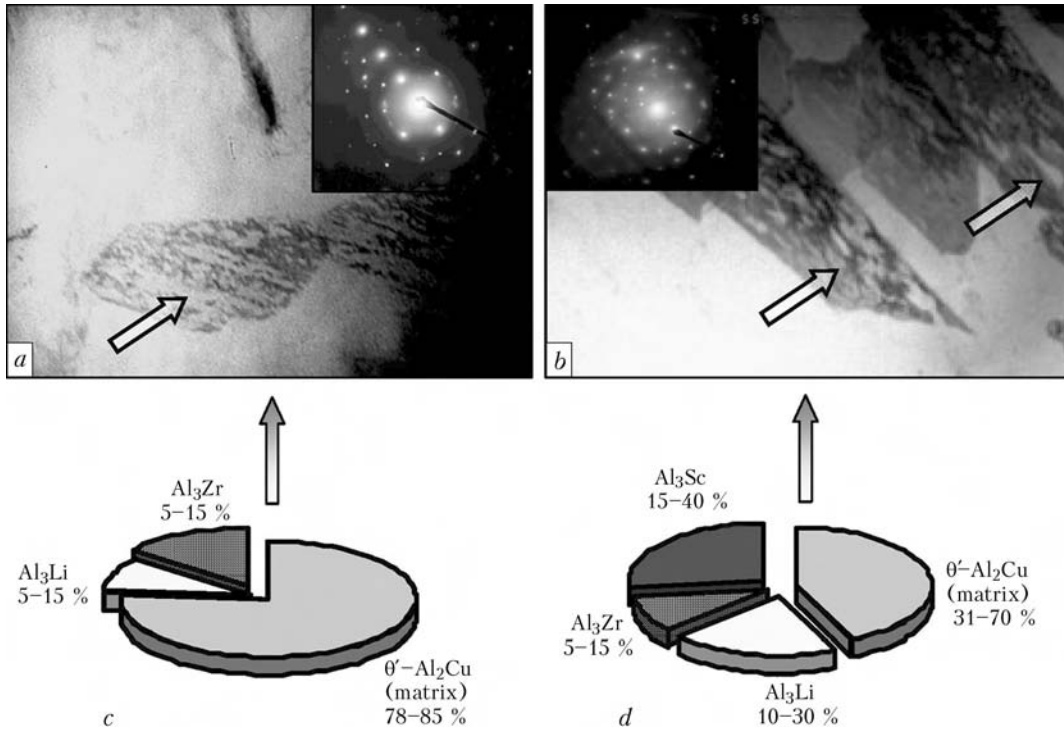
**Figure 9.** Changes (under heat treatment conditions at $T = 350$ °C, $t = 1$ h) in structure ($a$, $b$ — ×50,000) and composition ($c$, $d$) of θ'-phase formations in weld metal of the welded joint on alloy 1460 depending on the method of alloying without ($a$, $c$) and with ($b$, $d$) scandium

ries). The latter leads to dramatic gradients in the level of local internal stresses $\Delta\tau_{l/in}$ within the zone of contact of boundaries of the band structures and their internal volumes. As shown as a result of estimation of $\tau_{l/in}$ from the Konrad and Stroh relationships, allowing for the dislocation density [19], and comparison of these values with theoretical strength $\tau_{theor}$ of the material, the band boundaries are extended local raisers of internal stresses, where $\tau_{l/in}$ is 600–1500 MPa ($G/4.5–G/1.8)\cdot10$, this corresponding to $(0.22–0.55)\tau_{theor}$. Here $\tau$ is the shear modulus. In contrast to this, in the internal volumes of SBs the values of $\tau_{l/in}$ dramatically decrease (almost by two orders of magnitude) to a level of about 5–15 MPa (($0.0016–0.0055)\tau_{theor}$) (Figure 8, $a$). Thus, dramatic extended gradient $\Delta\tau_{l/in}$ of local internal stresses forms along the shear bands, i.e. $\Delta\tau_{l/in}$ corresponds to $0.55\tau_{theor}$ (SB boundaries)–$0.0055\tau_{theor}$ (SB volume).

Therefore, the directed local flow in the weld metal (at the absence of scandium) that leads to formation of extended raisers of internal stresses, combined with a directed dramatic gradient of such stresses along the SB boundaries, is a cause of cracking and, hence, decrease in level of not only strength and also ductility of the joints, which is proved also by a laminated character of microrelief of the surface with elements of quasi-brittle fracture of the weld metal (see Figure 5, $a$).

In the case of alloying with scandium a different type of structure forms in the weld metal under similar conditions of dynamic loading, this structure being characterised by a uniform distribution of dislocations and general refinement (fragmentation) of structure

(see Figure 7, $c$, $d$). Stable blocking of the forming slip systems by phase precipitates of a special type, i.e. phases of the conglomerate type with Sc-containing components (see Figure 9), is fixed in this case, this leading to fragmentation (dispersion) of structure and a more uniform distribution of internal stresses ($\tau_{l/in} \sim 75$ MPa or $0.027\tau_{theor}$) in the weld metal (see Figure 8, $b$). Formation of this type of the structures leads also to increase in the probability of plastic relaxation of internal stresses in the weld metal (especially under extreme conditions) due to involvement of additional rotation relaxation mechanisms, which is confirmed by a tough character of fracture of the joints (see Figure 5, $b$).

**CONCLUSIONS**

1. It was established that alloying the weld metal with scandium in argon-arc welding of Al–Li alloy 1460 leads to substantial dispersion of grain structure, increase in dislocation density and activation of the processes of formation of sub-structures and processes of phase formation (mostly Sc-containing phases) in the internal volumes of grains. Heat treatment ($T = 350$ °C, $t = 1$ h) in the case of alloying with scandium promotes levelling of intergranular structures (Li-containing zones, PFZs), which are a problem for the investigated alloys.

2. Analytical evaluations of the specific (differentiated) contribution of different structural-phase parameters to changes in the properties of strength $\Delta\sigma_y$, ductility $K_{1C}$ and crack resistance of the investigated welded joints were made. It was shown that alloying

with scandium leads to increase in the total (integrated) value of yield stress $\Sigma\sigma_y$ of the weld metal by about 20 MPa (10 %) in the as-welded state and by about 85 MPa (26 %) after heat treatment ($T = 350$ °C, $t = 1$ h). The maximal contribution to strengthening $\Sigma\sigma_y$ is made by phase formations (about 40 %), and the minimal contribution — by dislocation density (roughly up to 10 %).

3. Alloying with scandium leads to a more uniform distribution of growing local internal stresses and fragmentation of intensive SBs forming in the weld metal under dynamic loading, which is favourable for crack resistance of the welded joint and leads to increase in relaxation ability of the weld metal due to involvement of the additional (rotation) mechanisms of plastic relaxation to the dislocation ones.

1. Fridlyander, I.N., Chuistov, K.V., Berezina, A.L. et al. (1992) *Aluminium-lithium alloys. Structure and properties*. Kiev: Naukova Dumka.
2. Furukawa, M., Berbon, P., Horita, Z. et al. (1997) Production of ultrafine-grained metallic materials using an intense plastic straining technique. *Mater. Sci. Forum*, **233**/**234**, 177–184.
3. Ryazantsev, V.I., Fedoseev, V.A. (1994) Mechanical properties of welded joints on Al–Cu system aluminium alloys. *Svarochn. Proizvodstvo*, **12**, 4–7.
4. Tsenev, N.K., Valiev, R.Z., Obraztsov, O.V. et al. (1992) Mechanical properties of submicron grained Al–Li alloys. In: *Proc. of 6th Int. Aluminium Conf.* (Germany, Garmisch-Partenkirchen, Oct. 8–10, 1992), 1125–1135.
5. Ball, H.D., Lloyd, D.J. (1985) Particles apparently exhibiting fivefold symmetry in Al–Li–Cu alloys. *Scr. Met.*, **19**, 1065–1068.
6. Gayle, F.W., Vander Sande, J.B. (1984) Composite precipitates in an Al–Li–Zr alloy. *Ibid.*, **18**, 473–478.
7. Gufnghui, M., Huasyun, Y., Delin, P. et al. (2000) Fraction and phase spacing of fibrous intermetallic S-LiAl in hypoeutectic Al–Li alloys by unidirectional solidification. *Metallofizika. Nov. Tekhnologii*, 22(4), 58–61.
8. Furukawa, M., Miura, Y., Nemoto, M. (1987) Temperature and strain rate dependences of yield stress of an Al–Cu–Li–Mg–Zr alloy. *Transact. of JIM*, **28**, 655–665.
9. Darovsky, Yu.F., Markashova, L.I., Abramov, N.P. et al. (1985) Method of preparation for electron-microscopic analyses. *Avtomatich. Svarka*, **12**, 60.
10. Markashova, L.I., Grigorenko, G.M., Ishchenko, A.Ya. et al. (2006) Effect of scandium additions on structure-phase condition of weld metal produced by welding aluminium alloy 1460. *The Paton Welding J.*, **1**, 16–23.
11. Markashova, L.I., Grigorenko, G.M., Ishchenko, A.Ya. et al. (2006) Effect of scandium additions on the fine structure of weld metal in aluminium alloy 1460 welded joints. *Ibid.*, **2**, 20–25.
12. Markashova, L.I., Grigorenko, G.M., Lozovskaya, A.V. et al. (2006) Effect of scandium additions on structure-phase state of weld metal in aluminium alloy joints after heat treatment. *Ibid.*, **6**, 7–11.
13. Konrad, G. (1973) Model of strain hardening for explanation of grain size effect on metal flow stress. In: *Ultrafine grain in metals*. Moscow: Metallurgiya.
14. Petch, N.J. (1953) The cleavage strength of polycrystalline. *J. Iron and Steel Inst.*, 173(1), 25–28.
15. Orowan, E. (1954) *Dislocation in metals*. New York: AIME.
16. Ashby, M.F. (1983) Mechanisms of deformation and fracture. *Adv. Appl. Mech.*, **23**, 118–177.
17. Kelly, A., Nicholson, R. (1966) *Precipitation hardening*. Moscow: Metallurgiya.
18. Romaniv, O.N. (1979) *Fracture toughness of structural steels*. Moscow: Metallugiya.
19. Ivanova, V.S., Gordienko, L.K., Geminov, V.N. et al. (1965) *Role of dislocations in strengthening and fracture of metals*. Moscow: Nauka.

# MICROSTRUCTURAL FEATURES OF FATIGUE DAMAGEABILITY AND METHODS TO IMPROVE THE FATIGUE LIFE OF WELDED JOINTS FROM 09G2S STEEL

**V.D. POZNYAKOV, V.A. DOVZHENKO, S.B. KASATKIN** and **A.A. MAKSIMENKO**

E.O. Paton Electric Welding Institute, NASU, Kiev, Ukraine

The paper presents the results of investigation of the effect of cyclic bend loading on brittle fracture resistance of the HAZ metal, as well as accumulation of fatigue damages and structural changes in butt and T-welded joints in 09G2S steel. It is shown that presence of a sharp stress raiser at low temperatures (−40 °C and lower) leads to lowering of brittle fracture resistance of HAZ metal of welded joints with fatigue damages.

One of the main causes of failures and breakage of machines, mechanisms and engineering constructions is fatigue of structural materials in individual most loaded item components. These most often are weldments which have design or structural stress raisers. Despite the great success in studying the fatigue features and availability of various techniques to improve the fatigue life of welded metal structures, the number of accidents caused by fatigue is still considerable. In this connection, the results of investigations in fatigue area and, particularly, of fatigue damageability of structures are of great interest.

It should be noted that the majority of researchers are studying fatigue phenomena in metals and predominantly the dislocation structure both within the stable slip bands, and in the matrix using electronic microscopy [1]. Over the recent years research aimed at finding the possibility to predict the degree of fatigue damage of structural elements or equipment has been intensively pursued. Prediction of the time of safe operation of various structures and equipment should be based on investigation of metal fatigue features on the microlevel [2]. Without detailed investigations of processes occurring in these metal layers, it is difficult and sometimes impossible to give a well-substantiated statement about the extent of fatigue damageability development in the item at cyclic loading. Technical publications contain practically no information that would allow evaluation of the influence of structural changes, which occur as a result of fatigue phenomena, on mechanical properties of high-strength steel welded joints.

A basic point at definition of the research problem in this work was the fact that at present the number of loading cycles preventing fracture is considered as a function of cyclic deformations [2, 3] or stresses [4], causing fatigue damage accumulation. Accordingly, a distinction is made between two fatigue periods — incubation, in which fatigue damage accumulation occurs, and active, in which fatigue crack initiation and propagation occur.

In this work the influence of microstructural features of fatigue damageability under cyclic loading and manifestations of plastic deformation, formation of fatigue cracks, as well as the influence of cyclic loading of metal of HAZ of welded joints on their brittle fracture fatigue resistance at subsequent static loading of standard specimens, cut out of tee samples after cyclic loading, was studied in order to determine the critical stress intensity factor $K_{IC}$ and critical crack opening displacement $\delta_c$, depending on the number of cycles of tee joint loading.

Butt joints (B25) and tee joints with a stiffener from 09G2S steel of 30 and 10 mm thickness, respectively, transverse relative to the action of the forces (T8 to GOST 14771−76), were selected as the object of study. They were made by mechanized welding process with solid wire Sv-08G2S of 1.2 mm diameter in $CO_2$. Composition and mechanical properties of steels, as well as those of metal deposited with the above consumable, are given in Tables 1 and 2.

At the first stage of investigations samples 120 mm wide and 480 mm long were cut out of the welded joints, which were then subjected to symmetrical cyclic loading by bending at 14 Hz frequency. It is established that fatigue cracks more than 2 mm long in butt welded joints, which were tested at cycle stress $\sigma_a = 100$ and 130 MPa, formed after 200,000 and 110,000 cycles, respectively ($N = N_{Fr}$, where $N$ is the number of loading cycles; $N_{Fr}$ is the number of loading cycles, at which fatigue cracks form), and in tee welded joints, which were tested at cycle stress of 80 and 120 MPa, they were revealed after 880,000 and 490,000 cycles, respectively.

**Table 1.** Composition (wt.%) of 09G2S steel and metal deposited with Sv-08G2S wire

| Material | C | Mn | Si | S | P |
|---|---|---|---|---|---|
| 09G2S steel | 0.10 | 0.71 | 0.57 | 0.024 | 0.021 |
| Deposited metal | 0.08 | 1.30 | 0.80 | 0.017 | 0.019 |

**Table 2.** Mechanical properties of 09G2S steel and metal deposited with Sv-08G2S wire

| Material | $\sigma_y$, MPa | $\sigma_t$, MPa | $\delta_5$, % | $\psi$, % | $KCV$, J/cm$^2$, at $T_{test}$, °C | | |
|---|---|---|---|---|---|---|---|
| | | | | | +20 | −20 | −40 |
| 09G2S steel | 367 | 553 | 28 | 68 | 150 | 120 | 64 |
| Deposited metal | 375 | 508 | 23 | 66 | 145 | 65 | 15 |

At the second stage welded joints in as-welded condition, as well as after cyclic loading at achievement of $N$ = 0.45, 0.70 and 0.80 of $N_{Fr}$, were used to prepare standard specimens of 15 × 30 × 145 mm (butt joint) and 10 × 20 × 100 mm size (tee joint) for assessment of test results using fracture mechanics criteria. Specimens were cut out so that the tips of fatigue cracks, which initiate at the notch tip, were located only in the zone of localizing of metal plastic deformation. Such a region in welded joints is the line of weld fusion with base metal, where the natural stress raiser is located, which is due to weld geometry. Results of specimen testing for three-point static bending, conducted at the temperature from +20 up to −40 °C, are shown in Figure 1.

Results of testing specimens made from butt joints showed that at temperature from +20 to −20 °C, there are no noticeable changes in brittle fracture resistance of HAZ metal of 09G2S steel welded joints (Figure 1, a, b). Lowering of $K_{IC}$ and $\delta_c$ values was observed at $T_{test}$ = −40 °C in the case, when $N / N_{Fr} \geq$ 0.7. Similar regularities of decrease of $K_{IC}$ and $\delta_c$ values in the HAZ metal of welded joints, cyclic loading of which was interrupted at the stage preceding fatigue crack formation, were found also at testing specimens cut out of tee joints of 09G2S steel (see Figure 1, c, d). This is, obviously, related to the fact that during cyclic loading an essential accumulation of fatigue damage occurs in individual microvolumes, and ductile prop-

erties of metal are exhausted, as a result of which it loses its ability to effectively resist brittle fracture.

Investigation of the process of fatigue damage accumulation and features of microstructure changing under the impact of cyclic loading were performed on specimens cut out of butt and tee welded joints of 09G2S steel, which were loaded by different number of cycles. They were used to make microsections which were etched in 4 % HNO$_3$ solution in ethyl alcohol. After multiple periodical repolishing and etching of the surface, microstructure of microsections was studied in «Neophot-34» microscope, Philips scanning electron microscope SEM-515 and LECO microhardness meter M-40 under varying loads. X-ray structure analysis was performed in DRON-UM-1 diffractometer in monochromatic Cu$K_\alpha$-radiation by the method of step scanning. Graphite single crystal was used as the monochromator.

As shown by investigations, in metal of all types of welded joints subjected to cyclic deformation, indications of fatigue phenomena were found in the form of fatigue damage (stable slip bands, extrusion and intrusion) and fatigue changes of microstructure (Figures 2 and 3). They appeared after a certain number of deformation cycles, which was different for different types of specimens.
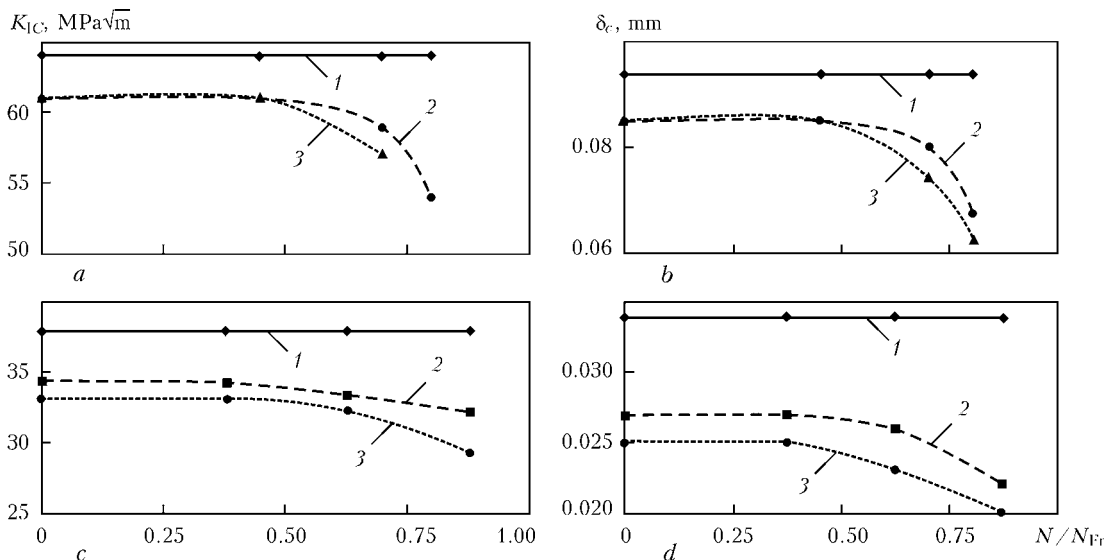


**Figure 1.** Change of $K_{IC}$ (a, c) and $\delta_c$ (b, d) values of HAZ metal of butt (a, b) and tee (c, d) welded joints of 09G2S steel with increase of the number of deformation cycles (cycle stresses for butt joints were 100 (a), 130 (b) MPa, and for tee joints — 80 (c), 120 (d) MPa): 1 — $T_{test}$ = +20 and −20 °C; 2, 3 — $T_{test}$ = −40 °C
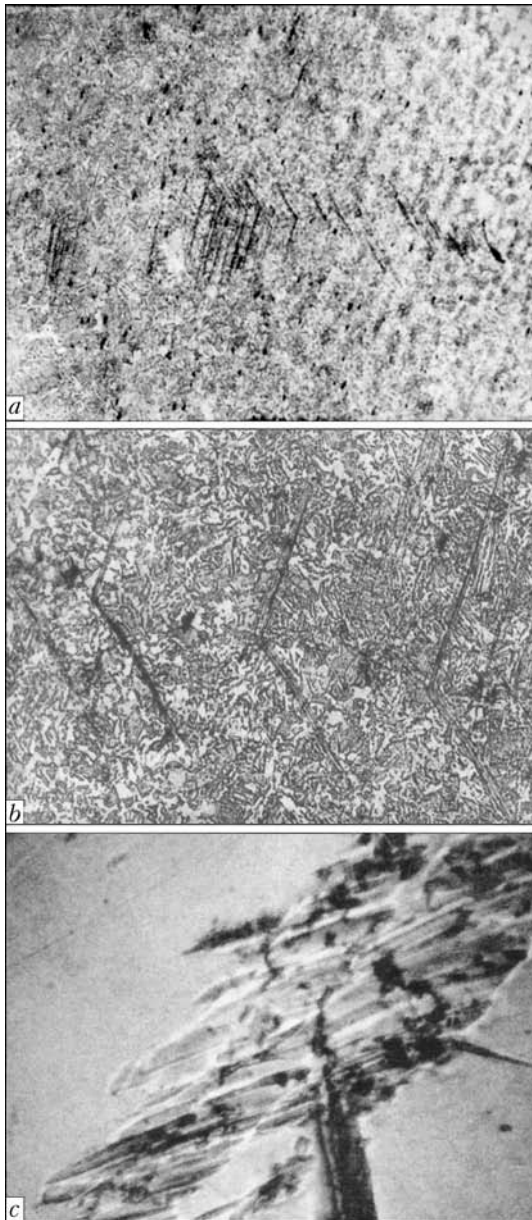
**Figure 2.** Slip bands, extrusions, intrusions in the metal of samples of 09G2S tee joints: $a$, $b$ — $N$ = 230,000 cycles, $\sigma_a$ = 120 MPa; $c$ — $N$ = 720,000 cycles, $\sigma_a$ = 80 MPa ($a$ — ×100; $b$ — ×500; $c$ — ×1000)

The most numerous of the detected fatigue damages in 09G2S steel welded joints both butt and tee, were stable slip bands, which did not disappear even after



**Figure 3.** Fatigue changes of microstructure of HAZ metal of 09G2S steel butt welded joints: $a$ — $N$ = 230,000 cycles, $\sigma_a$ = 120 MPa; $b$ — $N$ = 720,000 cycles, $\sigma_a$ = 80 MPa ($a$ — ×500; $b$ — ×1000)

multiple repolishing of the specimens. Irrespective of the types of welded joint, the number of slip bands rises with increase of the number of loading cycles, and the bands proper are a family of slip lines.

Considering that stable slip bands are located in slip planes and their orientation, as a rule, coincides with the direction of transverse sliding of dislocations [5, 6], it can be assumed that stable slip bands arose in those grains, where a certain dislocation density and critical stress level were achieved. As is known, after achievement of a critical stress level, dislocation movement starts in the direction close to their slip plane (transverse sliding of dislocations). Here critical stress depends primarily on the level of substructure development, and is inversely proportional to it. This accounts for the fact that in the HAZ metal, and, in particular, in the overheated region of the studied welded joints, slip bands formed more frequently than in the base metal. This is related to the fact that austenite transformation in this region during welding occurred by the shear diffusionless mechanism, unlike those regions of HAZ and base metal, where its transformation proceeded by the diffusion mechanism or did not occur at all. It should be noted that detection of stable slip bands in HAZ metal was difficult, because of the presence of a multitude of second phases in the structure.

Second phases obscure fatigue phenomena in the microstructure to an even greater extent, so that the latter are difficult to detect. As is seen from Figure 4, the main structural component of overheated zone of HAZ metal in butt and tee joints in the initial (as-welded) condition is bainite of globular (microhardness $HV50$ = 1880−2120 MPa) and plate-like morphology ($HV50$ = 2200−2430 MPa). Grain-boundary (hypoeutectoid) and seldom acicular ferrite are also present in the structure.

It is known [1] that depending on the initial structural state of material and cyclic loading conditions, material resistance to cyclic deformation can rise (and, therefore, material is strengthened), decrease or remain unchanged with increase of the number of loading cycles. In material softening zone such surface damage as extrusion and intrusion [2] develops, which is a consequence of material fatigue [2, 3].

In this work microhardness measurement was used to study the reaction of HAZ and base metal on cyclic deformation, depending on the number of loading cycles. Results of these investigations, given in Figure 5, are indicative of the fact that during cyclic loading of welded joints of 09G2S steel both strengthening and softening of HAZ metal and adjacent base metal regions take place. Strengthened and softened regions are of a local nature and alternate.

It is established that under the impact of cyclic deformation, fatigue changes (see Figure 3) occur in the HAZ metal structure of 09G2S steel welded joints, which consist in the change of the nature of dislocation
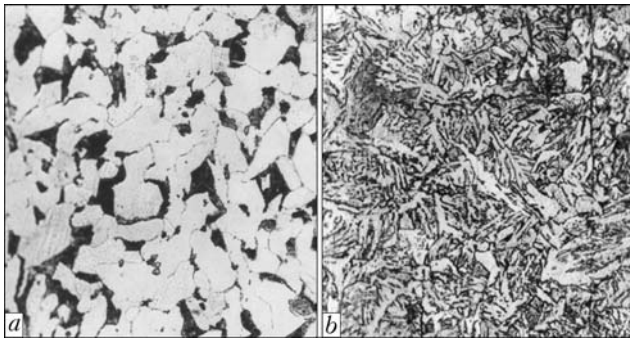
**Figure 4.** Microstructures (×500) of 09G2S steel (*a*) and HAZ metal (*b*) of tee welded joints

distribution, namely in their redistribution with formation of band structures. Degree of development of fatigue changes in the microstructure is different in different microvolumes, and, apparently, depends on their crystallographic sensitivity to the direction of load application axis, local stress concentration, as well as concentrational inhomogeneity as to impurity and alloying elements.

Alongside the stable slip bands, extrusions, intrusions and fatigue changes of the microstructure, transverse microshears were found on the surface of samples of tee joints subjected to cyclic deformation in different loading modes (Figure 6). The fact that under the same conditions of cyclic loading transverse microshears occur in samples of tee welded joints and are absent in butt joint samples, is, apparently, attributable to the initially higher rigidity of tee joints. A microshear, could, most probably, be initiated by dislocation clusters near the grain boundaries, carbide inclusions or second phase globules, as well as cleavages of non-metallic inclusions inside the grains.

In this work a specimen of 9 × 12 mm size was studied, which was cut out of cyclically deformed tee joint ($\sigma_a$ = 80 MPa and $N$ = 720,000 cycles, which is equal to $0.8N_{Fr}$), on the surface of which a region with a transverse microshear was found. Diffractometric studies of the specimens were performed using X-ray structural analysis. $D_{HKL}$ value of blocks of re-
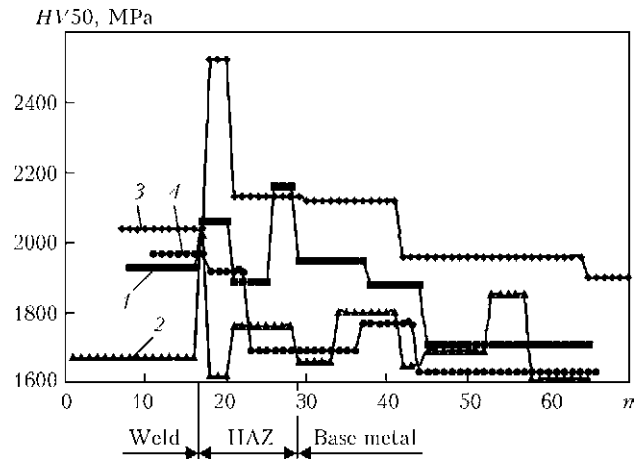


**Figure 5.** Microhardness of samples of tee welded joints of 09G2S steel after welding (*1*) and cyclic loading $\sigma_a$ = 80 MPa up to $N$ = = 400,000 (*2*), 700,000 (*3*) and 100,000 (*4*) cycles: *n* — number of measurements

gions, where microstructural changes and microstresses $\Delta a / a$, accompanying these changes, occur, was assessed. With this purpose two measurement points were selected: *a* — in the center of transverse shear; *b* — ahead of transverse shear. Time of exposure in the point was 40 s, and measurement step was 0.05°. Results of diffractometric studies given in Table 3 are indicative of the fact that microstress relaxation occurs in the region of transverse microshear. This is logical, because, as follows from references [1–3], the microshear, which is realized through atomic bond rupture under the impact of external stress, is the initial stage of submicrocrack growth. Rupture of such bonds occurs in the plane with the lowest atomic packing density, having the lowest values of surface energy. For metals with bcc lattice this is plane {100}.

As fatigue changes in welded joints occur in their local and quite definite zones, further studies were aimed at finding technological methods to improve the fatigue life of such joints and recovering their ability to resist brittle fracture. Effect of preventive repair by welding was studied, which is performed at the stage, preceding fatigue crack formation, and

**Table 3.** Results of diffractometric studies

| Measurement points | Measurement schematic | $D_{HKL}$, nm | $\Delta a / a \cdot 10^{-4}$ |
|---|---|---|---|
| *a* |  | $\to 0$ | $\to -\infty$ |
| *b* |  | 48.61 | 6.188 |
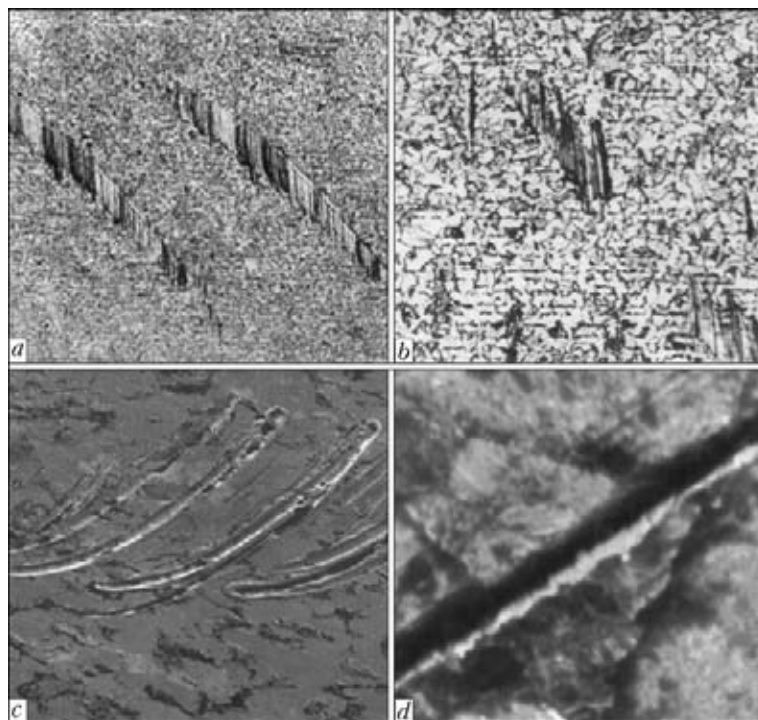
**Figure 6.** Microstructures with transverse microshears in samples of tee joints of 09G2S steel: $a$ — $\sigma_a$ = 120 MPa, $N$ = 400,000 cycles; $b$–$d$ — $\sigma_a$ = 80 MPa, $N$ = 720,000 cycles ($a$ — ×50; $b$ — ×125; $c$ — ×810; $d$ — ×5000)

which consists in deposition of additional beads along the edges of existing welds, as well as various kinds of metal strengthening (high-frequency mechanical peening, shock-wave or electric pulse treatment).

These investigations were performed by the limited fatigue life method for specimens cut out of tee joints of 09G2S steel 10 mm thick. After welding the samples were subjected to cyclic loading up to 400,000 cycles ($0.8N_{Fr}$) at cycle stress of 120 MPa. Then, they were repaired by welding or strengthened by various technologies, and then again subjected to cyclic loading at the above mentioned load up to formation of 2 mm fatigue crack. Other repaired or strengthened welded joints were used to make standard samples (type 11 to GOST 9454–78) for impact bend testing, which was conducted at $T_{test}$ = −40 °C.

Investigation results showed that after preventive repair by welding and high-frequency mechanical peening of welded joints their fatigue life rises 2–2.2 times. Fatigue life of welded joints after electric-pulse and shock-wave treatment increases somewhat less (1.4–1.8 and 1.4–1.5 times).

Impact bend testing showed that in as-welded condition impact toughness $KCV_{-40}$ of HAZ metal of 09G2S steel welded joints is equal to 10.0–13.1 J/cm$^2$, and as a result of cyclic loading it decreases to 6.8–8.2 J/cm$^2$. After preventive repair using welding and strengthening treatments $KCV_{-40}$ value rises but to different extent. In welded joints after preventive repair by welding impact toughness practically on the level of the initial condition ($KCV_{-40}$ = 10.1–10.8 J/cm$^2$) was recorded. It rose up to 9.2–10.2 and 8.9–9.6 J/cm$^2$ after high-frequency mechanical peen-

ing and shock-wave treatment. Electric-pulse treatment did not have any essential influence on impact toughness of HAZ metal of 09G2S steel welded joint.

**CONCLUSIONS**

1. At cyclic loading by bending ($N/N_{Fr} \geq 0.7$), accumulation of fatigue damage takes place in HAZ metal of 09G2S steel welded joints: stable slip bands, extrusions and intrusions form, their number increasing together with increase of loading cycle number.

2. Fatigue damages accumulated in HAZ metal of 09G2S steel facilitate its embrittlement and, as a result, lead to lowering of cold resistance by 20–40 %.

3. Fatigue life of 09G2S welded joints can be effectively increased 1.8–2.2 times and HAZ metal cold resistance can be restored to the initial condition through application of preventive repair performed at the stage preceding formation of fatigue cracks, by deposition of additional beads along weld edges and (or) performance of high-strength mechanical peening of the zone of weld-to-base metal transition.

1. Goritsky, V.M. (2004) *Diagnostics of metals*. Moscow: Metallurgizdat.
2. Yakovleva, T.Yu. (2003) *Local plastic deformation and fatigue of metals*. Kiev: Naukova Dumka.
3. Ivanova, V.S., Terentiev, V.F. (1975) *Nature of fatigue of metals*. Moscow: Metallurgiya.
4. Romaniv, O.N., Nikiforchin, G.N. (1986) *Mechanism of corrosion fracture of structural alloys*. Moscow: Metallurgiya.
5. Ivanova, V.S., Orlov, L.G., Terentiev, V.F. (1972) Specifics of dislocation structure development at static and cyclic loading of low-carbon steel. *Fizika Metallov i Metallovedenie*, 33(**3**), 617–633.
6. Wilson, D.V., Tromans, T.K. (1970) Effect of strain aging on fatigue damage in low-carbon steel. *Acta Metallurgica*, **18**, 1197–1208.

# EFFECT OF ADDITIONS OF ALUMINIUM TO FLUX-CORED WIRE ON PROPERTIES OF HIGH-CARBON DEPOSITED METAL

**S.Yu. KRIVCHIKOV**

E.O. Paton Electric Welding Institute, NASU, Kiev, Ukraine

Crack resistance and porosity of low carbon alloys in hardfacing using self-shielding flux-cored wire was investigated. It was established that alloying the deposited metal with over 0.7 wt.% aluminium leads to increase in its martensite phase content and decrease in its crack resistance. It was shown that maximal hardness of the deposited metal at an insignificant decrease in its crack resistance could be achieved at the 0.5−0.7 wt.% aluminium content.

The E.O. Paton Electric Welding Institute of the NAS of Ukraine developed self-shielding flux-cored wire PP-AN160 intended for wide-layer hardfacing of cast iron crankshafts of automobile engines[*]. Because of technological peculiarities of wide-layer hardfacing of crankshaft necks and a small diameter of flux-cored wire (1.8 mm), its core cannot contain more than 1.5 % of gas- and slag-forming components. However, this amount is insufficient for reliable shielding of the electrode metal drops and molten weld pool from air oxygen and nitrogen, which in turn leads to formation of porosity in the deposited metal. The main metallurgical method for prevention of porosity caused by air oxygen and nitrogen is adding the required amount of aluminium and/or titanium to the composition of the deposited metal in order to combine gases dissolved in the weld pool into insoluble compounds. An insufficient or excessive content of these elements may either incompletely suppress pore formation or partially participate in alloying and changing of physical-mechanical properties of the deposited metal.

The purpose of the present study was to investigate the effect of aluminium on porosity and properties of a wear-resistant alloy deposited by using self-shielding flux-cored wire PP-AN160.

Experimental self-shielding flux-cored wires with a diameter of 1.8 mm and different weight contents of aluminium in their core were manufactured for investigations. Multilayer hardfacing was performed under the following conditions: $I_h$ = 170−180 A, $U_a$ — 19−21 V, $v_h$ = 14 m/h, direct current of reverse polarity. Each next bead was deposited after complete cooling of the previous one. Chemical composition of the deposited metal (in the third layer) in the investigated specimens was as follows, wt.%: 2.2−2.4 C, 0.7−0.8 Mn, 1.6−1.8 Si, 0.2−0.3 Cr, 0.2−0.3 Ti, 0.035, 0.54, 0.82, 1.50 and 2.20 Al.

As shown by the experiments, independently of the content of aluminium (within the investigated limits) the beads had microcracks formed with a substantial sound effect during cooling of the deposited metal within the 450−250 °C temperature range, which allows them to be classified as cold cracks.

It was found in the course of metallurgical examinations that aluminium exerts a considerable effect on the quantity and morphology of microcracks in the deposited metal, as well as on its porosity. For instance, isolated microcracks and a large quantity of pores up to 2 mm in diameter were detected in the hardfaced specimens containing 0.035 wt.% Al (according to the data of chemical analysis, in the case of the absence of aluminium in the flux-cored wire core). The quantity of microcracks insignificantly grew, and that of pores decreased with increase of the weight content of aluminium to 0.54 %. Further increase of the aluminium content led to growth of length and opening displacement degree of the microcracks, whereas the microcracks affecting both deposited metal and fusion zone metal appeared in the deposited metal containing 2.20 wt.% Al (Figure 1). There were no pores in the specimens of the deposited metal containing over 0.54 wt.% Al.

Structure of the deposited metal containing no aluminium consisted of austenite decomposition products (ferrite-pearlite mixture) and a carbide-cementite phase. The latter had the form of a reinforcing net in section plane.

As established as a result of metallurgical examinations, alloying with aluminium within the investigated ranges does not have a substantial effect on the degree of dispersion of the solid-solution dendritic structure, but changes the spatial structure of the carbide-cementite phase. At 0.035 wt.% Al, it is formed not in all regions of the inter-arm spacing of dendrites. Therefore, it has the form (in section plane) of a bro-

---

[*]Krivchikov S.Yu. (2008) Improvement of tribotechnical characteristics of hardfaced cast iron automobile crankshafts. *The Paton Welding J.*, **12**, 31−33.
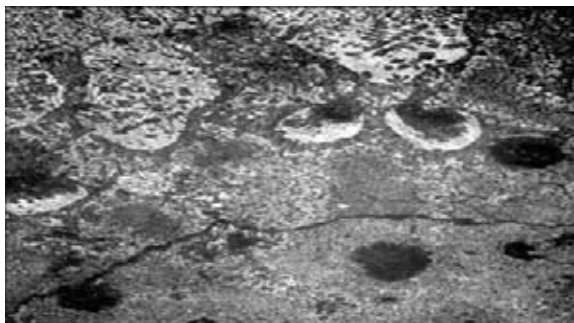
**Figure 1.** Microcrack in fusion zone of deposited metal containing 2.2 wt.% Al (×160)



**Figure 2.** Effect of aluminium on hardness $HV$ of deposited metal, microhardness $HV_a$ of solid-solution grains and microhardness $HV_c$ of carbide-cementite phase

ken net. Its branching grows with increase of the aluminium content.

Phase composition of the deposited metal also undergoes changes. Increase of the aluminium content to 0.50 wt.% leads to formation of approximately 3 % of martensite in structure of the deposited metal. Increase of the aluminium content to 2.20 % causes growth of the martensite content in structure of the deposited metal to 18 %. It is likely that formation of martensite is one of the causes of lowering of the level of crack resistance of the deposited metal at a weight content of aluminium above 0.50 %.

In addition to structural transformations, alloying with aluminium is also accompanied by a change in hardness of the deposited metal and its main phase components (austenite decomposition products and carbide-cementite net). As seen from Figure 2, the curves have maxima at a weight content of aluminium in the deposited metal equal to 0.7–0.9 %. Increase in hardness $HV$ of the deposited metal and microhardness $HV_a$ of solid-solution grains with increase of the aluminium content to the indicated level is caused by growing dispersion of the carbide-cementite phase and, probably, by participation of aluminium in strengthening of solid-solution ferrite (austenite de-

composition products). The graphitising effect of aluminium shows up with further increase in its weight content. This results in decrease of the cementite content, thus leading to decrease in hardness $HV$ of the deposited metal and microhardness $HV_a$ of solid-solution grains. Despite the fact that alloying with aluminium is accompanied by formation of martensite which has a relatively low hardness (4600–4900 MPa), it cannot act as obstacle to further decrease in $HV$. The cause of decrease in microhardness $HV_c$ of the carbide-cementite phase is likely to be related to a change in stoichiometric composition of carbide components of the deposited metal caused by alloying with aluminium.

It can be concluded on the basis of the investigations conducted that the maximal hardness, absence of porosity and satisfactory microcrack resistance are characteristic of the deposited metal containing about 0.5–0.7 wt.% Al.

# NEW TECHNOLOGY OF ELECTRIC ARC BATH WELDING OF RAILS ON TRAM AND CRANE TRACKS

**G.V. KUZMENKO, V.G. KUZMENKO, V.I. GALINICH** and **V.M. TAGANOVSKY**
E.O. Paton Electric Welding Institute, NASU, Kiev, Ukraine

New rail welding technology developed by the E.O. Paton Electric Welding Institute is described, and examples of its application at reconstruction and construction of tram and crane tracks are given. It is noted that after appropriate verification and authorization this method can be regarded as a serious alternative to the existing welding methods for performing operations in the railway track.

Continuously-welded track is the most advanced design of track structure, the main advantage of which is the possibility of practically complete elimination of rail butts that considerably reduces the dynamic forces and lowers train resistance (by 10 % on average). In addition, continuously-welded track extends the service life of track structure elements (from 1.3 to 2.2 times), reduces repair costs of track and rolling stock (up to 35 %), allows saving metal of web covers (5−7 t per 1 km), increases train velocity up to 160−200 km/h and more [1]. Despite the fact that the above advantages of continuously-welded track pertain to main-line railways, they are also realized to varying degrees at its application in all the kinds of railway transportation — on the tracks of industrial enterprises, metro, trams and cranes.

Rail welding is an integral part of trackworks, influencing the design and technico-operating parameters of track structure. Features of rail welding process are related to their material properties. Owing to high carbon content, rail steels are poorly weldable and are prone to hot and cold cracking. Their welding requires special welding consumables and specialized technologies. High requirements are also made of the accuracy of following the temperature modes of welding [2].

The weld should meet the same technical requirements as the rail proper. The latter is regarded as the load-carrying and guiding element of the track, which can stand static and dynamic loads, ensures a high smoothness of running, and is capable of resisting wear. In this connection the weld, similar to the rail proper, should meet safe operation requirements and create no hindrance to traffic. Welding process should ensure [3]:

• stable quality and satisfactory service properties of welded butt joints at minimum dependence on welder's qualification;

• maximum short total duration of welding process, particularly at track repair so as to fit within time widows allowed for these purposes;

• ability to apply portable welding equipment so that it could be easily transported and serviced;

• prevention of rail consumption or need to move them in the longitudinal direction;

• process adaptability to cross-sections of all types of used rails, as well as sufficient flexibility for application to rails with different degrees of wear;

• acceptable level of initial expenses for purchase of welding equipment and current expenses for performance of welding proper.

At present none of the applied processes of rail welding (flash-butt, gas-pressure, alumothermic, electric arc, bath welding) fully meets all of the above-listed requirements. In flash-butt welding providing the highest quality of welded joints and high efficiency (particularly in stationary conditions) cumbersome and expensive equipment is used, that makes its application in field conditions difficult and often not cost-effective or technically irrational, in particular, at performance of repair, when it is necessary to weld a relatively small number of butt joints. Application of this welding process is also complicated by the need to move welded rails and track opening. There are also certain difficulties in welding of frogs and switches with this process.

Gas-pressure welding was widely applied in 1930−1970s in the US railways mainly for joining rails in stationary conditions (in the shop and depot). However, increase of axial loads in 1980s lead to an essential increase of the number of butt joint failures, so that this welding process was ousted by flash-butt welding [4]. At present gas-pressure welding is rather widely applied in Japanese railways [5].

Alumothermic welding which has been applied for more than 100 years for joining various-purpose rails, features a high mobility and versatility, without, however, providing a sufficient stability or high quality of welded joints. At present the possibilities for im-

provement of this process in order to increase welded joint performance have been practically exhausted. Therefore, despite the numerous technological improvements and organizational measures taken by companies providing services on alumothermic welding, no breakthrough is to be anticipated in this area [6]. Moreover, this welding process did not develop in our country for decades, as a result of which quite expensive import consumables have to be purchased for its application.

At present coated-electrode arc bath welding is mainly widely accepted for joining tram and crane rails. This process, however, does not ensure a reliable quality of welded joints, as it essentially depends on welder's qualifications and is greatly inferior to other welding processes as to efficiency. In order to improve the efficiency, a process of semi-automatic arc bath welding of rail butts was developed, which was applied by Berlin Transportation Company in repair of metro rail tracks [7]. A special elongated current-carrying nozzle and self-shielded flux-cored wire were used. As a result, welding efficiency increased by 30 %, compared to manual coated -electrode arc welding. Arc bath welding was applied with success, in particular, at construction of high-speed Yamagata-Shinkansen line in Japan [8], where improvement of technology and welding consumables, as well as application of special heat treatment enabled a significant improvement of welded joint quality. Nonetheless, welding efficiency remained on a low level (time of welding a butt joint was 75 min) [9]. Nippon Steel developed a new process, intended to replace alumothermic welding and manual arc bath welding of rails in the future [9, 10]. It is based on a combination of gas-shielded welding by a rotating consumable electrode (welding of the rail foot) and electroslag welding (welding of rail web and head). The entire process is performed in the automatic mode using a computer-controlled unit.

This technology ensures much higher mechanical properties of welded joints than alumothermic welding does. However, the time of welding a butt joint is equal to about 100 min, although there is a possibility of shortening it to 50−60 min in the future that



**Figure 1.** ARS-4 unit for rail welding

will just bring this process closer to alumothermic welding in efficiency.

Several attempts were also made to develop the process of electroslag welding of rails [11−14]. However, despite the quite serious study of the subject, no satisfactory results have been achieved so far [15].

The E.O. Paton Electric Welding Institute of the NAS of Ukraine developed a new technology of rail welding, which was called automatic arc welding by bath method using consumable nozzle, or in short consumable-nozzle arc welding. It features application of self-shielded flux-cored wire, fed through a longitudinal channel in a special flat consumable nozzle, that allows welding to be performed in the gap of 12−16 mm, and in some cases − of up to 22 mm in the butt.

The proposed welding method, being a further development of arc bath welding, allows increasing the efficiency of operations 2−3 times owing to process mechanization, and at the same time significantly improving the quality indices of welded joints, while preserving the high mobility and versatility of the equipment.

It is designed, first of all, for welding the tracks of industrial enterprises, tram (also high-speed operation) and crane tracks, and in the long-term after appropriate verification and obtaining permission also for performance of on-line repair operations in main-line railways. Specialized equipment − ARS-4 unit was developed (Figure 1).

### Specification of ARS-4 unit

Rated DC supply line voltage, V ................................ 24
Power consumed by the
source, kV·A ...................... not more than 15 (3 × 380 V)
Rated welding current, A, at 100 % duty cycle ............ 350
Diameter of applied flux-cored wire, mm .................... 2.4
Ranges of adjustment of electrode wire feed
rate, m/h ....................................................... 50−300
Electrode movement speed, m/h ........................... 4−12
Transverse travel of electrode, mm ........................... 180
Electrode oscillation frequency, Hz ..................... 0.5−2.0
Amplitude of electrode end oscillations, mm ............. 0−20
Overall dimensions, L × W × H, mm ....... 1320 × 520 × 850
Unit weight without wire or
shoes, kg, ......................................... not more than 40

It features portability and owing to replaceable forming fixtures it is easily readjusted for welding rails of various typesizes. FORSAZh-500 inverter of Ryazan State Instrument-Making Plant (RF) is used as the welding source. Power can be supplied both from three-phase mains of 380 V voltage, and from self-sufficient electric generator of 25−30 kV·A power, with power consumed in welding being equal up to 15 kV·A. Average machine time of welding a butt joint of R65 type rails is equal to about 20 min that allows a combined team of five people (two welding operators and three trackmen) achieving the efficiency of up to 16 butts per shift.

Welding is performed with a consumable nozzle, making reciprocal motions of varying amplitude (Fi-

**Figure 2.** Schematics of nozzle displacement in arc welding of rails by bath method with a consumable nozzle



**Figure 3.** Welding crane tracks

gure 2) that ensures complete penetration of the edges being welded across the entire rail section. Foot welding is performed on a ceramic backing by multipass welding. After that a special lever mechanism is used to perform pressing down of copper shoes without interrupting the process, providing formation of weld side surfaces in welding of the rail web and head.

In most of the cases preheating before welding is not performed, butt preheating up to 250−300 °C is required only at the temperature below +5 °C, and welding can be performed at ambient air temperature down to −5 °C.

Consumable-nozzle arc welding was earlier introduced in mounting of crane tracks of bulker terminal of Tuapse Commercial Sea Port (RF) (2009−2010) and Iliichevsk Sea Fishing Port (Ukraine) (2011)

(Figure 3). In these facilities welding of butt joints of crane rails KR100 and KR120 was performed (Figure 4).

During 2009−2011 this method was also used to weld more than 900 butt joints of R65, T62 rails (Figure 5 *a*, *b*) and low-profile webless rails LK-1 (Figure 5, *c*) at reconstruction of high-speed tram line in Kiev and tram tracks in Lvov.

Developed special welding consumables and welding technology ensure rather high values of mechanical properties of welded joints. Hardness of metal of R65 rail welded joints is equal to *HB* 260−320; weld metal ultimate strength is 800−900 MPa. Breaking load at rail testing for static bending is 1500−1650 kN at bending of 16−22 mm.



**Figure 4.** Crane rails KR100 (*a*, *b*) and KR120 (*c*, *d*) after welding (*a*, *c*) and grinding (*b*, *d*)
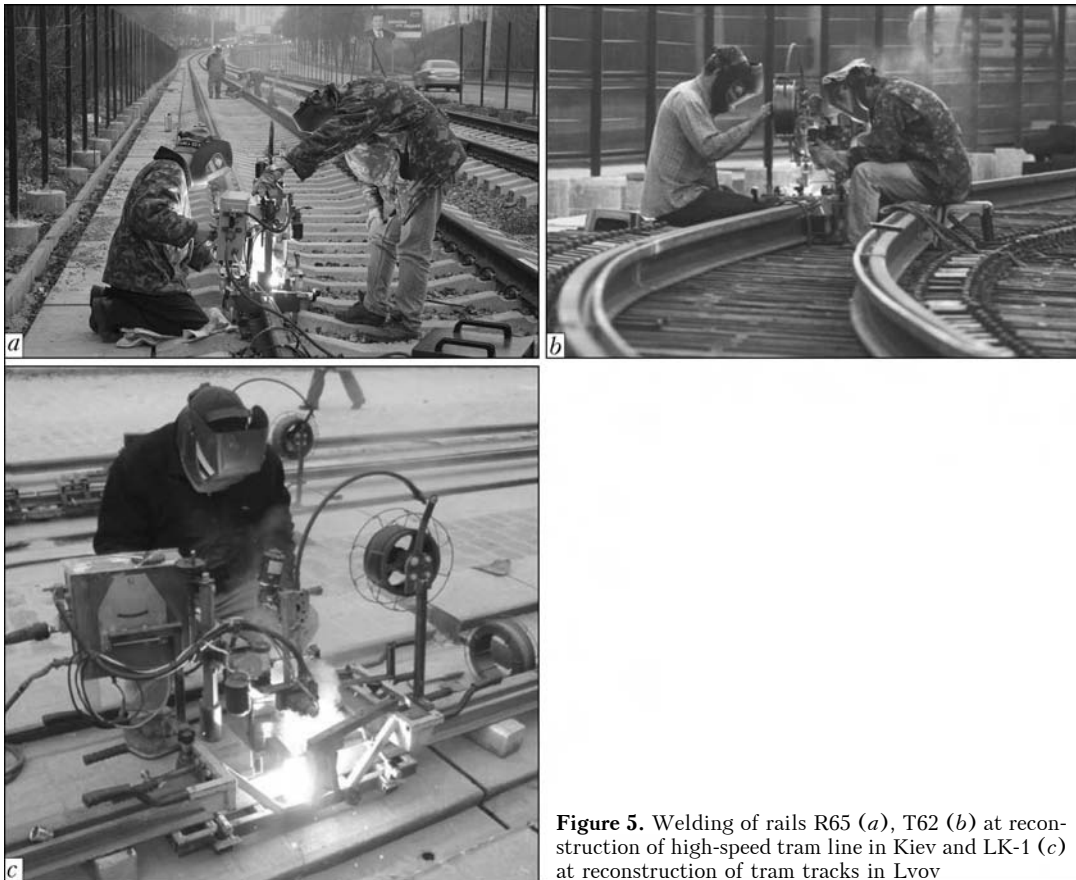
5/2012

35

**Figure 5.** Welding of rails R65 (*a*), T62 (*b*) at reconstruction of high-speed tram line in Kiev and LK-1 (*c*) at reconstruction of tram tracks in Lvov

This welding process offers the following advantages:

• higher and more stable quality of welded joints compared to manual arc bath welding and alumothermic welding;

• high efficiency — up to 16 butt joints per shift;

• no shielding gas or flux required;

• no preheating (at +5 °C and higher temperature) or heat treatment of the butt required;

• low power consumption (consumed power of up to 15 kV·A);

• easy readjustment of equipment for welding rails of various typesizes;

• high mobility that is particularly important at performance of repair operations.

Thus, the new process of electric arc welding by bath method with a consumable nozzle, developed at PWI, owing to its advantages, can be regarded as an alternative to the existing processes of welding during performance of operations in the track.

1. Kostyuk, M.D., Kozak, V.V., Yakovlev, V.O. et al. (2010) *Building and reconstruction of railway network of Ukraine for increase in track capacity and introduction of high-speed traffic of trains*. Kyiv: PWI.
2. Poznyakov, V.D., Kiriakov, V.M., Gajvoronsky, A.A. et al. (2010) Properties of welded joints of rail steel in electric arc welding. *The Paton Welding J.*, **8**, 16–20.
3. Sun, J., Davis, D., Steel, R. (2001) TTCI searching for improved in track welding methods. *Railway Track & Structures*, **1**, 13–15.
4. Sun, J., Kristan, J. (2003) Gas-pressure welding: is it feasible for North American railroads? *Ibid.*, **2**, 12–14.
5. Yamamoto, R. (2007) Advances in gas pressure welding technology for rails. *Railway Technology Avalanche*, **17**(3), 99.
6. Lonsdale, C.P. (1999) Thermit rail welding: history, process developments, current practices and outlook for the 21st century (PDF). In: *Proc. of AREMA 1999 Annual Conf.* Pt 2. The American railway engineering and maintenance-of-way association, Sept.
7. (2007) Stronger than a storm. *Weld+vision*, **19**, 14–15.
8. Takimoto, T. (1984) Latest welding technology for long rail and its reliability. *Tetsu-to-Hagane*, **70**(10), 40.
9. Okumura, M., Karimine, K., Uchino, K. et al. (1995) Development of field fusion welding technology for railroad rails. *Nippon Steel Techn. Rept.*, **65**(4), 41–49.
10. Tashikawa, H., Uneta, T., Nishimoto, H. et al. (2000) Steel welding technologies for civil construction applications. *Ibid.*, **82**(7), 35–41.
11. Svetlopolyansky, Yu.I. (1966) Semiautomatic electroslag welding of rails. *Avtomatich. Svarka*, **3**, 53–54.
12. Koperman, L.N., Mukanaev, K.K. (1967) Electroslag welding of crane rails. *Svarochn. Proizvodstvo*, **5**, 32.
13. Turpin, B., Danks, D. (2003) *Electroslag field welding of railroad rail* (Contract Number HSR-37). Washington, D.C.: Transportation Research Board, Jan.
14. Gutscher, D., Danks, D., Turpin, B. (2008) Electroslag welding: a potential alternative to conventional rail welding. In: *Proc. technology digest TD-08-043*. Pueblo, Col.: Association of American railroads, transportation technology center, Oct.
15. Gutscher, D. (2009) Development and evaluation of electroslag welding for railroad applications. *Railway Track and Structures*, **11**, 53–58.

# EQUIPMENT AND TECHNOLOGY OF EBW IN FINISHING SMOOTHING AND REPAIR OF REVERSE BEADS OF WELDS OF TUBULAR PRODUCTS

**L.A. KRAVCHUK**

E.O. Paton Electric Welding Institute, NASU, Kiev, Ukraine

Given are the hardware and technological solutions for the finishing smoothing and repair of linear reverse beads of weld of up to 1200 mm long inside the position extended tubular products of a rectangular shape using a system of electron beam refraction by 90°. As applied to titanium alloy VT20, the parameters of electron beam finishing smoothing were obtained providing the formation of a smooth transition from base metal to weld, smooth surface of molten metal and prevention of undercuts of up to 0.15 mm depth.

In EBW with a through penetration of position and rotating butts of long tubular products of round, square and rectangular shape an internal surface in a number of cases is working. To perform the finishing pass or repair for eliminating of roughness on the surface of weld reverse bead, small craters and undercuts along the edges of bead by an electron beam using a conventional method is not possible due to limited internal sizes of the product and difficult access to the site of treatment.

Known is the method of flashing the internal surface of tubular products using an electron beam deflected by electric field [1]. Application of a cooper reflector, mounted on a ceramic isolator, makes it possible to accumulate a charge in entry of electron beam on it and to create the field between the tube wall and reflector, with the help of which the beam is deflected along the preset trajectory to the internal surface of the tube being flashed. During control of electron beam deflection, the angle of inclined edge surface of the reflector, distance between the reflector and tube being flashed, shape of reflector and adjustment of parameters of primary electron beam are changed. The drawback of this method of flashing is the need in maintaining of a gap between the reflector and internal surface of the tube of not less than 3 mm, as well as the location of butt or reverse bead of weld at the depth of not more than 110 mm.

Investigations on repair and finishing smoothing of reverse beads of weld were performed in installation KL-138, designed at the E.O. Paton Electric Welding Institute and having computer control of all the parameters and systems. The installation is completed with a power complex on the ELA-60/60 base and electron beam gun, which is moved inside the vacuum chamber along the linear coordinates $X$, $Y$, $Z$, and

also rotated around the $Y-Y$ axis along the coordinate $QG$ by 0–90° angle. Vacuum chamber, having the 4500 × 3000 × 3000 mm internal size and 40.5 m$^3$ volume, is evacuated under the automatic condition of control to the operating vacuum of $2.66 \cdot 10^{-2}$ Pa ($2 \cdot 10^{-4}$ mm Hg) for less than 30 min. Application of cryogenerator of POLYCOLD type during pumping allowed decreasing significantly the time of evacuation and amount of moisture in vacuum chamber and butt of edges being welded that is particularly important in welding of titanium alloys [2]. At accelerating voltage $U_{acc} = 60$ kV the range of electron beam current $I_b = 0-1000$ mA is overlapped using two optics: 500 ($I_b = 0-500$ mA) and 1000 mA ($I_b = 0-1000$ mA). Accuracy of electron beam gun positioning along coordinates was not worse than 0.1 mm. Imaging of site of welding in secondary-emission electrons, as well as the coincidence of electron beam with a butt with an error of 0.1 mm was performed by the RASTR system.

To repair and to perform the finishing smoothing of linear and circumferential reverse beads of weld inside the tubular products of length of up to 1200 mm, and also to avoid the labor-consuming mechanical smoothing of a weld root part in welding, which is performed from the external side of the product, a system of electron beam refraction by 90° was designed, operating by the principle of effect of non-homogeneous magnetic field on electron beam in change of direct current in electric magnet coil. As is shown in Figure 1, the rotating system is mounted on the edge surface of the electron beam gun. It consists of a hollow pipe of a required diameter and length, and also water-cooled electromagnetic rotating system. Spatial position of the rotating system is selected so that after refraction by 90° the electron beam was directed strictly vertically downwards. Imaging of butt and reverse bead inside the tubular products, and also electron beam setting are made using a deflecting system, mounted in front of a rotating electric magnet, sensor of secondary-emission signal and RASTR system. The deflecting system of the main electron beam

**Figure 1.** 90° turning system for repair and finishing smoothing of weld reverse bead



**Figure 2.** Dependence of depth $h_p$ and width $B$ of penetration of alloy VT20 on beam current at $v_w = 3$ (*1*), 6 (*2*) and 10 (*3*) mm/s and $U_{acc} = 60$ kV, $l_{work} = 100$ mm

gun during operation of system of electron beam refraction by 90° is disconnected from the RASTR system, it is used for adjustment of electron beam and its setting in the interval between the pole tips of the electric magnet. It was found experimentally that the design of system of electron beam refraction by 90° guarantees the reliable and long-time operation at $I_b = 0$–100 mA.

The repair and finishing smoothing of linear reverse beads were made using a gun with 500 mA optics inside tubular products of a rectangular shape of up to 1200 mm length, manufactured of titanium alloy VT20, during movement of the system of electron beam refraction by 90° along the reverse bead. The selection of product material was stipulated by the non-uniform formation of reverse bead of weld with undercuts at the edges, especially typical at the through penetration by electron beam of titanium alloys of more than 6 mm thickness [3].

Selection of optimum parameters (beam current $I_b$, welding speed $v_w$, focusing current $I_f$ and working distance $l_{work}$ from edge of system of electron beam refraction by 90° to the product) of the process of electron beam finishing smoothing and repair was realized by making several penetrations on solid specimen of titanium alloy VT20 of 17 mm thickness.

After penetration at $l_{work} = 100$ mm and preparation of transverse macrosections the experimental dependence of depth $h_p = f(I_b)$ and width of penetration at the specimen surface $B = f(I_b)$ on beam current value in the range of $I_b = 10$–100 mA at $v_w = 3,6$ and 10 mm/s was obtained. As is shown in Figure 2, at $v_w = 6$ mm/s and $I_b = 20$ mA, $h_p \cong 2.5$ mm and $B \cong$ $\cong 5.3$ mm. This condition is recommended for the finishing smoothing of reverse bead of weld of 1–3 mm width. In making repair for elimination or decrease of the non-uniformities of formation of the reverse bead in length, and also small craters it is enough to increase the $I_b$.

In case of long tubular products of a rectangular shape it is necessary to determine the value of coefficient $K = \Delta l_{work} 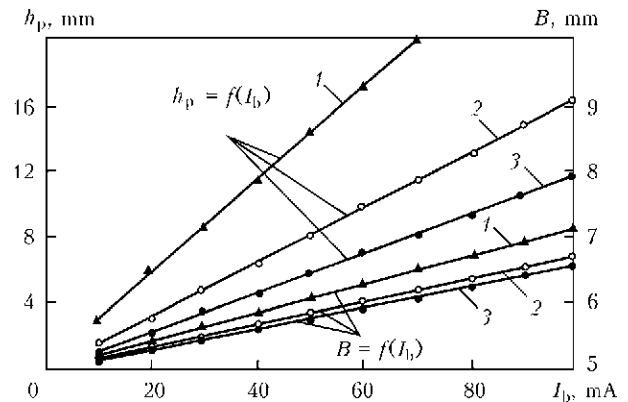/ \Delta l_f$ in change of position of reverse bead in height, i.e. with change of cross section in length of the product. It was found that for system of electron beam turning by 90° for 1200 m length at change of $l_{work}$ in the range of 100–200 mm the coefficient $K = 20$ mm/mA, i.e. the current of focusing lens of the electron beam gun with optics of 500 mA, is changed by $\Delta I_f = 5$ mA at changing the working distance by $\Delta l_{work} = 100$ mm. This weak relation $I_f = f(l_{work})$ proves that in this case a long focusing system is used.

Testing the conditions of finishing smoothing of reverse beads of welds using a system of electron beam refraction by 90° was performed on flat specimens of titanium alloys VT20 of 17 mm thickness. Welds and reverse beads were produced after making through penetration at a gravity position without backing of titanium specimens by a horizontal electron beam at $v_w = 30$ mm/s using a main electron gun of installation KL-138 without a system of electron beam refraction by 90° during a gun movement in horizontal plane [4]. By changing the amplitude of transverse oscillations of electron beam by a sawtooth law it was managed to form the defect-free face beads of weld and reverse beads with small undercuts of 1.2–2.0 mm width and height of 0.5–0.8 mm and without undercuts. As is shown in Figure 3, the finishing pass along the reverse beads of width of 1.2 (Figure 3, *a*, *c*) and 1.8 mm (Figure 3, *b*, *d*) at the selected condition ($U_{acc} = 60$ kV, $I_b = 20$ mA, $v_w = 6 =$ mm/s, $l_{work} = 100$ mm) made it possible to form a weld root part with smooth transitions from base metal to the weld, to produce a smooth surface without drops of molten metal and to eliminate small undercuts of depth down to 0.15 mm. Height of both reverse beads decreased and was not more than 0.4 mm, and the depth of penetration on the weld root side was 2.5 mm, that is correlated with results given in Figure 2.

The obtained results were realized in finishing smoothing of reverse bead of weld on the long tubular product of a rectangular shape of an intricate configuration with a reverse bead location on the lower surface. During movement of system of electron beam by 90° along the reverse bead, $l_{work} = 100$–250 mm. In
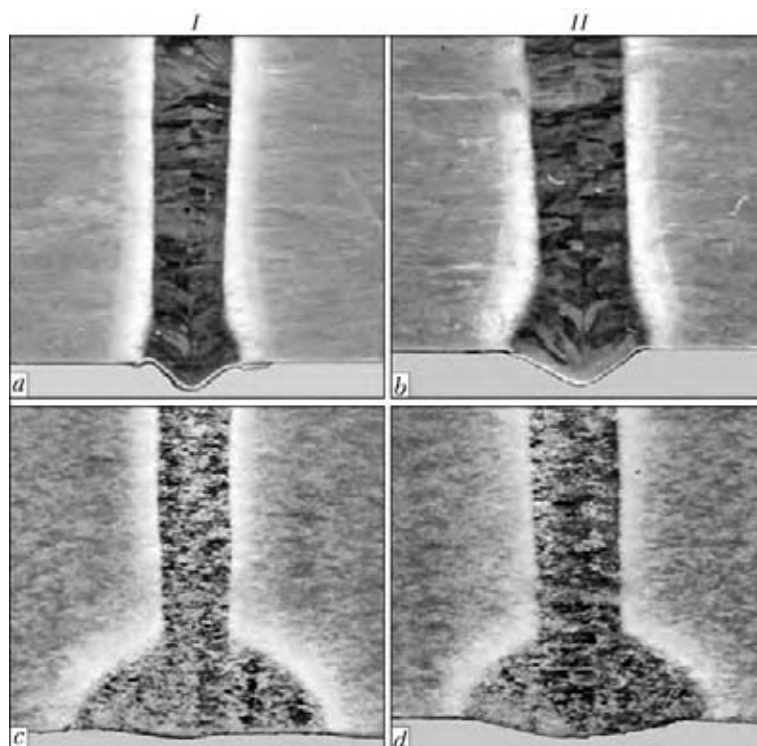
**Figure 3.** Macrostructure (×27.5) of welded joints of alloy VT20 and formation of weld reverse beads of 1.2 (*I*) and 1.8 (*II*) mm before (*a*, *b*) and after (*c*, *d*) their finishing smoothing

compiling the computer program of control of finishing smoothing all the parameters of electron beam are preserved constant, except the focusing current. This procedure allowed obtaining almost the constant width of penetration along the entire length of the product, which was $B \cong 5.3$ mm.

The investigations of finishing smoothing of linear reverse beads of weld can be fully applied in EBW with through penetration of position butts of long tubular products of a round shape. In this case the task of smoothing is simplified, as the working distance is preserved constant. In making EBW of long products of refractory materials with a depth of penetration $h_p \leq 6$ mm, for example such as waveguides and resonators [5], the application of system of electron beam refraction by 90° is the only possible variant

of finishing smoothing of weld reverse bead with a formation of a smooth surface without undercuts.

1. Borovik, V.M., Frolov, O.V., Shubin, F.V. (1991) Flashing of inner surface of cylindrical specimens by deviated beam. In: *Proc. of 11th All-Union Sci.-Techn. Conf. on Electron Beam Welding* (Nikolaev, 1–3 Oct. 1991). Leningrad: Sudostroenie, 73–74.
2. Nazarenko, O.K. (2008) Reduction of evacuation time of large-sized vacuum chambers of electron beam welding installations. *The Paton Welding J.*, **3**, 41–42.
3. Nudelman, Ya.B., Zadery, B.A. (1988) Weld formation in electron beam welding of titanium alloys up to 25 mm thickness. *Avtomatich. Svarka*, **5**, 29–30.
4. Kravchuk, L.A. (2010) Elimination of undercuts in EBW with complete and incomplete penetration. *The Paton Welding J.*, **6**, 22–25.
5. Zhdanevich, M.L. (1989) Deformation of resonators in electron beam welding. In: *Abstr. of All-Union Sci.-Techn. Conf. on Electron Beam Welding in Machine-Building* (Nikolaev, Sept. 1989), 41–42.

# DEVELOPMENT OF SURFACE CRACK-LIKE DEFECT IN WELDED JOINTS OF 06GB-390 STEEL AT CYCLIC LOADING

**A.Yu. BARVINKO, V.V. KNYSH, Yu.P. BARVINKO** and **A.N. YASHNIK**
E.O. Paton Electric Welding Institute, NASU, Kiev, Ukraine

The paper presents the results of experimental studies of a surface crack-like defect in a butt welded joint on flat specimens of 06GB-390 steel under cyclic loading to formation of a through-thickness crack. Dependence of growth of a surface crack-like defect in vertical butt welded joints on the loading cycle number was established for design rings of walls of oil storage tanks. It is shown that in the presence of surface defects in welded joints application of rolled plates of 06GB-390 steel for the design rings of tank wall provides a substantial improvement of their operational safety.

Operation of oil storage tanks with single or double walls (main and shielding) envisages everyday visual inspection of their surfaces with statement of the fact of the presence or absence in them of visually detectable surface cracks or oil spots from oil sipping through through-thickness cracks. Appearance of oil traces on the wall surface is the result of the final stage of development of a surface or inner crack-like defect. Surface crack after growing and reaching the opposite surface of tank wall is the most critical defect. Therefore, determination of the number of cycles of tank draining-filling with oil with its accepted operation mode that leads to formation of a through-thickness crack is an urgent task both for regular single-wall and for double-wall tanks. Determined cyclic fatigue life of welded joints of tank walls with the considered surface defects, allows precising their repair time and preventing further development of the through-thickness crack. Investigation of cyclic fatigue life of surface crack growing, including its reaching the opposite surface, is the first stage. It is necessitated by application over the recent years of new steels of grades S440, S390 and S350 for tanks of $V = 50-75$ thou m$^3$ capacity [1]. These steels differ from those recommended by normative document [2, 3] by a low content of carbon and sulphur, as well as mechanical properties (ductility, cold resistance, $KCV$), greatly exceeding the current requirements [2, 3].

It should be noted that steels of grade S390 of 10–30 mm thickness with required impact toughness $KCV \geq 50$ J/cm$^2$ at temperature $T = -20-40$ °C are practically absent in normative documents [2, 3] among those recommended for tank walls. This niche is occupied by new generation steels 06GB-390 and 09G2SYuch-U [1, 4] (steel grade will be omitted further on in designation of 06GB-390 steel). Rolled plates from 06GB steel have been successfully tried

out in construction of four tanks of $V = 50$ thou m$^3$ capacity in LPDS «Mozyr» (Belarus Republic). Steel of 8–50 mm thickness has $KCV > 118$ J/cm$^2$ at $T = +20 - -40$ °C [1]. $T = -40$ °C is the minimum design temperature for all the CIS and European countries. As the results of testing specimens at $T = +20$ and $-40$ °C are in the upper region of the curve of $KCV$ dependence on testing temperature, data obtained at $T = +20$ °C are extended to the entire upper plateau of this curve.

Figure 1 shows the schematic and dimensions of tested specimen of welded joints with a crack-like notch. PWI technology of welding rolled plates from 06GB steel ensures equivalent strength of the welded joint [5]. Transverse butt weld had through-thickness penetration. Mechanical properties of rolled plates of 06GB steel obtained on three specimens are as follows: thickness $\delta = 20$ mm; yield point $\sigma_y = 387.4$ MPa/mm$^2$; ultimate tensile strength $\sigma_t = 477.9$ MPa/mm$^2$; relative elongation $\delta_5 = 35.6$ %; relative reduction $\psi_z = 79.6$ %; impact toughness $KCV_{-40} = 232$ J/cm$^2$; $\sigma_y/\sigma_t = 0.81$.

At welded joint testing for static bending fractures ran though the base metal. Along the fusion line $KCV_{-40}$ of welded joint metal was equal to 341.1 J/cm$^2$ (average from three specimens).

Notch in welded joints was milled along the fusion line with rounding-off radius $r = 0.25$ mm, its depth being 6 mm, and length $-$ 39 mm (see Figure 1). All together nine specimens were tested, seven of them from 06GB steel. Three of them were pre-stretched before testing to obtain residual deformation $\delta_{res} = 0.8-1.0$ %. For comparison two specimens were made from 09G2S-12 steel with 0.01 wt.% S and 0.013 wt.% P content.

Specimens were tested at harmonic cyclic loading $P_{cyc}$ in TsDM-200pu pulsator with 5 Hz frequency. Maximum cycle stress was equal to $\sigma_{max} = 2/3\sigma_y$, that corresponds to values of maximum circumferential stresses in the tank wall, and minimum cycle stress $\sigma_{min} = 0.1\sigma_{max}$. Cross-section of specimens from 06GB
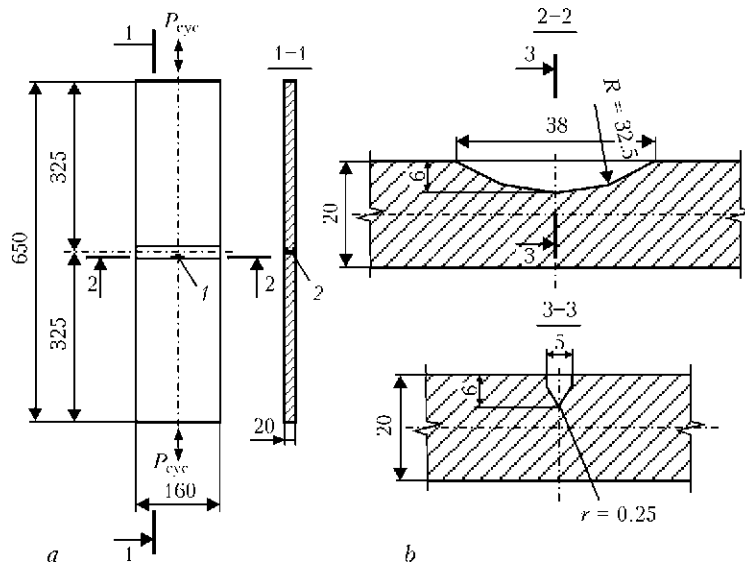
**Figure 1.** Schematic (*a*) and dimensions (*b*) of specimen of 06GB steel welded joints for cyclic crack resistance testing: *1* — notch along the fusion line in HAZ; *2* — weld reinforcement removed from two sides

steel was taken to be $160 \times 20$ mm, and that from steel 09G2S-12 — $160 \times 16$ mm. Dimensions and maximum stresses at cyclic loading allowed performance of crack resistance testing of welded joints with development of surface crack-like notch under the conditions of a plane-strain state up to formation of a through-thickness crack on the opposite surface and its propagation up to length $l = 2a$ ($30-40$ mm). Taken dimensions of the initial notch were close to visually detected cracks in vertical welded joints of the wall of tanks of $V = 10,000, 20,000$ and $50,000$ m$^3$ capacity. At the first stage of testing, number of loading cycles, corresponding to the moment of fatigue crack formation over the entire notch front was determined, and the sequence of the process of its development from the notch up to reaching the opposite surface was established. Schematic of formation of a through-thickness crack is given in Figure 2. Testing results are given in the Table.

On four specimens, which were tested without pretension, the average cycle number to crack initiation along the entire notch length was equal to 14.5 thou. Testing of two specimens (6, 7) at initial residual tensile deformation $\delta_{res} = 0.8-1.0$ % showed an increase of cycle number before crack initiation over the entire notch front by almost 30 %. Such a result was obtained due to reduction of the notch sharpness at pre-stretching of specimens before their plastic deformation. Crack growing on specimen 5 can be regarded as the result of notch deviation from the fusion line or absence of a clear-cut fusion line across thickness. After formation of a fatigue crack in specimens over the entire notch front the coefficient of stress concentration in their tips became the same. Under these conditions, the number of loading cycles in specimens 1–7 before fatigue crack reaching the opposite surface (taking scatter into account) was actually the same and was equal to $N = 10.3$ thou on average. Cracks on the notch surface and on the opposite side have the same length in all the specimens. Process of fatigue crack formation and its growing up to reaching the opposite surface is well-illustrated by Figure 3. Fracture symmetry is disturbed by the presence of a defect

Results of testing specimens with initial surface notch along the fusion line of the HAZ of 06GB and 09G2S-12 steel welded joint

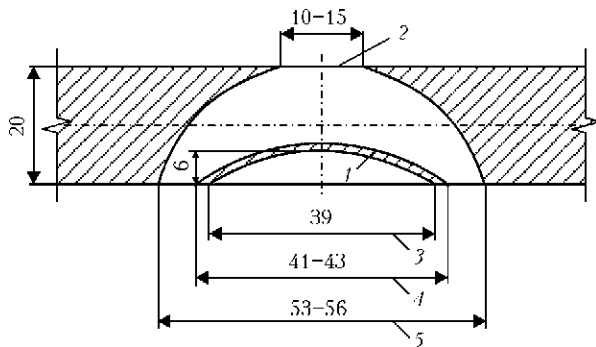| Specimen number | Steel grade | Welded joint state | Number of cycles by the moment of crack initiation over the entire notch front, thou | Initial length of crack on specimen surface, mm | Number of cycles from crack initiation over the entire notch front up to formation of through-thickness crack, thou | Crack length from the notch side at formation of through-thickness crack, mm | Length of through-thickness crack at its reaching the opposite surface, mm |
|---|---|---|---|---|---|---|---|
| 1 | 06GB | As-welded in free state | 16.9 | 42 | 13.4 | 59 | 15 |
| 2 | | | 12.6 | 40 | 10.0 | 56 | 10 |
| 3 | | | 14.2 | 42 | 12.8 | 56 | 10 |
| 4 | | | 14.2 | 40 | 10.0 | 57 | 10 |
| 5 | 06GB | Pre-stretching of specimen up to 0.8–1.0 % at residual deformation | 9.9 | 40 | 7.9 | 59 | 10 |
| 6 | | | 20.0 | 40 | 7.2 | 59 | 10 |
| 7 | | | 18.2 | 41 | 10.9 | 58 | 11 |
| 8 | 09G2S-12 | As-welded in free state | 20.4 | 41 | 13.6 | 54 | 12 |
| 9 | | | 49.2 | 41 | 13.3 | 49 | 8 |

Figure 2. Schematic of formation of initial crack from the notch and its growing up to through-thickness crack with reaching opposite surface: *1* — initial through-thickness crack; *2* — initial notch; *3* — length of crack-like mechanical notch; *4* — initial crack length; *5* — crack length at its growing to through-thickness crack



Figure 3. View of the surface of through-thickness fatigue crack (specimen 1)

in the weld (lack-of-fusion on the right side). In Figure 3 it is seen that at the beginning the fatigue crack about 5 mm deep forms over the entire notch front, and then it propagates across specimen thickness reaching its opposite surface (its initial length is equal to 10−5 mm).

Results of testing specimens from 09G2S-12 steel confirmed the known data that steels with a developed yield plateau have a high resistance to initiation and development of fatigue cracks [6, 7]. However, low cold resistance (by impact toughness value) of the above steels essentially limits their application in structures operating at low temperatures.

For practical application it is important to know the number of cycles of tank wall loading, time of fatigue crack initiation from the available surface crack-like defect (notch), and its growing across thickness up to formation of a through-thickness crack. Results of testing only specimens 1−4 having no softening of the notch sharpness were considered. Average cycle number was equal to 14.5 and 10.3 thou. For real structures assessment of results obtained on the specimens was made allowing for the safety factor per loading cycle number. Interstate Research Committee on Pressure Vessels recommends taking this coefficient to be equal to 20 [8]. Then the real number of loading cycles up to fatigue crack formation is equal to 725, and up to its growing with formation of a through-thickness crack — 515 cycles. Obtained data indicate that at application of 06GB steel for design rings of tank wall and annual number of loading cycles of 120 (operating mode of most of oil tank farms) fatigue crack initiation from a sharp surface notch 40 mm long present on the wall surface can be expected in 6 years. The process of transition of the formed fatigue crack into a through-thickness crack at tank wall thickness of 20 mm occurs during 4 years of operation. Obtained data are in good agreement with normative document [9], which specifies performance of partial examination of new tanks every 5 years (after 20 years of operation — every 4 years) and complete examination every 10 and 8 years, respectively. Such terms allow at partial examination performing visual determination of the presence of surface defect formed on the wall, and in the case of fatigue crack development from it — detecting it by
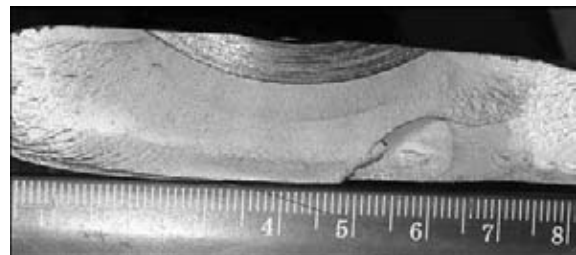
ultrasonic testing at the next complete examination of the tank.

Thus, presented results give an assessment of just the process of fatigue crack initiation from surface defect and its growing across specimen thickness up to its reaching its opposite surface. Fatigue crack, however, can also initiate from inner crack-like defects (lacks-of-fusion along the edges, different flat inclusions, etc.) or surface defect, located on tank wall inner surface. In this case, the surface crack will be manifested already at the stage of through-thickness one. This part of investigations is the second stage of the work, at which the process of propagation of through-thickness fatigue crack in the initial section of fatigue development diagram [8] along the fusion line of welded joint on 06GB steel 20 mm thick will be studied for walls of oil storage tanks. Results of these investigations will be published in one of the next issues of the journal.

**CONCLUSIONS**

1. Butt welded joints of rolled plates of 06GB steel in the case of walls of oil storage tanks have a high resistance to development of a fatigue crack from surface sharp defects in the direction of plate thickness under cyclic loading at plane deformation.

2. Terms of partial and complete examination of tanks from 06GB steel specified in normative documents allow detecting in their wall sharp surface defects before fatigue crack initiation from them, and in the case of its initiation allow taking the required safety measures and repairing the detected defects.

1. *TU U 27.1-05418923-085:2008*: Sheet products to be welded of quality steel of strength grade 355−590 for machine-building. Introd. 28.12.2006.
2. *GOST 31385−2008*: Steel vertical cylindrical tanks for petroleum and petroleum products. Introd. 02.06.2009.
3. *PB 03-605−03*: Rules of arrangement of steel vertical cylindrical tanks for petroleum and petroleum products. Introd. 09.06.2003.
4. *TU 14-1-5065−2006*: Amendments No.1. Plate iron of low alloy steel of grades 09G2SYuch, 09G2SYuch-U, 09KhG2SYuch and 09KhG2SYu-U. Introd. 27.12.11.
5. Poznyakov, V.D., Barvinko, A.Yu., Barvinko, Yu.P. et al. (2012) Cold resistance and lamellar fracture resistance of welded joints on steel 06GB-390. *The Paton Welding J.*, **3**, 35−39.
6. Novikov, V.I., Girenko, V.S., Bernatsky, A.V. (1985) Anisotropy of properties of rolled metal and serviceability of welded structures. *Avtomatich. Svarka*, **12**, 13−19.
7. Nikiforchin, G.N., Student, A.Z. (1981) Application of nonlinear fracture mechanics for evaluation of resistance to corrosion crack growing. In: *Transact. on Methods and Means of Corrosion Resistance Evaluation of Structural Materials*. Kiev: Naukova Dumka.
8. Nichols, R.V. (1975) *Design and technology of pressure vessech production*. Moscow: Mashinostroenie.
9. *DSTU-N B A.3.1-10:2008*: Recommendations for conducting technical diagnostics of steel vertical tanks. Valid from 2009.

# METHOD FOR MANUFACTURE
# OF LARGE-SIZED FORGED-CAST BILLETS
# USING ELECTROSLAG WELDING

**A.I. VOLOSHIN**[1], **K.P. SHAPOVALOV**[1], **V.A. BELINSKY, S.N. LITVINENKO, K.A. YUSHCHENKO**[2],
**I.I. LYCHKO**[2] and **S.M. KOZULIN**[2]
[1]Novo-Kramatorsk Machine-Building Works (NKMZ company), Kramatorsk, Ukraine
[2]E.O. Paton Electric Welding Institute, NASU, Kiev, Ukraine

Given are the results of application of a new technology for production of combined bimetal parts by using consumable-nozzle electroslag welding with the complicated-configuration welds.

Development of current machines and assemblies of press-forging, rolling-mill and power equipment tightly connected with manufacture of large-sized monolithic billets of up to 300 t and more weight. Two ways are mainly used to solve this at present stage. The first is application of corresponding capacities of steelmaking, press-forging and cast productions allowing obtaining of large-sized billets, and the second is enlargement of billets using welding.

Decisions about a method for obtaining of billets at Novo-Kramatorsk Machine-Building Works (NKMZ) are made by engineering services based on analysis of structural, technological and economic aspects of a problem. The aim at that is minimization of expenses and providing of necessary quality of the part. Considering this the Plant created technological capabilities for application of electroslag welding of rectangular sections of 5000 × 6000 mm size and automatic submerged arc welding of cylinder parts of up to 4000 mm in diameter at 500 mm wall thickness [1].

Calculations of strength and verification of structure serviceability (these procedures are carried out with the help of ABAQUS, SIMULATION and COS-MOS-MOTION programs at NKMZ) show that the whole structure has a non-uniform loading. Specifying of material for the whole part orienting at stressed state in places of maximum loading is economically unpractical. It is desirable to provide necessary me-chanical properties in the separate segments of the part minimizing at that excessive strength margins and surplus expenses, respectively.

Development of large-sized combined bimetal parts is used at the present time at NKMZ for solving this task. Significant reduction of expenses for production of quality billets, reduction of prime cost and increase of product competitiveness is promoted by means of application of forged inserts from alloyed steels in the places of maximum loading of the part manufactured from unalloyed steel cast.

Forged-cast structure of anvil block of stamping hammer, in which maximum level of stresses appears under the effect of work loading in the middle zone of the anvil block, can serve an example.

Decision about bimetal structure of the anvil block combining forged middle part from steel ITs-1A (analog of 16GNMA steel) with cast side pieces from steel 30L was made in development. Tables 1 and 2 show chemical composition and mechanical properties of applied materials, respectively. Parts of the anvil block were joined by traditional welds made using electroslag welding (ESW) and located in one plane (Figure 1). Such a welding technology is mastered and widely used at NKMZ.

New methods of strengthening of stressed places of the part (Figure 2) through obtaining of combined billets of more complex shape were developed by engineers of Chief Welder Department of NKMZ in the process of improvement of technique and technology

**Table 1.** Chemical composition of the materials used for anvil block manufacture, wt.%

| Material of the anvil block | C | Si | Mn | Ni | P | S | Mo | Cr |
|---|---|---|---|---|---|---|---|---|
| Steel 30L (GOST 977−75) | 0.27−0.35 | 0.20−0.52 | 0.4−0.9 | − | ≤ 0.04 | ≤ 0.04 | − | ≤ 0.3 |
| Steel ITs-1A (steel 16GNMA GOST 2246−80) | 0.12−0.18 | 0.17−0.37 | 0.8−1.1 | 1.0−1.3 | ≤ 0.04 | ≤ 0.04 | 0.40−0.55 | ≤ 0.3 |

**Table 2.** Mechanical properties of the materials used for anvil block manufacture ($T = 20$ °C)

| Material of the anvil block | $\sigma_t$, MPa | $\sigma_y$, MPa | $\delta$, % | $\psi$, % | $KCU$, kJ/m$^2$ |
|---|---|---|---|---|---|
| Steel 30L | 480 | 260 | 17 | 30 | 350 |
| Steel ITs-1A | 560 | 400 | 21 | 60 | 1200 |

of consumable-nozzle ESW for further reduction of prime cost of large-sized billets. The task at that is to master a technology of ESW of welds of П-shape.

Welds of such shape and sizes were not performed earlier in welding engineering practice on technical as well as technological reasons. First of all, corresponding specialized welding equipment is necessary for obtaining of П-shaped welds. Secondly, welding-in of such a called implantate simultaneously to three planes of rigid edges of massive billet (Figure 3) can be accompanied by formation of cracks in HAZ and
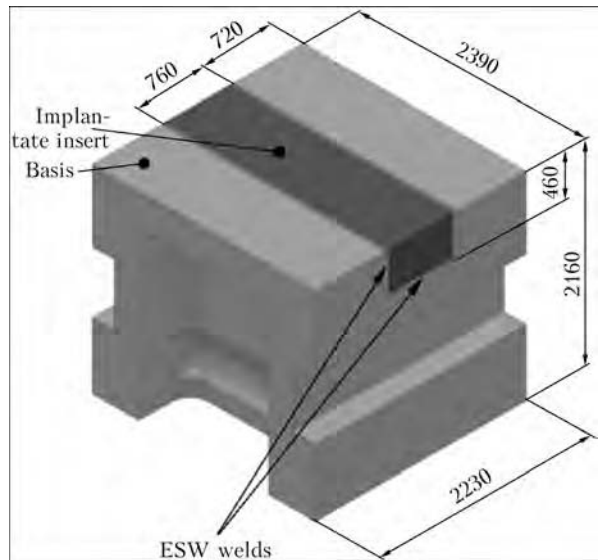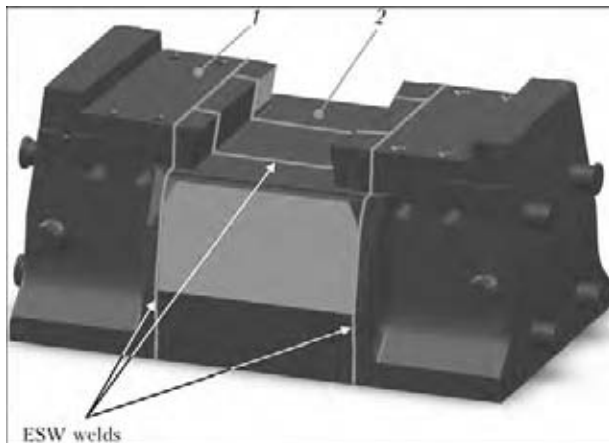


**Figure 1.** Location of ESW welds in manufacture of the anvil block: *1* — cast parts (steel 30L); *2* — forged-welded middle part of the anvil block consisting of three forged pieces from steel ITs-1A
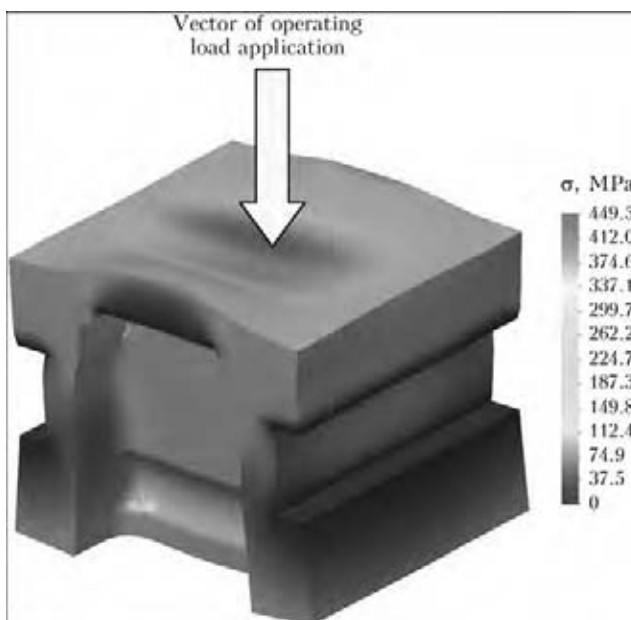


**Figure 2.** Stress-strain state of basis of the anvil block at the moment of application of operating load



**Figure 3.** Variant of combined bimetal basis with insert from 20KhN2M steel

weld. In this connection there can be hot as well as cold cracks.

Agreement was made between the NKMZ and the E.O. Paton Electric Welding Institute about a joint work in this important direction due to old industrial relations as well as their common interest to indicated complex task. Necessary temperature-time conditions of formation of welded joint in closed rigid space were determined considering technical capabilities of welding production of NKMZ [1] and obtained experience in ESW of the parts of large thickness [2]. At that the welded-in implantate suffers from influence of complex heat-deformation simultaneously along the whole weld perimeter. Technique and technology of consumable-nozzle ESW of complicated-configuration welds were developed as well as modes of further volume high-temperature treatment of welded part were selected. A decision was made about industrial-experimental testing of developed technique and technology using standard part, i.e. basis from parent metal of GS-45 steel (analog of steel 25L) with forged implantate of $420 \times 680 \times 2590$ mm size from steel 20KhN2M and П-shaped weld (Figure 4).
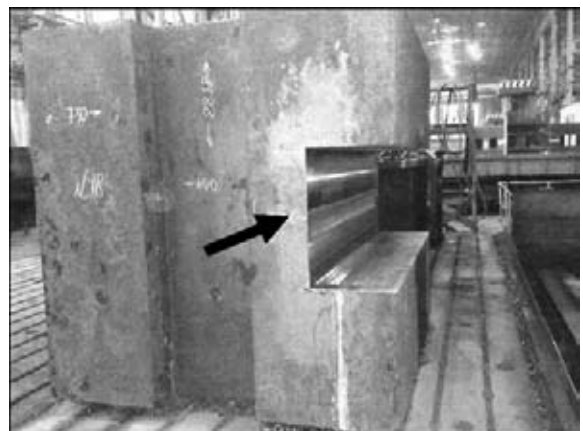


**Figure 4.** Appearance of the billet prepared for welding-in of forged implantate in the cast billet of anvil block basis using ESW method
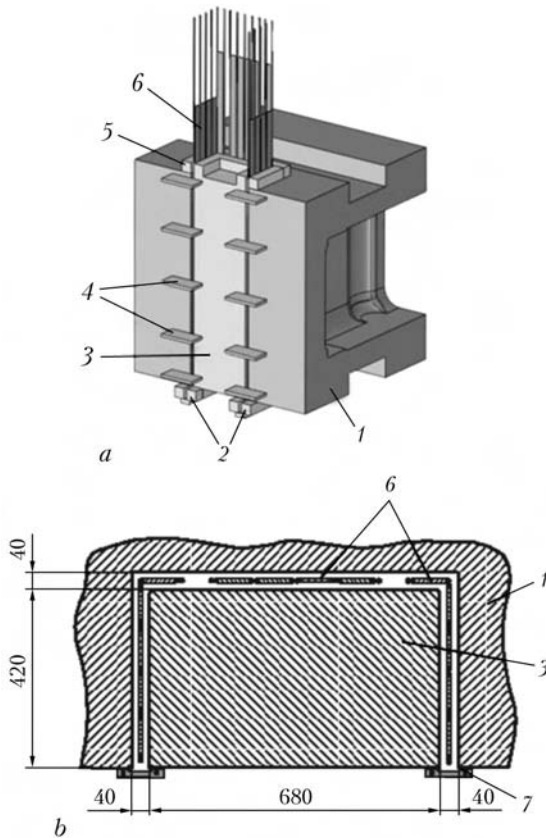
**Figure 5.** General view (*a*) and scheme of assembly for consumable-nozzle ESW (*b*): *1* — welded part; *2* — inlet implantate; *3* — forged insert (implantate); *4* — technological bars; *5* — outlet pockets; *6* — consumable nozzle; *7* — forming devices

Three sections of consumable nozzles, made from separate plates (Figure 5) and 1100 kg of welding wire was necessary for ESW of joint of complicated Π-shaped form and dimensions, indicated in Figure 5, *a*. At that system for duplicating of feeding of welding wire provided safe performance of complicated Π-shaped weld as in welding of welds in one plane.



**Figure 6.** Moment of welding-in of the implantate at plant complex

The welded part after mechanical and heat treatment (Figure 6) was subjected to ultrasonic testing. The latter confirmed high quality of welded joint obtained using new technology. Two similar parts have already been welded at present time.

Therefore, manufacture of welded parts as well as parts from metals with different properties was proposed for the purpose of reduction of prime cost of the manufacture of large-sized billets for components of rolling-mill, power and press-forging equipment. At that, selection of material for separate parts of the billet should be made based on analysis of stresses appearing in them under effect of operating loads. The new technology of ESW with the large-sized complicated-configuration welds was developed and successfully tested by the specialists of NKMZ and E.O. Paton Electric Welding Institute for the most efficient realization of the proposed concept.

1. Nevidomsky, V.A., Krasilnikov, S.G., Panin, A.D. et al. (2002) New machine for electroslag welding of large parts at JSC «NKMBF». *The Paton Welding J.*, **2**, 49–51.
2. (1980) *Electroslag welding and cladding*. Ed. by B.E. Paton. Moscow: Mashinostroenie.

*Scientific and Practical Seminar dedicated to ninety years since the birthday of Doctor of Technical Sciences, Prof. M.I. Razikov (1922—1975), a known scientist in the field of welding and surfacing, who had been working for many years as a head of the welding chair at the Urals Polytechnic Institute, was held in Nizhny Tagil on the 3rd of February 2012. Prof. Razikov was also the organiser and first leader of the branch surface laboratory at the Urals Polytechnic Institute. The Seminar was attended by over 80 specialists and managers of 35 enterprises and organisations from 17 cities of Russia and Kazakhstan, including a number of leading mining and metallurgical enterprises of the Urals region — Nizhny Tagil and Chelyabinsk metallurgical works, Kamensk-Uralsky and Serovsky metallurgical factories, Uralvagonzavod, Kochkanarsky and Vysokogorsky ore-dressing and processing enterprises, Uralmashzavod, etc. The Seminar considered in detail the subject of upgrading of repair of mining and metallurgical equipment parts by using plasma hardening. Below we give the paper presented by Dr. V.A. Korotkov, covering the experience of application of plasma hardening unit UDGZ-200 at different companies.*

*Editorial Board*

# EXPERIENCE OF APPLICATION OF PLASMA HARDENING UNIT UDGZ-200 AT ENTERPRISES OF THE URALS REGION

**V.A. KOROTKOV**

Nizhnetagilsky Technological Institute (subsidiary), Urals Federal University, Nizhny Tagil, Russia

It is well known that the constricted arc (plasma) is widely applied for welding, surfacing, deposition of protective coatings, surface hardening, etc. Company «Composite Ltd.» (Nizhny Tagil) developed and certified mobile unit UDGZ-200, allowing plasma hardening to be performed with a hand tool. The unit has a double-case design, weight of 20 + 20 kg, and is powered from the 380 V mains, the power consumption being 10 kW. Argon is used as plasma and shielding gas, the consumption of which is 20 l/min. Productivity of the unit is 25—85 $cm^2$ of the surface treated per minute. Depending on the grade of the steel being processed, hardness of the treated layer is $HRC$ 45—65, and its thickness is 0.5—1.5 mm. Carbon or tool steels are subjected to treatment. Therefore, no special cooling of a workpiece is required, this making the labour management much simpler. The required cooling rate is provided by removing heat into the bulk of a workpiece.

Plasma hardening of different-purpose dies has received considerable acceptance. For instance, application of plasma hardening unit UDGZ-200 at Uralvagonzavod allowed hardness of the leading edges of cutting dies made from steel 5KhV2S to be increased to $HRC$ 61, that from steels 5KhNM and 7Kh3 to $HRC$ 64, and that of steel U8 — to $HRC$ 58. Plasma treatment provided an approximately 2.7 times increase in resistance of the dies. The die block for cutting of receiver bottoms is shown in Figure 1. The discernible temper colours usually appearing in heating of metal do not lead to deterioration of parameters of surface roughness.

Plasma hardening of cast iron dies (inserts) for forming of large-diameter pipes is performed at the Chelyabinsk Pipe Rolling Mill (Figure 2). Earlier the Mill used gas flame hardening for such dies. Application of plasma hardening using a hand tool instead of gas flame hardening provided increase in hardness of



**Figure 1.** Die block for cutting of receiver bottoms after plasma hardening
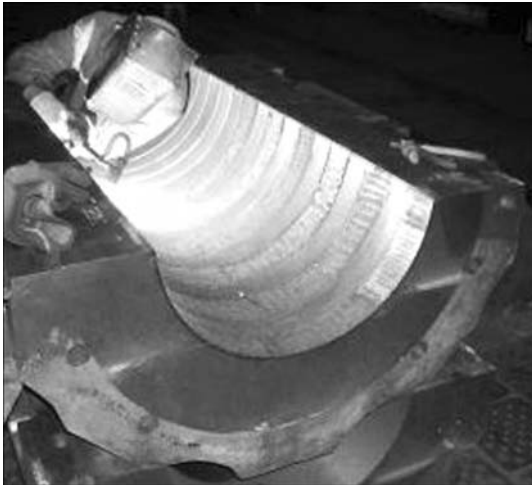
**Figure 2.** Plasma hardening of die performed at the Chelyabinsk Pipe Rolling Mill

the dies from *HRC* 50 to *HRC* 60. As a result, their resistance grew about 3 times.

Corporation VSMPO-AVISMA obtained positive results from application of plasma hardening for multi-ton dies of steel 5KhNM. For higher hardness and wear resistance, tempering of these dies after hardening from furnace heating was performed at a decreased temperature. But that affected strength of the dies — they began cracking. Surface plasma hardening allowed increasing the tempering temperature to prevent cracking without any decrease in hardness and wear resistance. As an experiment, this approach was applied at the Kamensk-Uralsky Metallurgical Factory (Figure 3).

Many large-size dies have a long-time manufacture cycle, involving cutting into relatively small parts for volume hardening in furnaces and subsequent labour-consuming fitting up of hardened fragments into a whole. The Volzhsky Motor Car Factory conducted an experiment by replacing volume hardening by surface plasma hardening (Figure 4), which allowed avoiding fitting up of the hardened parts (about 30 % of the total work content consumed for manufacture of a die), as they were manufactured as a whole following the drawing dimensions. A die used to make over 70,000 items (automobile cover tail beams) is still in a workable condition. The labour consumption for repair «conditionings» decreased approximately



**Figure 3.** Complex-configuration die after plasma hardening (KUMZ Ltd.)



**Figure 4.** Fragment of split die after plasma hardening

10 times due to reduction of frequency and duration of these operations.

The similar result was obtained also by the Gorky Motor Car Factory with experimental hardening of



**Figure 5.** Die block of GAZ car after plasma hardening of pressure loop



**Figure 6.** Die block for forming of large-diameter three-way pipes after plasma hardening



**Figure 7.** Plasma hardening of teeth of coarse-pitch gear

**Figure 8.** Plasma hardening of freight car centre plate collar and fragment of hardened surface



**Figure 9.** Shearing machine hopper lined with plates after plasma hardening

die blocks used for forming of right and left front car wings (Figure 5).

Three sets of die block for manufacture of formed-welded three-way pipes with a diameter of 530, 720 and 820 mm (steel 30GSL) fractured because of low hardness approximately after 50 forming operations at the Liskinsky Factory of Assembly Blanks. Plasma hardening with subsequent dressing of surfaces (Figure 6) allowed restoring performance of the die blocks. After the same quantity of formings they remained suitable for further operation.

Unit UDGZ-200 is successfully applied for hardening of gear and spline drives with modulus $m \geq 6$ (Figure 7). Plasma hardening is used to treat gear rings of mills, double-helical teeth and splines on gear shafts, transmission gears of railway locomotives, etc. As a result of plasma hardening the service life of gears is extended 2–3 times.

One of the most wearing locations on a freight car truck is a centre plate collar. Plasma hardening applied by Uralvagonzavod provided a two times increase in hardness of the collars (Figure 8), i.e. from $HB$ 180 to $HB$ 360, which resulted in a considerable reduction of their wear (from 1000 to 50 μm / 100,000 km).

This enterprise has experience in plasma hardening of transportation rails for wheelset axle production line. After manufacture of 200,000 axles the rails wore out by 3.2 mm in height. Similar rails after plasma hardening wore out only by 0.5 mm after manufacture of 320,000 axles. Therefore, wear resistance was increased more than 6 times as a result of plasma hard-

ening. At present, Uralvagonzavod is arranging application of plasma hardening for mass production of railway cars.

The similar result was obtained with rail tracks for workshop transfer buggies at the Chelyabinsk Pipe Rolling Mill. Before utilisation of plasma hardening the rails were replaced at a frequency of one to two times, and in the most heavy-loaded sections — up to six times a quarter. That created much tension, as the rails were of a special gauge, and they were imported from Germany. After plasma hardening of rails and wheels in 2006–2007 their wear slowed down dozens of times, and the rails were replaced only in 2011.

The Mill performed plasma hardening of heavy crane rails KR-100. Wear of the hardened rails was about 0.2 mm, and that of the non-hardened rails was approximately 2 mm, the operation life being identical.

To provide protection from fast wear, the working surfaces of Pilger mill stands are covered with face plates, which are usually replaced three times a year because of wear. The stand itself under the face plates wears out by up to 10 mm, and it is necessary to clad it once a year and then mill the deposited layer. Plasma hardening of the face plates and working surfaces of the stands provided decrease in the rate of their wear, and consumption of the plates and quantity of the claddings on the stand were reduced by a factor of 3. The similar effect was obtained with plasma hardening of lining plates of the shearing machine hopper at Metallurgical Works «Kamastal» (Figure 9).

At present, Composite Ltd. performs plasma hardening of up to 1000 m$^2$ of working surfaces of various parts by using units UDGZ-200. Such a unit was purchased by Uralvagonzavod, VSMPO-AVISMA, OR-METO-YuUMZ, Orsk and Bakal mining equipment factories, as well as enterprises of Kazakhstan and Ukraine.

*Memorable dates*

# LIGHT-WEIGHT WELDING TRACTORS
# OF THE E.O. PATON ELECTRIC WELDING INSTITUTE

65 years ago the E.O. Paton Electric Welding Institute developed a new generation of welding equipment, such as self-propelled welding device SAG-4 and a series of specialised tractors of the TS type for automatic submerged-arc welding. Welding tractor TS-17 held a longevity record among the arc welding devices.

Devices for automatic submerged-arc welding with a constant electrode wire feed speed, which had been developed by the E.O. Paton Electric Welding Institute during the Second World War, received wide acceptance in manufacture of tanks, air bombs and other arms.

About 700 suspended welding heads in a set with auxiliary equipment for movement of workpieces, or with carriages for movement of the heads were manufactured at workshops of the Institute and at factories. The post-war conversion required development of a more versatile equipment suitable for a wide range of parts and specialised assembly-welding units for conveyers. The main goal of the scientific and technological progress in the field of welding was to address the problems of rise in productivity and stability of functioning of the equipment, improvement of working conditions, saving of labour, etc. It was necessary to develop apparatuses for mechanised submerged-arc welding, including for making of relatively short welds, as well as devices for welding in spatial positions other than the flat one.

Upgrading of the equipment was dictated by the necessity to improve reliability of feeding of flux, directing of the electrode tip along the weld axis, failure-free ignition of the arc, and maintaining of energy input into the welding zone in real time without operator's interference. A pressing problem was to preserve succession and unification of assemblies and components of the already proven samples of the equipment. Similar problems were addressed also by welders in the USA, Great Britain, Germany and other countries.

To handle these problems, the E.O. Paton Electric Welding Institute used a system analysis of all components of the welding equipment, studied the experience gained in machine and apparatus building, as well as the specific features of the welding process. To decrease the required skill of welders and avoid difficulties in debugging, it was necessary to simplify control of the apparatuses.

Portable tractor TS-6 designed in 1945 at the E.O. Paton Electric Welding Institute (Vladimir E. Paton) opened up a series of specialised light-weight welding apparatuses. Compared to the heads of the war period, this tractor was less cumbersome and permitted a wider range of adjustment as to the height, inclination angle and turning radius. The quantity of control buttons and knobs was minimised.

During a period of 1945–1947, the E.O. Paton Electric Welding Institute developed a series of specialised tractors TS-11 and TS-12 (for butt welding with and without edge preparation, respectively), and TS-13 (for gravity fillet welding), which provided the welding speed of 22 to 44 m/h at currents of 600–1000 A. Weight of the tractors without wire and flux was about 40 kg. However, many industries needed a versatile portable hand-held apparatus for automatic



Stringent acceptance of model of tractor TS-6



TS-17 in field camp of Dashava–Kiev gas pipeline

The Paton WELDING JOURNAL

TS-17 in production line

submerged-arc welding. In 1947, V.E. Paton developed tractor TS-17 for butt and fillet welding. This apparatus featured an optimum combination of comparatively small dimensions, low weight (42 kg) and simplicity in operation. A copying element of the tractor was the apparatus itself, where the front or rear wheels were replaced by wedge-shaped rollers, depending on the type of a welded joint. Several variants of adjustment made the tractor versatile, as among other things it also allowed making of circular welds inside vessels.

Tractor of the TS-17 type quickly became popular in many industries, and was in operation for several decades. Moreover, it served as a prototype for a range of welding mechanisation facilities. Devices for thin-wire arc welding, welding of aluminium over a flux layer, plasma arc welding (A-1044, A-1054), single-arc butt welding of sheet materials in one pass on a sliding water-cooled copper backing with simultaneous formation of the reverse side of the weld (TS-32 and TC-44), etc. were developed on its base with minor redesigns. Tractor TS-17 and its modifications had no analogues abroad and up to now are considered among the best in the world.

At the same time, the work on welding heads, mostly for stationary machine tools and units, was in progress in the Soviet Union. In 1947, the E.O. Paton Electric Welding Institute developed self-propelled heads SAM and then USA-2, which moved on carriages along rails. They were manufactured by workshops of the Institute and by the «Iskra» Factory. Tending to typification and unification, the staff of the Institute (P.I. Sevbo, V.E. Paton et al.) designed the ABS head featuring a constant electrode wire feed speed. Assemblies of this apparatus served as a base for the development of a series of unified devices, including heads A-348, A-639, etc. Welding head ABS and its modifications manufactured several decades ago are still in operation.

*Dr. (History) A.N. Kornienko*

## INVESTIGATION OF FATIGUE RESISTANCE OF WELDED JOINTS ON ALUMINIUM ALLOYS MADE BY MODERN WELDING METHODS

### The research work on the above subject was completed in 2011 by the E.O. Paton Electric Welding Institute
(supervisor – Prof. V.I. Kyrian)

Quantitative estimation of factors (stress concentration, residual stresses, etc.) caused by the modern processes of welding of thin-sheet aluminium alloys (TIG, MIG, FSW), which affect service properties of the welded joints, was performed. It was established that the residual stressed state can be simulated with comparatively narrow (80−100 mm width) specimens in fatigue tests of the welded joints on 1−3 mm thick aluminium alloys. Fatigue resistance of the welded joints made by the above methods was investigated. Optimal parameters were identified for high-frequency mechanical peening (HFMP) of the welded joints on thin-sheet aluminium alloys to improve their fatigue resistance by bringing it closer to the level of the base metal. It was proved that HFMP is an efficient method for reducing the concentration of stresses caused not only by convexity of the weld but also by angular deformation. The investigations completed showed a high potential of widening of a range of thicknesses of aluminium alloys with different alloying systems from 1 to 3 mm for the high-productivity MIG welding technology (in contrast to requirements of GOST 14806−80) to manufacture transport-application structures operating under alternating loading conditions. The values of fatigue limits of the welded joints required for design and evaluation of service life of the transport-application structures were calculated

# THESIS FOR A SCIENTIFIC DEGREE

**E.O. Paton Electric Welding Institute of the NAS of Ukraine.**
**O.I. Olejnik** (PWI) defended on April 18, 2012 the Candidate's thesis on the subject «Improvement of effectiveness and safety of main gas pipeline repair by arc welding in service».

The thesis is devoted to improvement of the effectiveness of measures which ensure safe performance of arc welding during repair operations in the main gas pipelines under pressure and serviceability of repaired sections.

Numerical procedure for assessment of the risk of failure of defective sections of the main gas pipelines is developed, and principles of damage ranking by hazard level at repair in service are defined. Fundamental possibility of determination of repair order during the predicted term is shown both for isolated defects and entire sections of the main gas pipeline. Influence of factors ensuring safety at repair of pipe wall thinning by welding was studied. Calculated dependencies for determination of critical defect dimensions in the longitudinal and circumferential directions were established for various typesizes of pipes (Dn 1000, 1200, 1400 mm), material characteristics and service conditions (5.5 and 7.5 MPa pressure). Diagrams of admissible linear dimensions of defects were constructed, which allow determination of the minimum required level of pressure lowering in the main line for guaranteeing safety at performance of repair operations. Degree of influence of the conditions of welding and operation of the main lines on the risk of cold cracking in welded joints at repair of pipe wall thinning was assessed. Influence of diffusible hydrogen penetrating into the HAZ through pipe wall from inside of the pipeline is considered in detail. It is shown that the quantity of this gas cannot influence the probability of cold cracking. Conditions are defined, which ensure the effectiveness of application of welded leak-tight couplings of various designs at repair of the main gas pipelines under pressure. It is established that avoiding spontaneous failure of pipe wall can be ensured through pressure regulation in the main line during repair and tensioning of the structure at its mounting on the pipeline. As regards couplings with a filler, it was determined that to achieve the required level of structure performance the most effective is increasing the coupling wall thickness with simultaneous increase of weld width.

A system of procedural measures is proposed, which ensure effectiveness and safety of repair by welding at performance of operations in the main gas pipelines in service.

# OUR CONGRATULATIONS!

*Collective of the E.O. Paton Electric Welding Institute of the NAS of Ukraine and Editorial Board of «The Paton Welding Journal» heartily congratulate* **Igor V. Krivtsun** *with election to full members of the NAS of Ukraine and* **Vladimir M. Nesterenkov** *with election to corresponding-members of the NAS of Ukraine. Wish them to be healthy and happy, make new achievements and further much creative success!*

I.V. Krivtsun graduated from Physical faculty of the Taras Shevchenko National University of Kiev; has been working at the E.O. Paton Electric Welding Institute of the NAS of Ukraine since 1976; head of the Department of Physics of Gas Discharge and Plasma Technique since 2004; Deputy Director on Scientific Work since 2008; Cand. of Phys.-Math. Sci. on specialty «Theoretical and mathematical physics» (1987), Dr. of Tech. Sci. on specialty «Electrothermal processes and installations» (2003); corresponding member of the National Academy of Sciences of Ukraine on specialty «Materials science, welding of metals» (2006); author of more than 170 scientific works, including three monographs and seven patents.

I.V. Krivtsun is a widely known scientist in area of physics of gas discharge and theory of welding processes who has made an outstanding contribution in a development of specified scientific directions. His main works are dedicated to investigation of physical effects taking place in low-temperature technological plasma (welding arcs, plasma jets and other types of gas discharge) as well as processes of interaction of electric arc plasma and laser irradiation with treated material under conditions of arc, plasma, laser and hybrid welding, surfacing and coating deposition.

I.V. Krivtsun performs large educational and scientific work along with fruitful scientific activity. He has become a professor of the Department of Laser Technique and Physico-Technical Technologies of the NTUU «Kiev Polytechnic Institute» in 2009 and being a head of this department since 2010; head of postgraduate study and study for obtaining of doctor's degree at the E.O. Paton Electric Welding Institute and he has prepared two candidates and one doctor of sciences. He is a permanent member of specialized counsels on defense of theses at the NTUU «KPI» and at the E.O. Paton Electric Welding Institute, member of the Editorial Board of «The Paton Welding Journal». I.V. Krivtsun is a full member of American Welding Society (AWS), member of Materials Information Society (ASM International) and cooperates on active basis with different scientific-and-technical organizations of Germany, Russia, USA, China and other countries.

V.M. Nesterenkov graduated from Bryansk Transport Machine-Building Institute on specialty «Technology and equipment of welding engineering»; has been working at the E.O. Paton Electric Welding Institute of the NAS of Ukraine since 1973; defended thesis for Cand. degree in 1980 and thesis for Dr. degree in area of electron beam welding of large thickness metals in 2004; now he is a Chief Scientific Associate and Head of Department of Investigation of Physical Processes, Technology and Equipment for Electron Beam and Laser Welding, laureate of State Prize of Ukraine 2006.

V.M. Nesterkov is a well-known scientist who has made a significant contribution in development of theoretical basics of physical-metallurgical processes of electron beam welding of large thickness metals and determination of criteria of stable behavior of weld pool in various spatial positions. He investigated hydrodynamic processes in vapor-gas channels of large depth and developed technological processes of welding of low-alloyed steels of up to 200 mm thickness and high-strength aluminum alloys of up to 300 mm thickness. V.M. Nesterenkov proposed the scientifically proved recommendations on application of parallel beam scanning and spatial orientation of welded joint in electron beam welding of large-dimension parts of critical application as well as appropriateness of modification of weld metal in order to increase the strength and service reliability of the joints. Works on 25 contracts with Framatome, Aerospatiale (France), Airbus (England), HBC, WBC (Chine) and K+S Services and Alcoa (USA) companies were fulfilled using scientific achievements of V.M. Nesterenkov.

V.M. Nesterenkov published the basics of his scientific investigations in 72 works, including 12 author's certificates. The results of his scientific research were presented and discussed at multiple international conferences on electron beam technologies.

## NEWS

# MANUAL INSTRUMENT FOR MECHANICAL PEENING

Portable ultrasonic equipment of new generation US-TREAT-1.0, designed for manual performance of high-frequency mechanical peening of the welded joints



was developed at the E.O. Paton Electric Welding Institute in cooperation with G.V. Kurdyumov Institute for Metal Physics. Plastic deformations of the surface of metal as well as effect of ultrasound on metal structure take place as a result of treatment. This provides:

• increase of characteristics of fatigue strength and rise of fatigue crack life of welded elements of metal structures at manufacture;

• increase of residual fatigue crack life of welded metal structures under operation at the stage of damage accumulation up to formation of fatigue crack;

• increase of characteristics of fatigue resistance of repair welds;

• relieving of welded residual tensile stresses and inducing of residual compression stresses in zones of peening;

• geometric stability of thin sheet welded structures.

**Technical characteristics**

Frequency of ultrasonic oscillations, kHz .................... 26
Amplitude of oscillations, μm ............................... 15, 25
Weight of manual tool with changeable impact head, kg ............................................... 1.7
Weight of ultrasonic generator, kg ........................... 3.5

# THE MOTTO IS FASTER, HIGHER, STRONGER...

Well-known company «NAVKO-TEKh» (Kiev) specializes in the field of mechanization, automation and robotization of production of welded structures. The following can be noted among its deliveries in 2011:

• robotic complex IU-01 for measurement of deformations of castings of rail frogs;

• set from two machines AS333-1250 for TIG welding of longitudinal welds and one machine AS357 for TIG welding of circumferential welds of «pencil-box» part;

• machine AS364 for multi-pass MIG/MAG welding of switch blades;

• machine AS349 for MIG/MAG welding of bodies of fire-extinguishers;

• batch of machines AS333 for TIG welding of longitudinal welds.

The following equipment was delivered to the customers from the beginning of 2012:

• 11 machines AS333 for TIG welding of longitudinal welds;

• machine AS381 for MIG/MAG welding of branch pipe and body of oil automobile filter;

• machine AS308-2 for welding of longitudinal welds of thin shells of bodies of fire-extinguishers;

• 4 machines UDS711 for MIG/MAG welding of disc with rim of automobile wheels;

• machine AS337 for MIG/MAG welding of automobile shock absorbers.

# PRESENTATION OF TECHNOLOGY OF ARC WELDING
# OF POSITION BUTTS OF PIPES OF MAIN PIPELINES

In the period of March 19–20, 2012 on the initiative of ARKSEL Ltd. (Donetsk), CJSC ITS (St.-Petersburg), PJSC Electric Machine-Building Plant «Firma SELMA» (Simferopol) on the technical base of Inter-Industry Training-Attestation Center of the E.O. Paton Electric Welding Institute of the NAS of Ukraine in the presence of representatives of «Ukrtransgaz», «Naftogaz Ukrainy» and specialists of scientific departments of the E.O. Paton Electric Welding Institute the of technology of position welding of butts of pipes of steel of K60 strength class of 1420 mm diameter with wall thickness of 24 mm using welding wires of the types ARCSEL-13-O, POWER PIPE 60R, POWER BRIDGE 60M of ARKSEL Ltd. production (Figures 1 and 2) was demonstrated.



Figure 1



Figure 2

During presentation two welding technologies were demonstrated:

1st — semiautomatic welding of a root weld using a solid wire ARKSEL-13-O of 1.14 mm diameter in $CO_2$ + automatic welding of filling and finishing layers of weld using a flux-cored wire POWER PIPE 60R of 1.2 mm diameter in mixture of shielding gases Ar + 25 % $CO_2$;



Figure 3
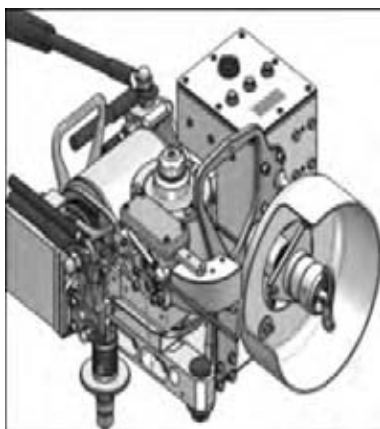


Figure 4
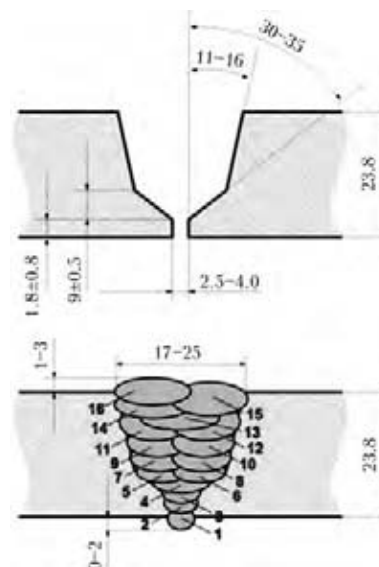


Figure 5

| No. of layer | Number of passes | Welding method | Welding current, A | Arc voltage, V | Welding speed, mm/s | Input energy, kJ/mm | Kind of current, polarity |
|---|---|---|---|---|---|---|---|
| 1 | 1 (root) | 135 | 140−160 | 13.5−15.5 | 16−20 | 0.56−0.60 | DC, reversed |
| 2 | 1 (filling) | 136 | 220−240 | 20.0−22.5 | 52−59 | 0.40−0.44 | |
| 3, 4 | The first 2 filling | 136 | 190−220 | 20.5−23.0 | 24−26 | 0.78−0.94 | |
| 5, 6, 7, 8 | The last 8 filling | 136 | 190−220 | 20.5−23.0 | 24−26 | 0.78−0.94 | |
| 9 | Finishing 3 | 136 | 220−260 | 21.0−24.0 | 23−24 | 0.97−1.25 | |
| Welding equipment: rectifier VDU-508U3, VD-506DK U3, wire feed mechanism PDGO-511 U3.1, welding heads VOSKhOD. | | | | | | | |

2nd— semiautomatic welding of a root weld using metal flux-cored wire POWER BRIDGE 60M of 1.0 mm in $CO_2$ + automatic welding of filling and finishing layers of weld using a flux-cored wire Power Pipe 60R of 1.2 mm diameter in the mixture of shielding gases Ar + 25 % $CO_2$.

Both technologies envisaged the application of welding rectifier VD 506DK U3, wire feed mechanism PDGO-511 U3.1 (Figure 3) (semiautomatic welding), welding heads VOSKhOD (Figure 4) of production of «Firma SELMA» plant (automatic welding).

The welding was performed according to preliminary technological instructions on welding pWPS 001 and pWPS 002. Edges preparation for welding, assembly and weld parameters are given in Figure 5. Welding parameters are given in the Table above.

To prove the demonstrated welding technologies the results of mechanical tests of specimens of pipes welded joints, carried out preliminary, were presented.

The results of tests of specimens proved that these technology provide mechanical properties of welded joints meeting the requirements of standard documents for main pipelines. According to test result the E.O. Paton Electric Welding Institute certified the presented welding technologies.

The presentation rose enormous interest among the specialists of «Ukrtransgaz», «Naftogaz Ukrainy», «Ukrgazpromstroj», who consider these technologies to be challenging in repair and construction of national gas pipelines. During presentation the issues of training and attestation of spe-

| Results of tests (2nd technology of welding) | | |
|---|---|---|
| Ultimate tensile strength, MPa | Bending angle, deg | Macroscopic examination |
|  |  |  |
| 575.8<br>587.9<br>Rupture in base metal | No cracks | Defects were not revealed |

| Impact toughness Temperature −20 °C | Type IX GOST 6996−66 | Size, mm 10×10×55 | | Requirement 47 J /cm² |
|---|---|---|---|---|
| Site of notch | Values | | | Mean |
| | 1 | 2 | 3 | |
| Weld metal | 143.9 | 161.3 | 141.7 | 145.6 |
| Near-weld zone | 335.4 | 342.5 | 349.4 | 342.4 |

Hardness
Type / load: $HV10$
Requirement: ≤250

Base metal: 1-188, 2-188, 3-182, 4-182, 5-182, 6-182, 7-188, 8-188, 9-188, 10-171, 11-171, 12-171

HAZ: 13-213, 14-217, 15-213, 16-213, 17-213, 18-192, 19-192, 20-188, 21-197, 22-197, 23-182, 24-182

Weld metal: 25-182, 26-188, 27-182, 28-190, 29-197, 30-197

Site of measurements (sketch)


cialists of welding production for «Naftogaz Ukrainy» on the technical base of the Inter-Industry Training-Attestation Center of the E.O. Paton Electric Welding Institute were discussed as well.

*M.V. Karasev (St.-Petersburg)*
*A.M. Mikitenko (Donetsk)*
*P.P. Protsenko, N.A. Protsenko (Kiev)*